drones

MDPI

Review

Remote Wind Turbine Inspections: Exploring the Potential of Multimodal Drones

Ahmed Omara [1], Adel Nasser [1], Ahmad Alsayed [2] and Mostafa R. A. Nabawy [1,3,*]

[1] Department of Mechanical and Aerospace Engineering, School of Engineering, The University of Manchester, Manchester M13 9PL, UK; ahmed.omara@manchester.ac.uk (A.O.); a.g.nasser@manchester.ac.uk (A.N.)
[2] Department of Mechanical Engineering, Umm Al-Qura University, Makkah 5555, Saudi Arabia; aaasayed@uqu.edu.sa
[3] Aerospace Engineering Department, Faculty of Engineering, Cairo University, Giza 12613, Egypt
* Correspondence: mostafa.ahmednabawy@manchester.ac.uk

Abstract: With the ever-increasing demand for harvesting wind energy, the inspection of its associated infrastructures, particularly turbines, has become essential to ensure continued and sustainable operations. With these inspections being hazardous to human operators, time-consuming and expensive, the door was opened for drone solutions to offer a more effective alternative. However, drones also come with their own issues, such as communication, maintenance and the personnel needed to operate them. A multimodal approach to this problem thus has the potential to provide a combined solution where a single platform can perform all inspection operations required for wind turbine structures. This paper reviews the current approaches and technologies used in wind turbine inspections together with a multitude of multimodal designs that are surveyed to assess their potential for this application. Rotor-based designs demonstrate simpler and more efficient means to conduct such missions, whereas bio-inspired designs allow greater flexibility and more accurate locomotion. Whilst each of these design categories comes with different trade-offs, both should be considered for an effective hybrid design to create a more optimal system. Finally, the use of sensor fusion within techniques such as GPS and LiDAR SLAM enables high navigation performances while simultaneously utilising these sensors to conduct the inspection tasks.

Keywords: multi-modal drones; wind turbines; remote inspection; sensors; renewable energy; rotor-based designs; bio-inspired designs; hybrid designs

Academic Editor: Abdessattar Abdelkefi

Received: 9 November 2024
Revised: 11 December 2024
Accepted: 19 December 2024
Published: 24 December 2024

Citation: Omara, A.; Nasser, A.; Alsayed, A.; Nabawy, M.R.A. Remote Wind Turbine Inspections: Exploring the Potential of Multimodal Drones. *Drones* **2025**, *9*, 4. https://doi.org/10.3390/drones9010004

1. Introduction

To combat climate change and meet the world's growing energy demands, renewable energy sources have become increasingly important in the recent shift in the global energy landscape. Wind energy is one of these renewable energy sources that has become increasingly important, progressively gaining traction as a clean and sustainable substitute for traditional fossil fuels. The growing number of both offshore and onshore wind farms highlights the crucial role that wind turbines currently play in our effort to create a more sustainable and environmentally friendly future. In fact, this exponential rise in wind energy exploitation is supported by innovations and technological advancements within the industry. However, because of their immense size, intricate designs and distant locations, wind turbine systems encounter substantial hurdles in their efficient operation and maintenance. To maximise energy output and maintain economic viability, it is essential to ensure the optimal working and longevity of these turbines.

The development of drones has completely changed the way wind farms inspect and maintain their infrastructure. Previously, inspecting turbines required a lot of manual labour, time and risk to workers' safety, particularly when climbing tall structures. On the other hand, drones with sophisticated sensing skills have quickly emerged as indispensable tools for maintaining the functionality and health of wind turbines. In fact, numerous benefits are provided by these drone solutions for wind farm maintenance, as schematically illustrated in Figure 1. They can provide thorough and accurate evaluations of the structural integrity, operating effectiveness and general health of the turbines. Moreover, they allow access to hard-to-reach places and enable anticipating potential problems before they become serious, which improves preventive maintenance techniques and reduces costs associated with the operation and maintenance of these wind turbines.

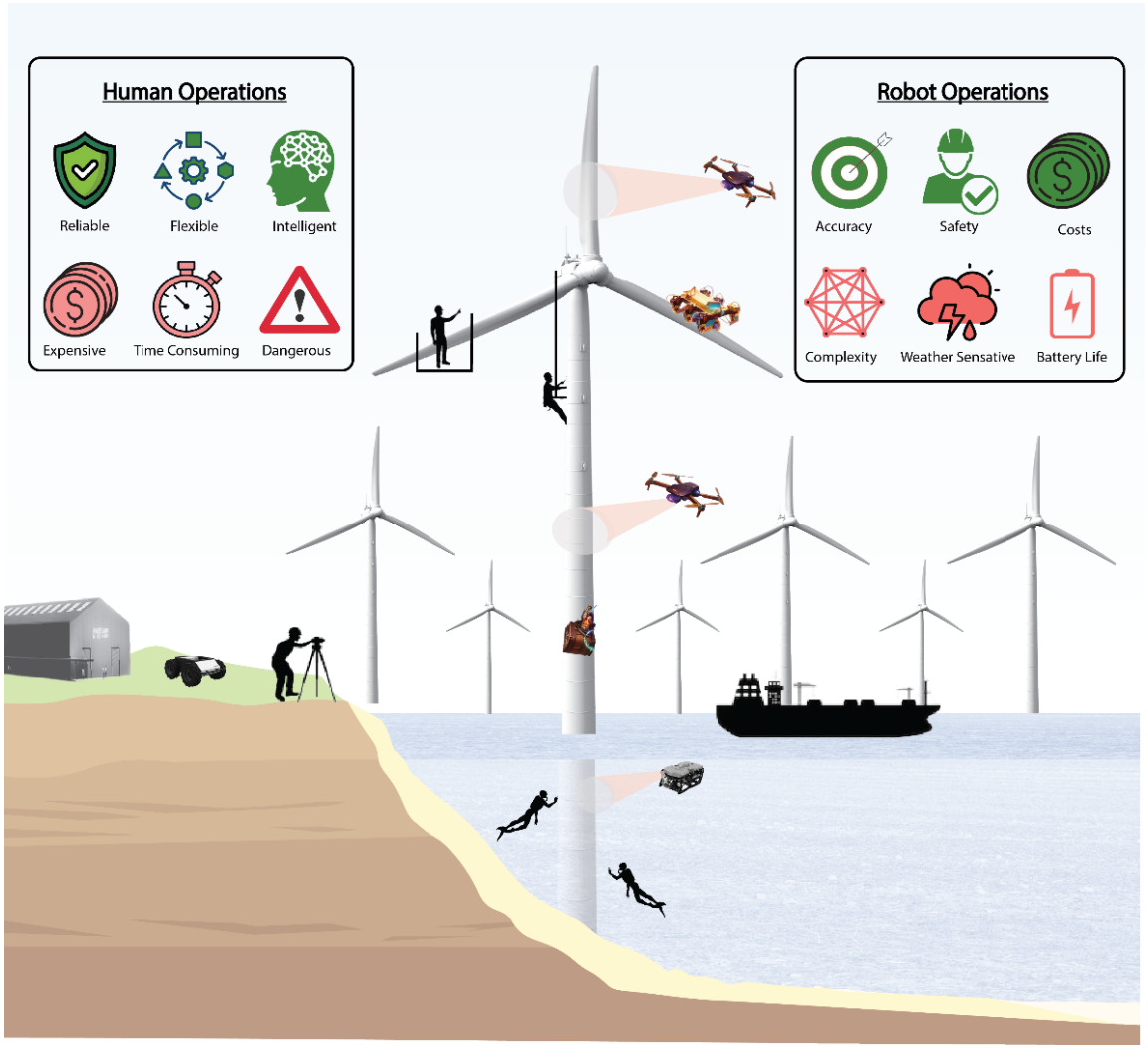

Figure 1. Illustration of the different aspects of operation and maintenance required for wind turbines, highlighting the different human and drone inspections, with their benefits (in green) and drawbacks (in red) highlighted.

Drones can be deployed either sequentially or concurrently to conduct wind turbine inspections. Each drone solution has its own advantages and disadvantages, which are summarised in Table 1, and these should be considered when deciding on the best solution for specific wind turbine inspections. Despite the aforementioned benefits that come with adopting single-mode and collaborative drone solutions, the field of wind turbine maintenance and inspection has the potential to undergo a radical change with the intro-

duction of multimodal drones (see Figure 2 for a generic representation of a multimodal drone). These sophisticated robotic systems combine several features, including various sensors, manipulators and mobility mechanisms and can change morphologies between different environments. As such, synergistically combining these features offers a novel way to improve the accuracy and efficiency of wind turbine health assessments. In particular, the newly offered mobility features are essential for reaching difficult-to-reach or isolated wind turbine locations and manoeuvring through tight spaces, vertical surfaces and complicated terrain, giving multi-modal drones unmatched access to every aspect of the turbine structure. While multimodal drones have great potential, it is fair to acknowledge that collaborative drones also provide a different approach to inspections with their own advantages and disadvantages, as discussed in Table 1. However, this field has been extensively considered in prior studies, such as [1–3]. Therefore, this paper only focuses on the growing potential of multimodal drones and how these can be applied to the field of wind turbine inspections.

Table 1. Definition and comparison of different types of drones in the field of wind turbine inspections.

Drone Type	Definition and Application	Advantages	Disadvantages
Climbing	Close-range drone that operates on the surface of the structure	- Can carry heavy payloads - Detailed damage assessment	- Low modularity and used on only one turbine - Slow inspections
Aerial	Long-range drone that flies around the structure and scans for defects	- Quick inspections - Full range of motion and can be used on multiple structures	- Low weight payloads and relatively high energy consumption - Cannot detect low-level defects
Terrestrial	Long-range drone that drives on land, and can be used for transportation and ground inspections	- Low energy consumption - Easy to control	- Cannot inspect high altitude and underwater components
Aquatic	Long-range drone that operates underwater for offshore environments, scanning underwater components	- Needed for underwater inspections	- Designs are typically heavy and require waterproofing - Control is complex
Collaborative	A multitude of single-mode drones that communicate accordingly to conduct inspections alongside each other	- Allow for multiple inspection methods simultaneously - Multiple inspections can be done concurrently with lower payloads	- Requires a strong communication link - Requires multiple drones and personnel
Multimodal	A combination of two or more modes of operation to conduct multiple inspections on a single platform	- Fewer drones and personnel needed, reducing costs - No wireless communication between multiple drone mechanisms	- Design needs to be highly optimised - Depending on the design, inspections may need to be conducted sequentially

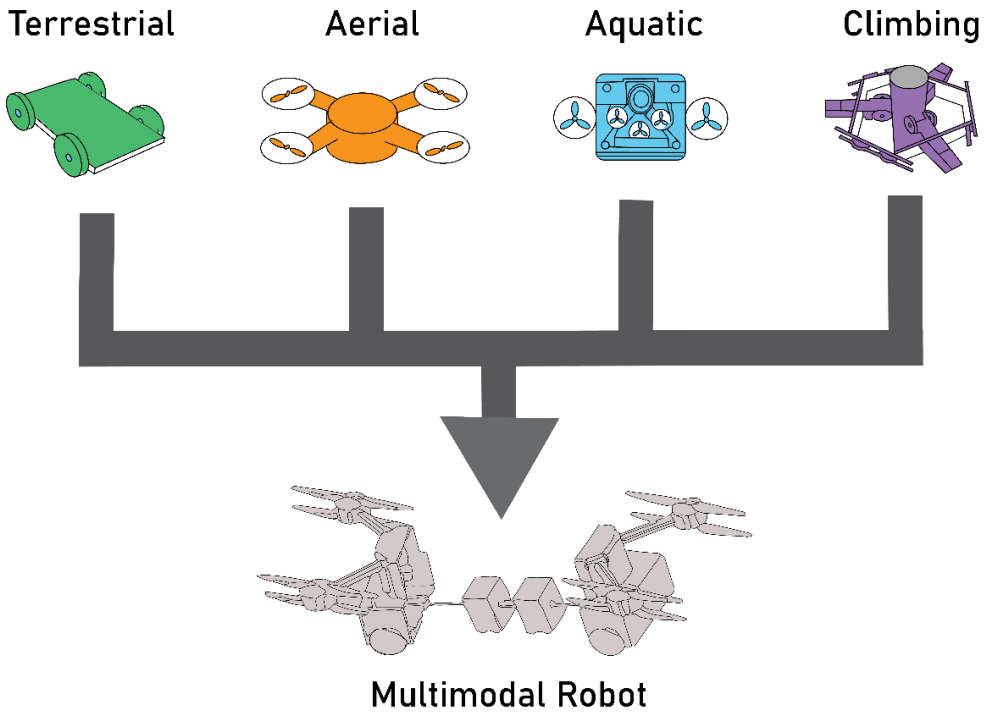

Figure 2. Illustration of a multimodal drone and its single-mode components.

As the demand for renewable sources increases, in line with global targets such as those outlined by the United Nations (UN) Sustainability Development Goals, the need to inspect these systems becomes more important [4]. One of the objectives of this study is to highlight the technologies developed and examined in wind turbine inspection research, as well as the challenges encountered. We particularly focus on the potential of multimodal drones within this field in the last decade, an angle that is typically overlooked in existing review papers. For clarity, the scope of this review encompasses work involving drone inspection methods and multimodal designs and their feasibility in this field. Other inspection technologies and methods, such as artificial intelligence, digital twins and human inspections, have been extensively covered in previous reviews, such as [3,5,6]. In fact, these reviews provide insight into past and current trends in wind turbine inspections, including sensing technologies, damage assessments and various technologies used in the field. Therefore, these aspects are not considered in this review. It is worth mentioning though that in this year alone (2024), there have been some notable advances presented in the field of wind turbine inspections, such as [7–11], highlighting the innovative technologies being developed in the field.

The keywords considered when compiling the research studies for this review included 'wind turbine inspections', 'drone inspections', 'wind turbine damage assessments' and 'wind turbine sensing technologies', as well as a combination of these terms. Furthermore, specific drone and inspection synonyms were used, such as 'UAV' and 'monitoring'. Relevant publications were collected from a wide variety of online databases, such as Google Scholar, IEEE Explore, Web of Science, ResearchGate and Scopus, as well as other journal websites relevant to this field. Figure 3 shows the increasing frequency of *review* studies directed towards wind turbine inspection technologies. Evidently, the figure illustrates the increasing interest in reviewing wind turbine damage assessment and inspection technologies as well as their impact. However, all previous reviews typically omit the growing potential of multimodal drones for these inspections, hence creating the motivation for this work. In fact, this review angle is believed to be important as the field of multimodal

drones has recently shown remarkable growth with new design concepts, such as [12–16], providing insight into the potential of future technologies in this field.

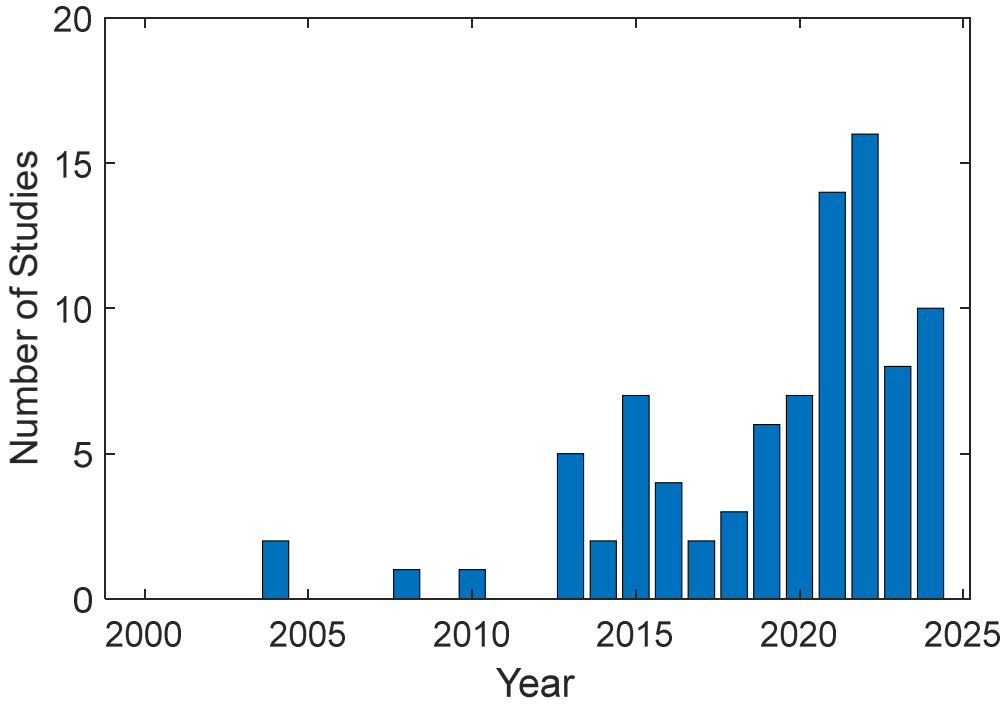

Figure 3. Frequency of review papers involving wind turbine damage assessment and inspection technologies from 2004 to 2024. References and information from which the figure is based can be found in Table S1 of the electronic Supplementary Materials.

In terms of processing the collected literature and following the collection of the first set of relevant papers, a backward citation search was conducted to collect more papers, i.e., the citations at the end of each article were carefully examined to determine their relevance to the current investigation. Following this, a forward citation search was conducted to identify new research articles on the subject, i.e., papers that cited the first set of articles were also investigated. After compiling all papers, the scope of each was objectively evaluated. For each paper of relevance, we extracted information including the technique used, the application demonstrated and the most important findings such as the performance and design approaches of each proposed drone.

The layout of this review is as follows: Section 2 overviews the current movement to renewable energy sources as well as the current issues observed with wind turbines. Section 3 delivers a review of the current methods used to inspect wind turbines, particularly highlighting the current drone technologies employed. Section 4 discusses the potential of multimodal drone designs and discusses the benefits of the different design approaches available. Section 5 then discusses the different methods of achieving the desired method of locomotion and discusses their suitability for wind turbine inspections. Section 6 follows by offering an insight into the different techniques required to control the drone in the relevant environments. The paper then finishes off with Section 7 presenting the key discussion points, critical remarks, and future outlooks into the potential research directions for this field.

2. Wind Turbine Installations and Challenges

2.1. The Transition to Renewable Energy

Herraiz et al. [17] mention that from 2000 to 2017, there were a substantial number of new installations of wind turbines (≈160 GW), solar photovoltaic cells (≈110 GW) and natural gas (≈90 GW). This trend can be extended globally, and as can be seen from Figure 4a, renewable sources are on the rise on a yearly basis, while fossil fuels are decreasing each year. This indicates the growing demand for renewable energy. Hence, inspections are needed to keep these systems operating effectively for as long as possible while minimising costs as much as possible. Currently, wind turbines are *primarily* inspected by humans, consequently causing downtime issues, which usually contribute 25–30% of the costs within the lifetime of the wind turbine. To give an example, this is estimated to lead to a cost of around €12 m/year for a 500 MW offshore wind farm situated 50 km in the North Sea [18]. As such, suitable solutions are clearly required to optimise the inspection process for wind turbines.

To create a more zoomed-in view of the current situation, Figure 4b shows how wind power is becoming extremely in-demand in comparison to all the other energy sources (only overtaken by Solar) [19,20]. In fact, the projections illustrated in Figure 4b show that by 2027, the total number of yearly installations could increase substantially. With the increase in installations comes a rise in costs, and a breakdown of the distribution of these costs per wind turbine can be seen in Figure 4c. Nash [21] concluded that maintenance and operation costs demonstrated by the Operational Expenditures (OPEX) collectively cover 41% of the total operational expenditures, and in a different study by Röckmann et al. [22], 53% of the OPEX was attributed to Operation and Maintenance. Overall, this shows that a good portion of the costs is attributed to maintenance. Note that this is only second to the Capital Expenditures (CAPEX), which contributes 52% of the costs, whereas the Development expenditures (DEVEX) and Decommissioning Expenditures (DECEX) are negligible in comparison, as seen in Figure 4c.

2.2. Types of Damage

Following installation, the clock starts ticking with respect to the lifetime of a wind turbine. Without regular inspection and maintenance, this lifetime will become much shorter depending on the environment in which it is placed. That said, wind turbines have various levels of damage, where some are obvious and seen readily and others are far more discrete and are much harder to spot, making detecting these defects much more difficult. Figure 5 illustrates some examples of the distinct types of damage that occur in many stages and in different forms across the wind turbine, including nacelle damage, blade damage, tower damage and mooring damage.

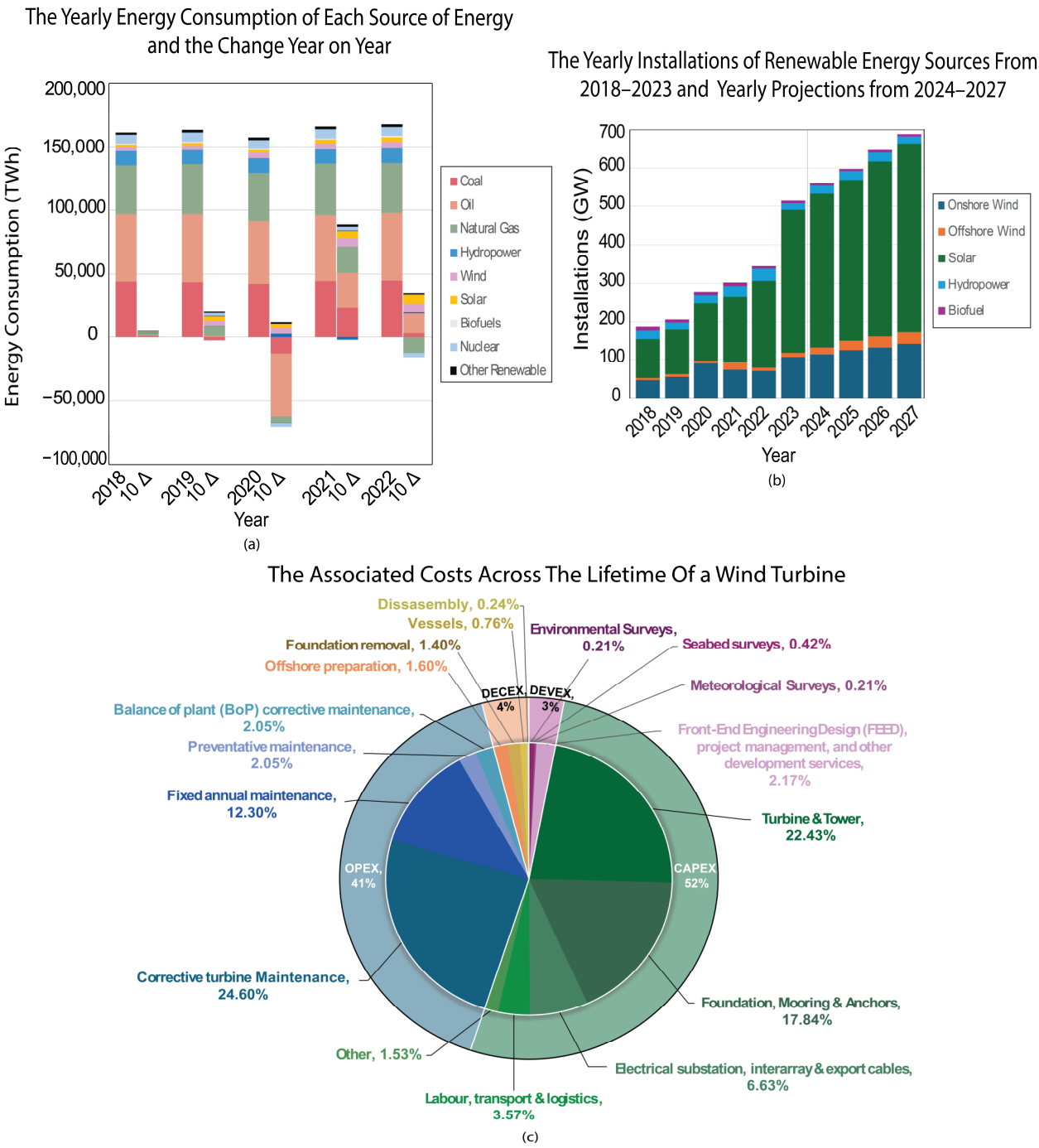

Figure 4. Evolution of renewable energy trends and resources: (**a**) Yearly consumption by type, where 10Δ is an amplified representation of the change year on year (i.e., yearly change, Δ, is multiplied by 10 for visual clarity). (**b**) Yearly installations of renewable energy. (**c**) Associated costs of wind turbines along their lifetime. Data used to create the figure were acquired from [19,21,23,24].

The first main type of damage is that involved with the nacelle. The damage involved within this type can be classed as either mechanical or electric failures of the systems enclosed (as seen in Figure 5a). Another form of damage is that involved with the chassis. As the structure is typically designed to be able to withstand heavy winds and survive for a long time, this damage needs to be detected as early as possible [25]. Following this, blade damage presents significant challenges and is by far the most important form of damage to inspect as it directly affects the operation of the system (as seen in Figure 5b). In this respect, Zhao et al. [26] concluded that lightning damage accounts for 7~10% of damage to wind

turbine blades, and this in turn causes average maintenance costs of US$150,000 per blade. Additionally, leading-edge erosion accounts for approximately 7% of the damage and has significant consequences on the aerodynamics performance [27,28]. This damage typically comes from rain exposure, hailstone impact, ultraviolet light, sea spray, and particulate matter such as sand and dust [29]. Finally, icing, which involves ice accumulation on the blades, incurs power losses of up to 17% in cold regions [30,31].

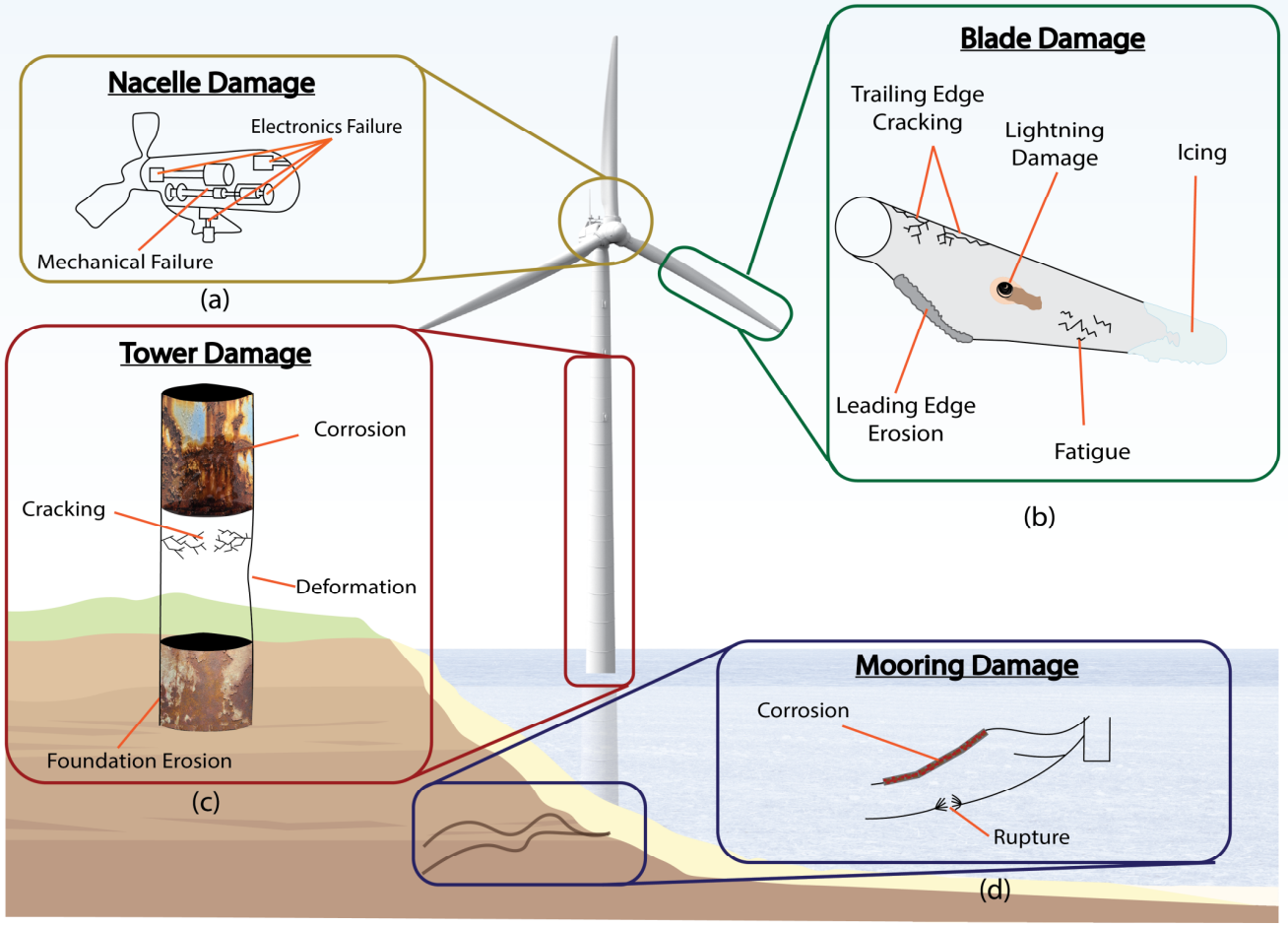

Figure 5. Different forms of wind turbine damage: (**a**) nacelle damage, (**b**) blade damage, (**c**) tower damage, and (**d**) mooring damage.

Another two types of damage are those within the tower and mooring systems (as illustrated in Figures 5c and 5d, respectively). For both of these systems, corrosion and erosion are the main contributors to these damages [32,33]. Another type of damage is fatigue-based damage, such as cracking, deformation and rupture, which are arguably very extreme and need to be detected as early as possible [34,35]. Fatigue can be classified into three categories: high, medium and low, with varying damage levels in the matrix [36]. Higher damage levels are typically visible and severe, including fibre pull-out and through penetration. Medium damage involves visible but less severe damage cases, such as matrix cracks and surface buckling. Finally, lower damage cases involve defects that may not be visible and, hence, can be overlooked [37]. The evolution of fatigue for composite materials has been studied by Katsaprakakis et al. [38]. Due to the wind turbines typically being made of composite materials, there are structural non-linearities in the material, which affect the health of blades including geometric, material and status nonlinearities [39]. All the previously discussed types of damage need to be detected using suitable and effective

sensing technologies, which will be discussed in Section 3. For further details on wind turbine damage, the reader is referred to [36,38,39].

3. Wind Turbine Inspection Techniques

3.1. Inspection Methods and Sensors

For inspections, there are usually two different approaches with their respective benefits and drawbacks: long-range and close-range inspections. Long-range inspections are important because they provide an overview of damage without the need for close contact with the wind turbine structure. They can come in many forms, as illustrated in Figure 6a–e. These methods provide various levels of context for the wind turbine structure using different camera and radar technologies. However, they can only capture surface-level damage and have limited abilities for more sophisticated types of damage in which close-range inspection is then required. There are a multitude of technologies that can be used for close-range inspection, as summarised in Figure 6f–k. However, while the tower, nacelle and mooring systems can be inspected during the operation of the wind turbine, the blades cannot be inspected during operation due to the high speeds of operation and the instability that an external inspection system may induce on the blades. As such, the turbine would need to be switched off for the inspection to be initiated. For interested readers, further information about wind turbine inspection technologies can be found in [18,36,40,41]. It is important to recognise here that each of these sensing methods can be applied to specific drones and have specific requirements to be used efficiently. These factors are compared and discussed in Table 2.

The selection of sensing technologies to be deployed on a drone should be performed carefully while assessing its suitability for the chosen design. This is even more critical in the context of multimodal drones as these are required to operate in multiple modes, requiring a multitude of sensors that have different requirements. In Table 2, it can be seen that relatively lightweight sensors that have a large sensing range are compatible with aerial drones, while low sensing range and heavy sensors are more compatible with climbing drones, with imaging and ultrasound sensors being suitable for underwater scans. Therefore, when combining these for multimodal operation, the weight constraints of the drone need to be met while having reasonable dimensions. The sensing range is also critical to the selection of sensors, and for an ideal multimodal drone, a mix of long- and close-range sensors is needed to fulfil the multimodal sensing requirements on wind farms, which is not an easy engineering challenge.

Currently, the interval of inspections for a regular environment (not susceptible to frequent lightning storms, excessive heat and increased humidity) is every six months for visual inspections and every one/two years for a comprehensive check as per the international codes [42,43]. For more extreme environments, this is usually reduced to monthly visual inspections and twice yearly for comprehensive checks [42,43]. Clearly, the wider inspection intervals are typically due to the difficulty of deployment and the costs involved with the inspection process. However, if these costs are reduced and the process of inspections is streamlined, then more comprehensive inspections can be conducted more frequently for better upkeep of wind farms and improved longevity of wind turbines. Therefore, carefully selecting compatible sensors within a multimodal solution can provide the potential for increasing inspection intervals while lowering inspection costs. In the following section, current wind turbine inspection solutions are assessed, highlighting their designs and sensing technologies.

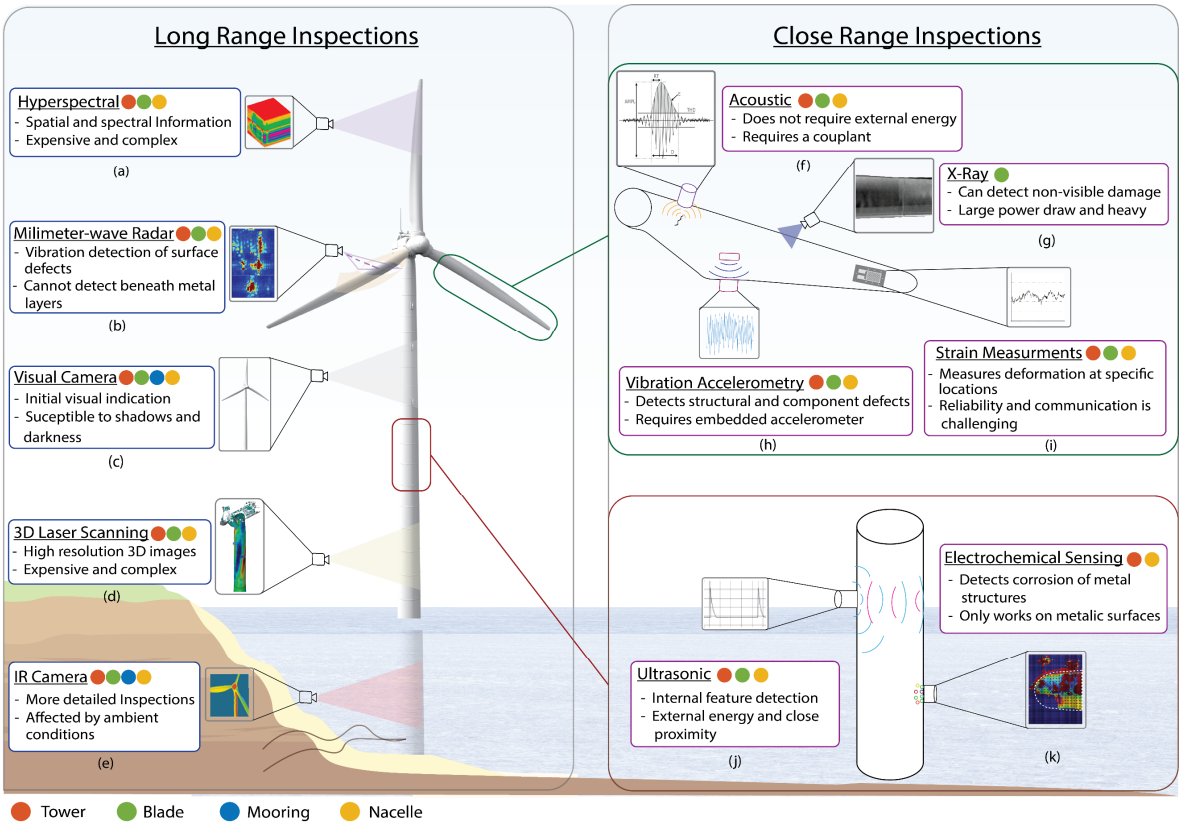

Figure 6. Inspection techniques used for a wind turbine (with illustrations of potential output formats, such as images and waveforms): (**a**) hyperspectral, (**b**) millimetre-wave radar, (**c**) visual camera, (**d**) 3D laser scanning, (**e**) infra-red (IR) camera, (**f**) acoustic, (**g**) X-ray, (**h**) vibration accelerometer, (**i**) stain measurements (**j**) ultrasonic and (**k**) electrochemical sensing.

Table 2. Specifications of the different sensors and their drone compatibility in the context of wind turbine inspection applications.

Imaging		
Sensor	**Specifications**	**Compatible Drone**
Hyperspectral [44–47]	- Weight: 0.1–5 kg - Size: approximately 0.1 m × 0.1 m × 0.1 m - Cost: approximately £100 - Sensing range: 5–20 km	- *Aerial* due to relatively low weight and high sensing range
Visual camera [48]	- Weight: 0.1–15 kg - Size: approximate height: 0.1 m, approximate diameter: 0.1 m - Cost: £10–£100,000 - Sensing range: several cm to several km	- *Aerial* due to compatible weight and high sensing range - *Aquatic* due to high sensing range and the sensor can be waterproofed
IR camera [49,50]	- Weight: 0.1–2 kg - Size: approximately 0.1 m × 0.1 m × 0.1 m - Cost: £10–£50,000 - Sensing range: several cm to several km	- *Aerial* due to compatible weight and high sensing range - *Aquatic* due to high sensing range and the sensor can be waterproofed
X-ray [51,52]	- Weight: 10–2000 kg - Size: approximately 1 m × 2 m × 1 m - Cost: £1000+ - Sensing range: contact–50 mm	- *Climbing* due to very high weight and low sensing range
3D laser scanning [53]	- Weight: 0.5–10 kg - Size: approximately 0.1 m × 0.1 m × 0.1 m - Cost: £ 100–£30,000 - Sensing range: approximately 500 m	- *Aerial* due to relatively low weight and high sensing range

Table 2. *Cont.*

Waves		
Sensor	**Specifications**	**Drone**
Millimeter-wave radar [54,55]	- Weight: 0.1–2 kg - Size: approximately 0.1 m × 0.1 m × 0.01 m - Cost: £10–£500 - Sensing range: 0.1 m–20 m	- *Aerial* due to low weight and high sensing range - *Climbing* due to compatible sensing range
Acoustic [56–58]	- Weight: 0.1–1 kg - Size: approximate height:0.01 m, approximate diameter: 0.1 mm - Cost: £100–£1000 - Sensing range: approximately 2 m	- *Climbing* due to low sensing range
Vibration accelerometry [59]	- Weight: 0.1–100 kg - Size: approximate height:0.1 m, approximate diameter: 0.01 mm - Cost: £1–£2000 - Sensing range: In contact	- *Climbing* due to very low sensing range
Ultrasonic [60–62]	- Weight: 0.1–10 kg - Size: approximately 0.1 mm × 0.1 mm × 0.1 mm - Cost: £10–£10,000 - Sensing range: few cm to several m	- *Climbing* due to flexible sensing range - *Aerial* due to relatively low weight and high sensing range - *Aquatic* due to high sensing range and the sensor can be waterproofed
Mechanical		
Sensor	**Specifications**	**Drone**
Strain measurements [63]	- Weight: 0.01–10 kg - Size: approximately 0.01 m × 0.1 m - Cost: £1–£2000 - Sensing range: In contact	- *Climbing* due to very low sensing range
Chemical		
Sensor	**Specifications**	**Drone**
Electrochemical sensing [64,65]	- Weight: approximately 1 kg - Size: approximately 0.1 m × 0.01 m × 0.01 m - Cost: approximately £50–£1000 - Sensing range: In contact	- *Climbing* due to very low sensing range

3.2. Drone-Based Inspections

Currently, many inspections are conducted by human operators, which is evidently risky and costly. These inspections involve the deployment of sensing technologies manually by climbing up the towers. Within this field, several previous studies have demonstrated advancements in damage assessment, including the sensing technologies required. Some notable studies include [66–70], which highlight the different technologies being deployed that do not rely on drones.

Obviously, a drone can be deployed in place of a human operator and can be monitored remotely from afar. This removes the risk to human workers and minimises costs if the drone cost is low enough in comparison to the potential losses [71,72]. There are many designs that have impacted this field, which are discussed in this section and summarised in Figure 7. Furthermore, Figure 8 illustrates the frequency of publications in this field, demonstrating how the number of drone solutions throughout the years has been steadily increasing. This demonstrates the effectiveness of these solutions as well as their need. Remarkably, collaborative solutions (i.e., drones that operate simultaneously for a common goal, relying on exceptional communications between the different systems) have become increasingly popular in the last few years, with multimodal solutions showing promise as well.

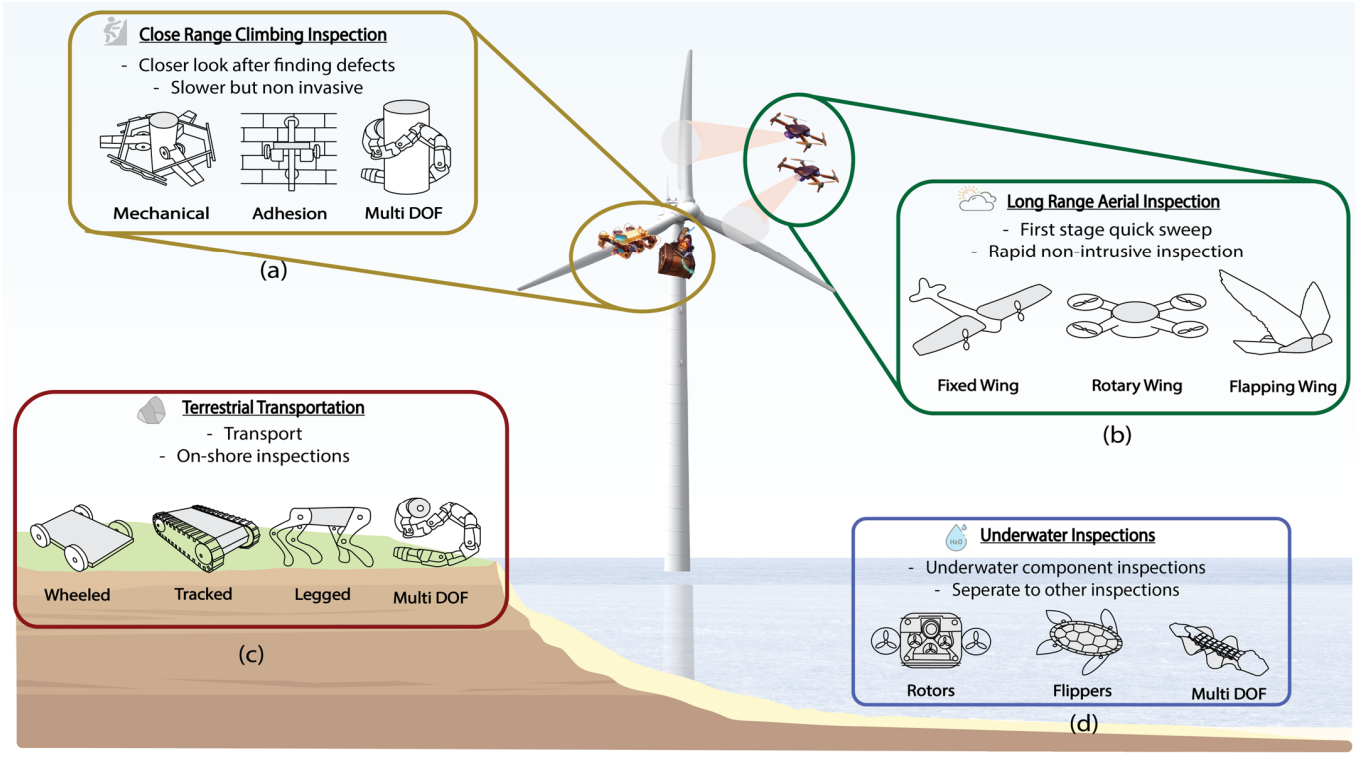

Figure 7. Possible drone solutions for the different systems of wind turbines and the diverse types of inspections involved: (**a**) close-range climbing, (**b**) long-range aerial, (**c**) terrestrial and (**d**) underwater inspections.

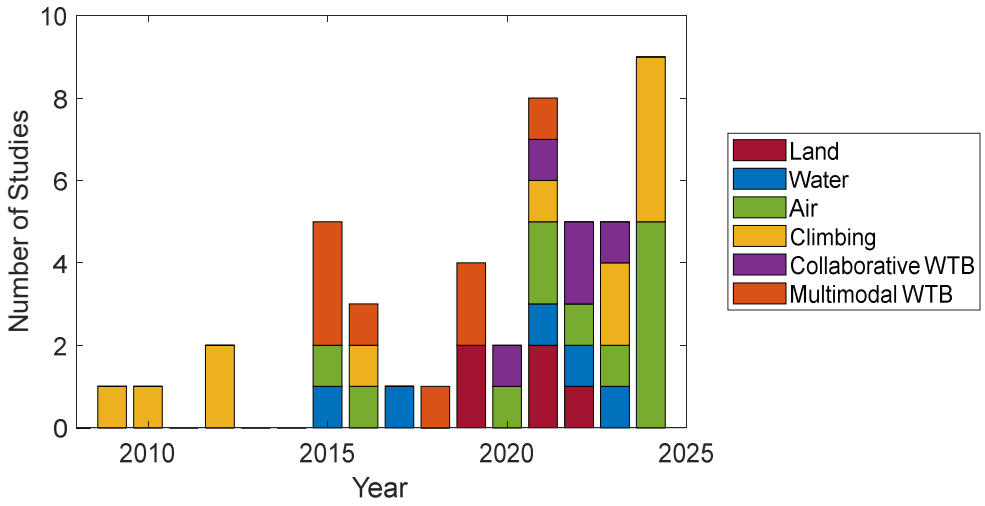

Figure 8. Frequency of wind turbine inspection drone designs from 2009 to 2024. References and information from which the figure is based can be found in Table S2 of the electronic Supplementary Materials.

Drones have been typically employed in all sorts of inspection missions, including infrastructure, construction sites, radiology, industrial sites and stockpiles [73–81]. Within wind turbine inspections, there have been several technologies deployed, including edge analytics, digital twin technology, real-time anomaly detection using AI algorithms and autonomous drones [3,5,6]. These are all attributed to lowering the Levelized Cost of Energy (LCOE) [82]. The Levelized Cost of Energy (LCOE) is defined as the average cost of the unit (kWh) generated by a system and is calculated by the ratio of the total annualized cost of the system to the total electrical load served [83]. Studies by Kabbabe et al. [71] and

Shafiee et al. [84] have indeed highlighted the benefits of drone inspections, particularly by reducing the personnel needed for inspections as well as achieving cost savings. In particular, it was shown that the usage of UAVs can reduce costs by 70% and downtime losses by 90%. Liu et al. [2] investigated various robotic platforms for evaluating various offshore wind turbine (OWT) components, demonstrating the usefulness and need for multiple drone platforms for effective inspections. In addition, Lee [85] highlighted the significance of a complete sensor suite for efficient operation. As such, drones and AI have already started to improve the inspection process and have the potential to improve with new technologies.

As presented in Table 3, many drone designs have been deployed in the field of wind turbine inspections. For onshore operations, both climbing and aerial drones are typically utilised. It can be observed that the most popular climbing drone designs (as illustrated in Figure 7a) are those of ring and wire climbing. These provide a simple method for reliable tower climbing with a high adhesive capability and a high payload capacity. However, the surface contact may cause wear to the tower. On the other hand, aerial designs (as illustrated in Figure 7b), most notably, Unmanned Aerial Vehicle (UAV) designs, operate without contacting the structure. These designs usually use Light Detection and Ranging (LiDAR) and Global Positioning System (GPS) capabilities for mapping and navigation, allowing for effective mapping and perception. This method also significantly reduces the downtime and costs associated with the system, resulting in a quick method for long-range inspections [71]. Nonetheless, UAV designs can only broadly inspect wind turbine structures and, as such, cannot be used singlehandedly for effective inspections.

While not immediately useful for wind turbine inspections, terrestrial drones (as illustrated in Figure 7c) have shown promise in other fields of inspection, such as those in bridge and confined space inspections. In fact, the evolution of sensors, actuators and control systems in technology has led to a major evolution in ground drones intended for inspection and monitoring, such as autonomous operations. Remarkably, the techniques created for bridge inspections can be modified to provide wind turbines with automated problem detection and high-quality 3D maps, improving safety and maintenance procedures [86,87]. In addition, for OWT applications, aquatic designs (as illustrated in Figure 7d) are vital for inspecting submerged structures. From Table 3, it is evident that Remotely Operated Vehicles (ROVs), Autonomous Underwater Vehicles (AUVs), Autonomous Surface Vehicles (ASVs) and Launch and Recovery Systems (LARS) are popular options due to their reliability and capability to operate at high depths. Despite that, the widespread usage of monitoring systems continues to present challenges such as data quality and sensor longevity, thus more robust and dependable technologies need to be developed.

Subsequently, from Table 3 we can observe that collaborative drones have been utilised in recent years. Popular collaborative designs include multi-drone systems, as well as detachable climbing drones attached to UAVs. This provides a method for concurrent operation across the wind turbine, which reduces downtime and optimises the operation across the structure. One notable system is that demonstrated by the Goliath UAV and blade-bug-legged drone [88,89]. This solution allows for both long- and close-range inspections by using two drones simultaneously. However, having multiple drones is costly, requiring more personnel to deploy, as well as being dependent on robust communication. As such, multimodal solutions have shown promise in combining these capabilities into one platform. However, the current designs have limited operation time and payload capacity, as well as high energy consumption.

It is important to note that the size, weight and endurance requirements of drones and their onboard sensors are critical to the design of a robust drone capable of satisfactorily performing wind turbine inspections. In particular, the weight of a drone is highly

influenced by the sensor payload it carries. Each sensor has different characteristics and requirements for operation; therefore, when designing the drone, these factors should be accounted for as demonstrated in Table 2. Table 3 shows, where information is available, the sensors used on the different drones used for the inspection of wind turbines. Examples include X-ray sensors primarily being used in climbing drones due to their weight and energy consumption, which are both major concerns within aerial drones as they need to be as lightweight and efficient as possible. As such, other solutions such as cameras and lasers are often more used on aerial drones due to their long-range nature and lower weight constraints.

Table 3. Examples of wind turbine inspection drone contributions.

Climbing				
Drone [Ref]	**Schematic**	**Design Purpose and Configuration**	**Performance and Findings**	**Inspection Sensors**
[37]	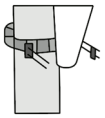	- Ring-climbing drone prototype - Actuated using three wheels - Model weight is 3 kg - 1:10 scale prototype for a 30–45 cm test tower	- Maximum prototype payload of 2 kg - Maximum climbing speed of 10 m/min	- X-ray
[90]	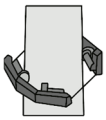	- Ring-climbing drone prototype - Actuated using four wheels with two body frames - Model weight is 8.2 kg - Dimensions 500 mm × 164.96 mm × 45 mm	- Maximum prototype payload of 8.2 kg - Average climbing speed of 120 mm/s	- N/A
[91]		- Full-size wire ring-climbing drone deployment with three degrees of freedom - Drone weight is 1.9 tons - Dimensions: 5.2 m × 5.2 m × 0.8 m	- Withstands wind speeds up to 6.51 m/s - Demonstrated successful phased array ultrasonic imaging	- Ultrasonic
RIWEA [92,93]	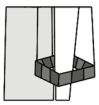	- Wire ring-climbing drone for inspection and cleaning with three degrees of freedom	- Drone can move vertically at 0.1 m/s with water jet pressures up to 145 bar	- IR camera - Ultrasonic - Visual camera
Inchworm [94]	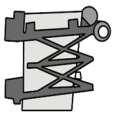	- Inchworm-type ring-climbing - Actuated using wheels and multiple links - Weight of 30 kg - Dimensions: 962.9 mm × 571.8 mm × (311.3~1074.1 mm)	- Drone design concept that can climb blades based on adaptive guide mechanism	- Visual camera - X-ray - Ultrasonic - IR camera
Aerial				
Drone [Ref]	**Schematic**	**Design Purpose and Configuration**	**Performance and Findings**	**Inspection Sensors**
[95]	-	- Autonomous machine vision for UAVs using distance error to tower and edge detection	- Real-time processing times around 7–11 Hz	- Visual camera
[96]	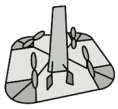	- Automated quadcopter UAV with LiDAR for wind turbine inspections	- Prototype development and 3D mapping presented	- LiDAR
[97]		- Quadcopter UAV with LiDAR for wind turbine inspection	- Successful Gazebo simulations and full-scale tests with maximum distance error of 0.1315 m	- LiDAR

Table 3. *Cont.*

Aquatic				
Drone [Ref]	**Schematic**	**Design Purpose and Configuration**	**Performance and Findings**	**Inspection Sensors**
[98]	-	- Fully coupled numerical model for ROV, ASV, and LARS	- ROV follows mooring accurately with 0.15 m errors	- Ultrasonic
[99]	-	- Advanced control and navigation for ROV manipulators	- Accurate motion of floating platform	- Visual camera
Seacat [100]	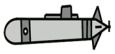	- Submarine-shaped drone with rear propeller and fins for control for underwater inspections - Maximum weight of 180 kg - Dimensions: 2.7 m × 0.58 m × 0.67 m	- Algorithm for AUV presented with field trials for the path planning and sensing	- Ultrasonic - Visual camera - LiDAR
RoboFish [101]	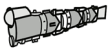	- Development of fish-inspired underwater ROV for underwater OWT inspections - Weight of 30 kg - Total length of 1.9 m with inner body cylinder diameter of 9.3 cm and 43 cm long	- Prototype tested for watertightness and control in minimum lake trials	- Ultrasonic - Visual camera
Collaborative				
Drone [Ref]	**Schematic**	**Design Purpose and Configuration**	**Performance and Findings**	**Inspection Sensors**
[1]	-	- Collaborative strategies for various types of UVs for wind turbine inspections	- UVs are limited when operating alone but are more flexible when operated together	- N/A
[102]	-	- Multi-drone system (UAV, ring, and magnetic climbing) for inspection of wind turbines	- Robot Operating System (ROS) used for process control, collision-free path planning, and vision-based control using the Bezier Library	- Visual camera - LiDAR - IR Camera - Ultrasonic
Goliath and Blade-bug [88,89]	**-**	- Deployment and recovery of climbing drones using UAVs for wind turbine inspections - Combined weight: 15 kg + 3.5 kg - Total dimensions: 0.8 m × 0.8 m × 0.5 m	- Effective autonomous retrieval on standalone blade with wind speeds over 10 m/s	- LiDAR
[103]	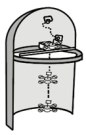	- Quadcopter tethered to wheeled climbing drone that may be used for wind turbine inspections - Weight of 0.5 kg - Climbing robot dimensions of 0.15 m × 0.18 m × 0.12 m	- Experimented with varying duct shape testing stability on a common ceiling	- Visual camera - Radiation
Multimodal				
Drone [Ref]	**Schematic**	**Design Purpose and Configuration**	**Performance and Findings**	**Inspection Sensors**
[17]		- Legged climbing drone design with six adhesive legs for NDT of wind turbines - Weight of 4.42 kg - Diameter of 52 cm	- Drone design fabricated including mechanisms and sensors	- Ultrasonic - Visual camera - Acoustic - IR camera
[104–106]	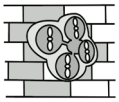	- Development of quadcopter climbing drone with the ability to tilt to 90 degrees for wall climbing	- Successful wall climbing vertically at 90% success	- Ultrasonic

Table 3. *Cont.*

Multimodal				
Drone [Ref]	**Schematic**	**Design Purpose and Configuration**	**Performance and Findings**	**Inspection Sensors**
[107]	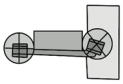	- Design and validation of four-wheeled drone with four tiltable drone motors for wall climbing - Weight of 3 kg - Ducted fans of 70 mm diameter	- As tilt angle increases from 0 to 90 degrees, tensile force decreases with fewest failures at 40–60 degrees	- Ultrasonic
[108]	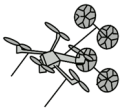	- Design concept of a drone for bridge inspections useful for wind turbine inspections - Total mass of approximately 5 kg - Diagonal wheelbase of 450 mm	- Maximum propulsion force of 2 N with wall distance of 0.78 m and wheel reaction of 0.5 N	- Visual camera

Based on the inspection methods briefly discussed in this section, it is evident that the current methods of inspection primarily focus on ring-climbing drones for close-range inspections, quadcopter drones for aerial inspections and ROV drones for aquatic inspections. While each of these different methods is viable for their given task, they do face several limitations. Some of these include time limitations and the inspection interval required. In particular, due to the difficulty and inefficiency of climbing deployments, a longer interval between close-range inspections is typically required in comparison to long-range inspections. This provides a significant shortcoming in the current methods, where comprehensive inspections are rarely conducted while visual inspections are more frequently conducted.

4. Multimodal Drone Designs

4.1. Overview

Currently, wind farm inspection drones mostly operate in a single mode of operation (as discussed in Section 3). This approach can be costly and inefficient due to the need to achieve different tasks at once, including long-range and close-range inspections. Hence, these systems need to be designed effectively and communicate accurately with each other with the potential addition of human operators, which all contribute to the added costs. This section will outline the different multimodal designs used for different applications (some examples can be seen in Figure 9a–g) and analyse their suitability for wind turbine inspection applications.

Based on Figure 9, we classified drones into multiple subgroups based on their locomotion modes and how that mode is achieved. For all discussions in this manuscript, the following definitions are used:

Modal classification:

- Bi-Modal = Drone with two modes of locomotion.
- Tri-modal = Drone with three modes of locomotion.
- Quad-modal = Drones with four modes of locomotion.
- Terrestrial Aerial (TA) Drone = A drone that can operate both on land and in the air.
- Amphibious Drone = A drone that can operate on land and in water.
- Wall-Climbing Robot (WCR) = A drone that can operate on land and can climb.
- Aerial Aquatic (AA) Drone = A drone that can operate in the air and in water.
- Aerial Climbing (AC) Drone = A drone that can operate in the air and can attach to a surface without the ability to operate effectively on land.
- Aerial Wall-Climbing Robot (AWCR) = A drone that can operate in the air and on land, while having the ability to climb.

- Triphibian Drone = A drone that can operate on land, in the air and in water.

Mode-realisation classification:

- Rotor-Based Drone = A drone that operates using only rotor kinematics.
- Bio-Inspired Drone = A drone that operates using only nature-inspired kinematics.
- Hybrid Drone = A drone that combines rotor and bio-inspired kinematics.

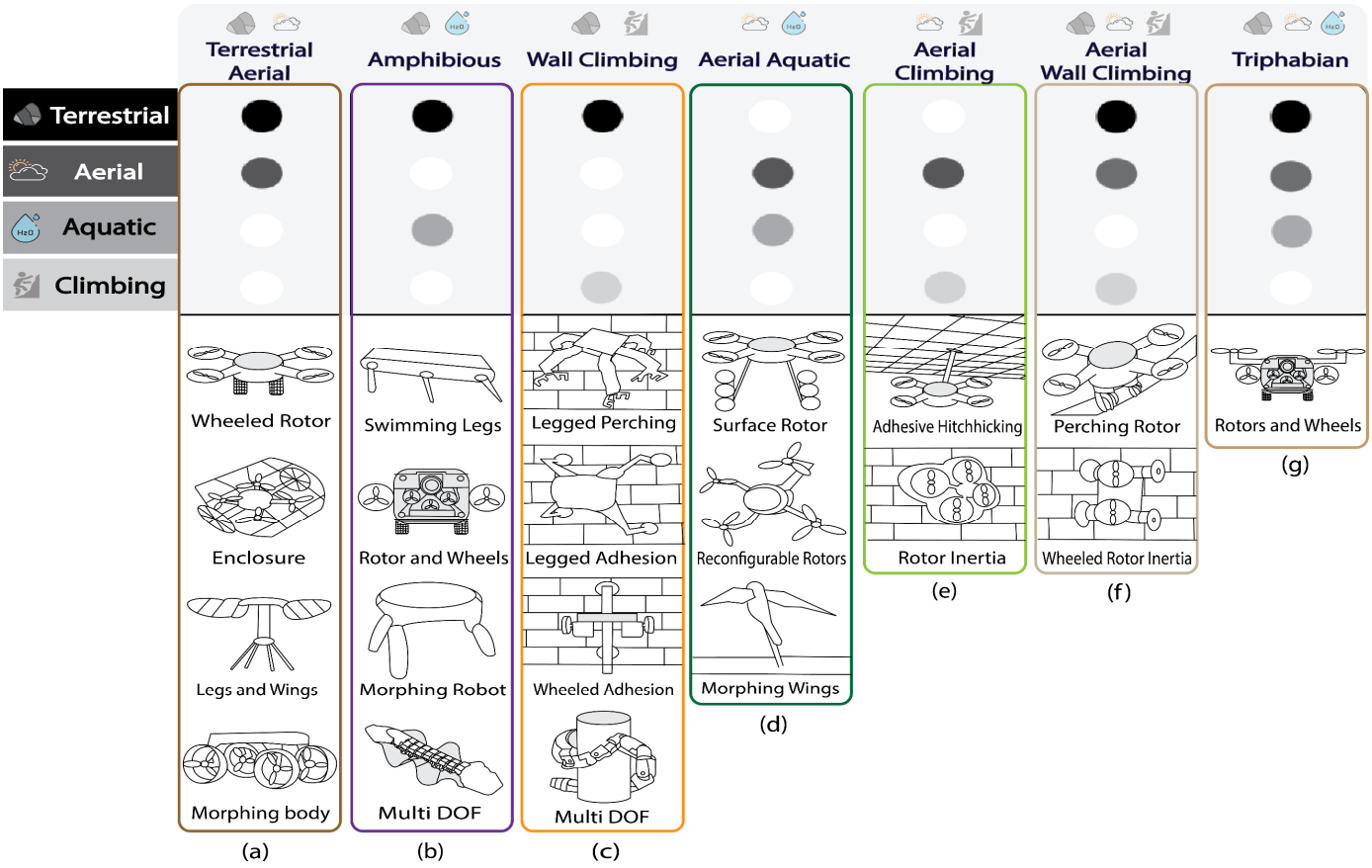

Figure 9. Types of multimodal drone configurations: (**a**) terrestrial aerial, (**b**) amphibious, (**c**) wall-climbing, (**d**) aerial aquatic, (**e**) aerial climbing, (**f**) aerial wall-climbing (perching) and (**g**) triphibian. The monochromatic circles demonstrate the modes of locomotion used within each classification (the colours match the background colour of the mode of operation seen on the left of the figure) while outlining the limitations of each class with white circles, representing the environments that cannot be traversed in a wind farm setting using this drone configuration.

Notably, the frequency of studies on multimodal robotics research (as seen in Figure 10a) has been rising throughout the years. Remarkably, the figure shows that there is a significantly sparse number of climbing multimodal drones. It can also be seen that tri-modal and quad-modal drones are either rare or non-existent, as are aquatic climbing drones. Figure 10a shows the same data shown in Figure 10b: the former classifies designs using modal classification, whereas the latter classifies designs based on how locomotion was realised. Evidently, the frequency of studies that considered rotor-based drones in comparison to bio-inspired drones is much higher as these are easier to prototype and control. Notably, hybrid designs are gaining momentum, and their numbers are demonstrating an increasing trend.

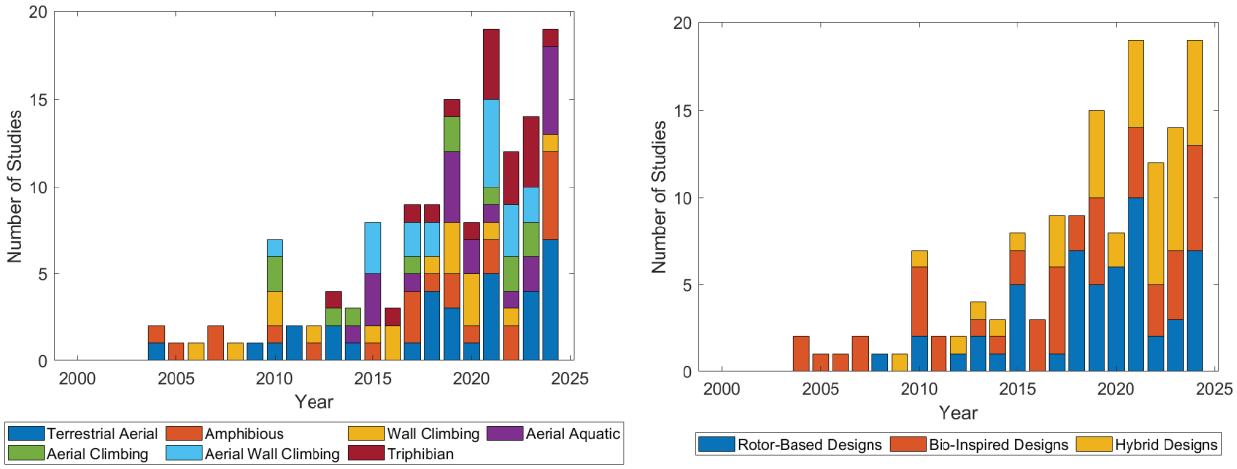

(a) (b)

Figure 10. Frequency of multimodal drones from 2004 to 2024 based on (**a**) modal classification and (**b**) mode-realisation classification. References and information from which the figure is based can be found in Table S3 of the electronic Supplementary Materials.

Multimodal drones can come in the form of additive or adaptable designs, as demonstrated in Figure 11. Additive designs add separate actuation modes together to individually perform the required motions. While this is much easier to implement, it requires separate mechanisms for the separate systems, which in turn affects weight and power consumption. Alternatively, adaptable morphology has become a more interesting and promising field of research in recent years. These drones, which typically take their cues from biological systems, can change their structural makeup and form to adapt to various tasks and environments. This was discussed by Mintchev and Floreano [109] as well as Ramirez and Hamaza [110] who considered different methods of achieving adaptable morphology such as soft materials, structures modelled after origami and mechanisms with variable stiffness. Despite the benefits, these designs obviously typically invite additional complexity. As a final note, the designs presented within the whole section are meant for all types of applications and are not exclusive to wind turbine inspection applications. This allows for identifying their main design aspects and, hence, assessing their potential for the application at hand.

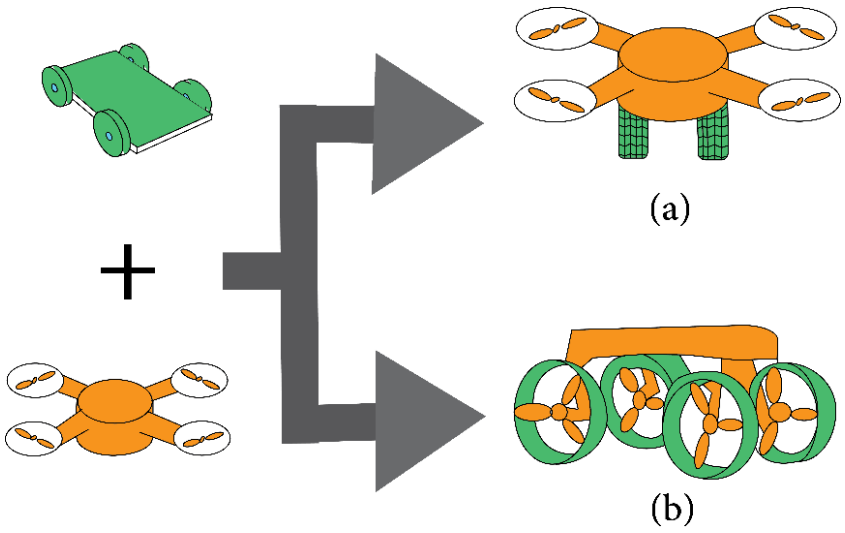

Figure 11. An illustration of additive and adaptive multimodal designs: (**a**) additive and (**b**) adaptive.

4.2. Rotor-Based Designs

Rotor-based actuation (as illustrated in Figure 12) simplifies control, design and deployment but affects size, weight and energy consumption. As such, these factors need to be optimised according to the environment of choice. This section considers multiple designs and assesses them within the context of wind turbine inspections.

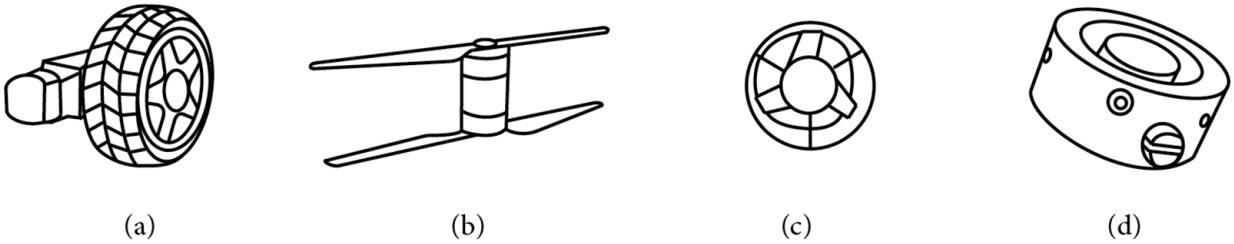

Figure 12. Rotor-based drone actuation methods applied within different contexts: (**a**) terrestrial, (**b**) aerial, (**c**) aquatic and (**d**) Bernoulli pad used for climbing.

As can be gathered from Figure 10 and Table 4, rotor-based bi-modal designs are attracting increasing attention. These designs include TA drones, amphibious drones, WCRs, AA drones and AC drones. Common TA drones include a combination of wheels and propellers in an additive configuration due to the simplicity of integration involved. However, this configuration lacks the flexibility required for curved and uneven surfaces, as well as lacking climbing or aquatic actuation. Common amphibious drones have wheels and aquatic impellers in spherical or wheel paddle configurations. Spherical designs provide simple additive control mechanisms, with a sealed waterproof enclosure, while wheel paddle approaches provide adaptive wheels for water surface locomotion. That said, having a paddle or spherical design can damage the structures involved, as well as having low surface contact. Following this, WCRs usually combine wheeled locomotion, with some sort of adhesive mechanism, such as pneumatic adhesives for pneumatic WCRs (PWCRs). These have remarkably high adhesive strength while allowing the drone to traverse various surfaces. Nonetheless, these systems consume a remarkably high amount of energy and do not have any aerial capabilities. Frequent AA drone designs include drones with buoyant landing balls. This design allows the drone to land on the water surface and transition in a simple manner. Even so, this design does not work underwater and does not effectively move along the water surface. Finally, AC drones, on the other hand, involve drones that can perch on a vertical structure. This allows for unconventional manoeuvres for aerial drones while utilising inertial methods in addition to usual drone control mechanisms. Be that as it may, these designs consume a lot of energy and are not optimised for uneven surfaces, such as those seen on wind turbine blades.

Table 4. Examples of rotor-based multimodal drones.

Terrestrial Aerial Drones			
Drone [Ref]	**Schematic**	**Design Purpose and Configuration**	**Performance and Findings**
HyTAQ [111]	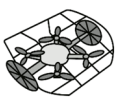	- Quadcopter drone with two side wheels connected by a cage, forming one uniform wheel	- Terrestrial range up to 11 times greater than aerial - Power of 120 W at flight take-off
[112]	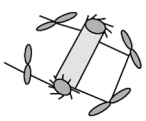	- Foldable quadcopter drone with whegs wheels for versatility - Weight of 340 g - Dimensions: 370 mm × 300 mm × 80 mm in aerial (largest) mode	- Hovering range of 7.1 km in 15.6 min - Terrestrial range of 12.4 km in 6.8 h

Table 4. *Cont.*

Terrestrial Aerial Drones			
Drone [Ref]	**Schematic**	**Design Purpose and Configuration**	**Performance and Findings**
[113]		- Foldable drone with adaptable size to fit confined spaces with tracked wheels for crawling	- 75% success to small misalignments and travel in 34% smaller paths than nominal size
[114]		- Foldable drone with propeller wheels that can be used for both flying and driving - Weight of 318 g - Dimensions: 290 mm × 76 mm × 120 mm on ground	- Drone requires 70 W to take off and hover with about 50 N lift force
WAMORN [115]		- A small, wheeled quadcopter with two large wheels, with supporting castor wheels - Weight of 329 g - Dimensions: 300 mm × 240 mm × 260 mm	- Drone can climb slopes of 26 degrees and can perform controlled landings
Rollocopter [116]	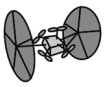	- Design and evaluation of a Rollocopter formed of a quadcopter with two large wheels	- Rolling mode is five times more efficient than flying
[117]	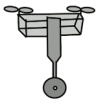	- Development of a half-drone wheeled inverted pendulum	- Did not converge to desired position after 100 s with real drone, but converged in simulation
BogieCopter [118]		- A quadcopter setup with four adjustable wheels - Weight of 4 kg - Dimensions: 695 mm × 693.5 mm × 302 m	- Stable flight and works on 61-degree slopes
[119]	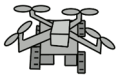	- Additive quadcopter setup with a four-wheel drive drone - Weight of 1.8 kg - Dimensions: 21.4 cm × 11.5 cm × 9.2 cm	- Vehicle faced challenges due to weight
[120]	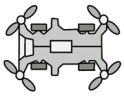	- Quadcopter design with four wheels, inline	- Power consumption of 105 W for a 630 s flight time
[121]	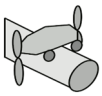	- Wheeled UAV on a pipe with bi-copter setup with side rotors, with a four-wheel drive setup	- Robustness of controller under various conditions with LQR approach in simulation
Amphibious Drones			
Drone [Ref]	**Schematic**	**Design Purpose and Configuration**	**Performance and Findings**
MAR [122]	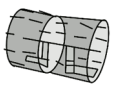	- A new archaeology exploration with an enclosed design with large, spiked wheel enclosure - Weight of 120 kg - Internal volume: 500 dm^3	- Buoyant prototype fabricated and tested in lake with successful swimming and land locomotion
WSP-Bot [123]	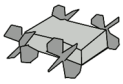	- A wheel-spoked drone with adaptive four-wheel drive structure with flipper wheels - Weight of 1.34 kg - Dimensions: 280 mm × 316 mm × 120 mm	- Maximum linear wheel speed of 0.8 m/s and paddle speed of 26 m/s

Table 4. *Cont.*

Amphibious Drones			
Drone [Ref]	**Schematic**	**Design Purpose and Configuration**	**Performance and Findings**
SeaDog [124]	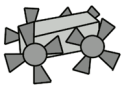	- Whegs-wheeled drone for land and water locomotion - Weight of 25.1 kg - Dimensions: 114.5 cm × 44.5 cm × 38 cm	- Climbing of 48 cm obstacles and basic aquatic paddling demonstrated
[125]	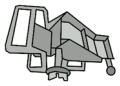	- Wheel paddle trash collecting drone prototype with two-spiked wheels	- Payload of 7 kg with 45 W, in still water and 90 W against the stream
[126]	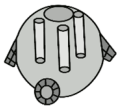	- Spherical drone with three mecanum wheels for omni-motion, with underwater thrusters - 32.5 cm diameter chassis with 20.6 cm internal drone triangular length	- Successful 12-degree incline during wheeled locomotion and underwater operation
[127]	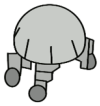	- Spherical robot with four wheels for land motion and thrusters for underwater operation - Maximum weight of 403 g - Maximum diameter of 40 cm	- Maximum velocity of 36.7 cm/s at 100% duty cycle
Wall-Climbing Robots			
Drone [Ref]	**Schematic**	**Design Purpose and Configuration**	**Performance and Findings**
[128]	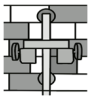	- Two-wheel drive drone with two Bernoulli pads for wall adhesion - Weight of 234 g - Dimensions: 224 mm × 156 mm	- Drone shows effective adhesion on glass with overall 12 N adhesive force
[129]		- Four-wheel drive drone with a ducted fan with a bottom restrictor - Weight of 1 kg - 0.6 kg payload	- Suction force greater with restrictor than other options with a −3.4 kPa suction pressure
Wall-C [130]	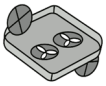	- Design and control of a wall-cleaning drone with two wheels with two ducted fans - Dimensions: 235 × 230 × 70 mm	- Maintained pressure difference within safe limits on curved and gapped surfaces
UOTWCR [131]	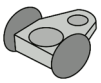	- A magnetic wheeled drone with two wheels with magnets - Weight of 520 g	- Operated with a climbing speed of 0.1 m/s
[132]		- Shape adaptive magnetic wheeled drone with two magnetic spherical wheels	- Successful flat, convex, and 90-degree climbing
Aerial Aquatic Drones			
Drone [Ref]	**Schematic**	**Design Purpose and Configuration**	**Performance and Findings**
Hydrone [133,134]	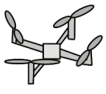	- Development of a mathematical model for an aquatic drone	- Distance of 51.5 m reached during underwater navigation with 3.883 kJ of energy consumed
MEDUSA [135]	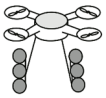	- Underwater sample acquisition drone of quadcopter design with buoyant balls	- Lake tests with horizontal turn speeds of 100 deg/s and forward speed of 0.35 m/s

Table 4. *Cont.*

Drone [Ref]	Schematic	Design Purpose and Configuration	Performance and Findings
Aerial Aquatic Drones			
TJ-FlyingFish [136]	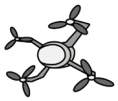	- Quadcopter drone with tiltable rotors for air and underwater - Weight of 1.63 kg - Dimensions: 380 mm wheelbase	- Dual-speed gearbox enhances aquatic propulsion
Naviator2 [137]	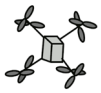	- Design of aerial aquatic Quadcopter UAV - Weight of 2 kg	- Transitions between air and water under 2 s
[138]	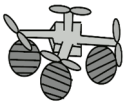	- Design of origami floating devices for UAV water landing with origami balls - Weight of 1.5 kg - Wheelbase: 550 mm	- Hovering accuracy of 2.5 m horizontally and 0.8 m vertically
Aerial Climbing Drones			
Drone [Ref]	**Schematic**	**Design Purpose and Configuration**	**Performance and Findings**
[139]		- Semi-autonomous quadcopter UAV applying normal force to wall using supports - Weight of 20 kg	- UAV maintained stable flight with 5 N to vertical wall
MMAR [140]	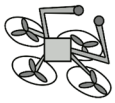	- Design of quadcopter drone with passive wheels with robust motion planning	- UAV can stabilise to altitude with/without disturbances
CAROS [141,142]	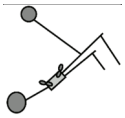	- Development of wall-climbing drone with rotary arms and passive wheels	- Link mechanism controlled the angle to follow target with maximum climbing speed of 0.8 m/s
CAROS-Q [143]	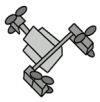	- Reconfigurable tri-copter that can extend to move central body accordingly - Weight of 1.9 kg	- Maintained position while pitching from 0 to 90 degrees
[144]		- Design of a quadcopter UAV with adhesive pads for surface perching - Weight of 32 g - Dimensions: Approximately 5 cm × 5 cm	- In comparison to flight, perching leads to energy savings of 40% for ceiling perching and 80% for wall perching
[145]	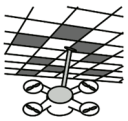	- Design of quadcopter drone with adhesive on an extended rod based on impedance control - Weight of 0.65 kg - Dimensions: 45 cm × 45 cm	- Effectiveness of adhesion mechanism demonstrated with 10 N force
Aerial Wall-Climbing Robot			
Drone [Ref]	**Schematic**	**Design Purpose and Configuration**	**Performance and Findings**
Vertigo [146–148]	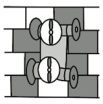	- Design of a Four-wheel drive drone with two propellers for flight and wall adhesion - Weight of 2.35 kg - Dimensions: 600 mm × 200 mm × 200 mm	- Wall-climbing speed of 0.25 m/s
FCSTAR [149]		- Foldable quadcopter design with wheels attached and reverse thrust - Weight of 1.3 kg - Dimensions: 24 cm × 34 cm	- Lift force three times larger than drone weight with ground speeds up to 3.2 m/s

Table 4. *Cont.*

Aerial Wall-Climbing Robot			
Drone [Ref]	**Schematic**	**Design Purpose and Configuration**	**Performance and Findings**
LAWCDR [150]	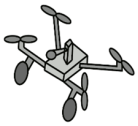	- Land-air wall crossing drone inspired by gecko landing with quadcopter setup and four wheels - Weight of 3 kg	- Drone successfully operates in land, air, and wall areas
[151]	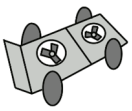	- Design of cost-effective efficient wall-climbing drone with four wheels and two propellers - Weight of 650 g - Dimensions:460 mm × 460 mm × 200 mm	- Vertical climbing at speeds of 15 inches/s
Triphibian Drones			
Drone [Ref]	**Schematic**	**Design Purpose and Configuration**	**Performance and Findings**
[152]		- Multimodal drone design concept for multi-environment locomotion with quadcopter and wheg wheels	- Multimodal drone categories discussed - Design concept for triphibian drone proposed
OmnibotV2 [153]		- A Quadcopter UAV drone with a screw-drive system	- Improved flight performance with aerial speed of 4.05 m/s and 372 W power consumption
[154]	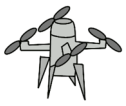	- A tri-habitat drone of a quadcopter setup with spherical design and landing legs - Weight of 0.45 kg	- At 1873 revs/min for the propellers, the drone can be suspended hovering in the air
[155]		- A mechatronic triphibian drone with tri-copter setup with underwater impellers and mecanum wheels - Dry weight of 7.5 kg - Dimensions: 1148 mm × 1108 mm × 75 mm	- Ground speed of 0.3 m/s at 20-degree slope
[156]	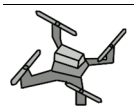	- Design concept for triphibian drone with quadcopter setup with reconfigurable propeller wheels	- Structural simulation of the drone frame provided a stress value of 34.3 MPa
TR-TRS [157]	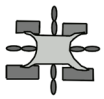	- Design of triphibian drone with tilting rotors, buoyant body, and four wheels - Weight of 4 kg - Dimensions: 550 mm × 500 mm	- Velocity control during transitions shown - Drone needs to flip 90 degrees to manoeuvre underwater
MUWA [158]		- Design of a ring-shaped triphibian quadcopter where ring acts as wheel and buoyant ring - Weight of 2.1 kg - Diameter of 910 mm - Thickness of 120 mm	- Successful flying and mono-wheel modes with 8.5 m/s^2 tornado mode angular acceleration
[159]		- Design of a triphibian drone for motion in spherical mode with wheels and foldable propellers	- Design concept for triphibian transport vehicle proposed with adaptive morphology
[160]		- A novel all-terrain cyclocopter with four wheels that can also drive on water surface - Weight of 1010 g - Dimensions: 0.51 m × 0.43 m × 0.30 m	- Can sustain hover at 232 W - Aquatic translation at 1.3 m/s at 19 W - Terrestrial translation at 2 m/s at 28 W

Tri-modal designs mainly include two configurations: triphibian drones and AWCR drones. Triphibian designs usually combine wheels, propellers and aquatic propellers in an additive fashion to allow for motion in all operational mediums with simplified control. These designs suffer from not being optimised for close-range climbing, which is critical to the inspection procedure of wind turbines. As such, AWCR drones show promise by building upon climbing drones with the addition of terrestrial motion, allowing for flexible long- and close-range operations. However, payload capacity, energy efficiency and adaptive control algorithms are common challenges for this class of vehicle.

4.3. Bio-Inspired Designs

Bio-inspired multi-modal drones (as exemplified in Figure 13) show promise in traversing different environments more efficiently and flexibly [161]. These mechanisms can be extraordinarily complex and more energy-demanding. As such, the drone needs to be effectively designed to ensure that the trade-off between flexibility and complexity is functional for a given environment.

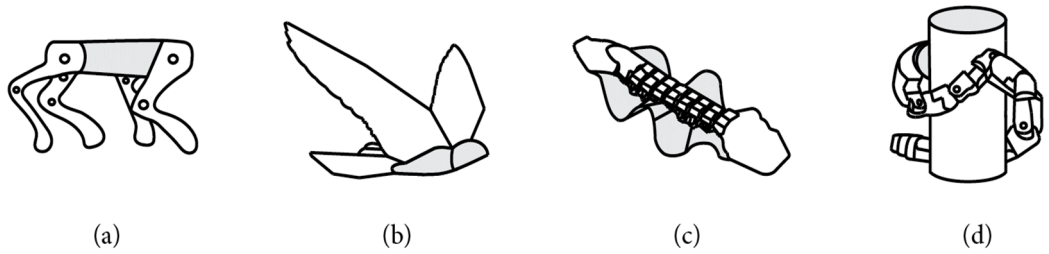

Figure 13. Bio-inspired robotic design exemplifications: (**a**) terrestrial, (**b**) aerial, (**c**) aquatic and (**d**) climbing.

From Table 5, and as previously illustrated in Figure 10, bio-inspired terrestrial bimodal designs have shown many innovative designs. TA drone designs include gliding drones and winged ornithopters, allowing for flexible flight and controlled landings. In contrast, these mechanisms are overly complex with small payloads and no hovering or climbing abilities, which are critical for our current application. Similarly, amphibious drone designs include flipper designs, as well as other multi-DOF designs (such as fin and fish designs). These designs demonstrate great degrees of flexibility and adaptability as well as adaptable morphologies, which results in fewer mechanisms overall. However, these drones have issues with transitioning, require complex control systems and are very demanding in terms of computation and energy. Furthermore, WCR designs involve various adhesion mechanisms inspired by animals such as snails, geckos and caterpillars. These designs usually involve legged or multi-DOF mechanisms for locomotion along the structures. These provide more adaptable methods to climbing as well as flexible methods to traverse different obstacles along the structure. That said, the limited payload of these designs and the lack of aerial or aquatic modes of operation make direct deployment to wind turbine inspection applications challenging. Common AA drone designs include winged propulsion systems operating in water and air with propellers and wings, transitioning through the water barrier using some sort of jet propulsion. These design concepts demonstrate high manoeuvrability with adaptable locomotion and efficient forward flight. Even so, these designs often do not support hovering flight functionality and we believe require more research to be effectively used in practice within both aerial and aquatic terrains. On the other hand, AC drones have effective designs, such as fixed-wing drones with microspines for wall perching. These allow the drone to momentarily land on structures in the air with high manoeuvrability. Despite that, these designs do not provide the required payload and hovering functionality for wind turbine inspection applications.

Table 5. Examples of bio-inspired multimodal drones.

Terrestrial Aerial Drones			
Drone [Ref]	**Schematic**	**Design Purpose and Configuration**	**Performance and Findings**
[162]		- Study on self-righting mechanisms in geckos, squirrels, insects, and shuttlecocks for drone designs	- Mid-air orientation can be achieved in as little as 20 ms
[163,164]	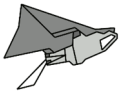	- Pteromyini-inspired gliding drone design - Weight of 0.42 kg - Dimensions: 0.34 m × 0.041 m × 0.021 m	- Stable gliding with a glide ratio of 2.14 achieved in simulations
MALV [165]	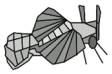	- Design for autonomous missions with wings and wheg legs on a miniature scale - Weight of 100 g - 30 cm wingspan	- Capable of flying several kilometres on single use
[166]		- Entomopter design with adaptive wings that can be used for flying and walking - Weight of 50 g	- Enhanced lift and manoeuvrability reported
BOLT [167]		- Design of lightweight bipedal ornithopter - Weight of 11.4 g - Wingspan of 28 cm and a length of 17.5 cm	- Maximum velocity of 0.5 m/s with maintained stability
DASH+ [168]		- Design of lightweight hexapedal ornithopter - Weight of 0.54 g per wing - Wing is 0.124 m long with an average chord of 0.064 m	- Maximum running speed of 0.68 m/s and flapping of 1.29 m/s
Amphibious Drones			
Drone [Ref]	**Schematic**	**Design Purpose and Configuration**	**Performance and Findings**
[169–171]		- Design of a quadruped utilising Klann linkages with duck-inspired feet - Weight of 1890 g - Volume: 1575 cm^3	- Velocity of the feet computed as 0.03125 m/s
ART [172]		- Design of a turtle-inspired quadruped with soft morphing limbs for swimming and walking - Weight of 9 kg - Dimensions: 0.32 m × 0.96 m × 0.358 m	- limb took around 100 s to morph in water and 50 s to morph in air at 22 °C
AQUA [173,174]	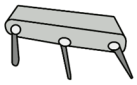	- Amphibious hexapod design with six flipper legs that can be used for swimming and walking	- Successful testing up to 40 feet underwater
HAMR [175]		- Design of micro quadruped with pads for water surface walking using electrowetting - Weight of 1.6 g	- Water movement 18% more energy consuming than land - 2.9 g maximum payload
[176]	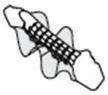	- Aba knifefish-inspired drone design with multiple degrees of freedom	- Maximum restoring moment of 4 Nm at 30-degree heel angle
AmphiBot I [177]	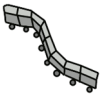	- Design of an amphibious snake drone with multiple degrees of freedom with wheels - Segment dimensions of 7 cm × 5.5 cm × 3.3 cm	- Max motor angular frequency of 0.75 Hz, at which maximum amplitude of 45 degrees cannot be reached

Table 5. *Cont.*

Amphibious Drones			
Drone [Ref]	**Schematic**	**Design Purpose and Configuration**	**Performance and Findings**
AmphiRobot [178,179]		- Design of an amphibious snake drone with multiple degrees of freedom with whegs wheels - Weight of 3.81 kg - Dimensions: 700 mm × 320 mm × 150 mm	- Successful steering and underwater swimming
Wall-Climbing Robots			
Drone [Ref]	**Schematic**	**Design Purpose and Configuration**	**Performance and Findings**
[180]	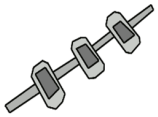	- Snail-inspired drone with three actuated sections connected by a single bar moving one by one	- Cosine line actuation allows for effective motion with peak linear speed of 7.67 mm/s
[181]	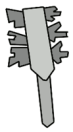	- Cockroach- and gecko-inspired legged drone design with microstructure adhesives	- Climbing velocities are on average at 0.2 m/s
[182]	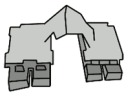	- Serica orientalis-inspired bipedal drone design with spiny feet - Weight of 78 g - Dimensions: 150 mm × 60 mm × 40 mm	- Maximum adhesive forces bearing 300 g loads
[183]		- Caterpillar-inspired climbing drone design with multiple degrees of freedom - Weight of 19.2 g - Joint module dimensions of 35 mm × 37 mm × 30 mm	- Maximum step length of 5 mm in 1.8 s while climbing on glass with vacuum adhesion
GLEWBOT [184]	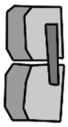	- Woodpecker-, Leech-, and Gecko-inspired bipedal drone for wall climbing - Weight of 1.4 kg - Dimensions: 420 mm × 105 mm × 115 mm	- Adhesive force of 55 N with 74.6% defect detection
Aerial Aquatic Drones			
Drone [Ref]	**Schematic**	**Design Purpose and Configuration**	**Performance and Findings**
AquaMAV [185,186]	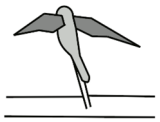	- Design of aquatic bird-inspired drone with fixed wings and jet propulsion for mode transitions - Weight of 0.2 kg - Wingspan: 0.59 m	- Successful jet propulsion water air transition
[187]	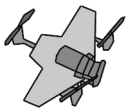	- Aerial aquatic drone inspired by wild ducks with a tri-copter setup on fixed-wing chassis - Weight of 1.55 kg - Dimensions: 56.2 mm × 35 mm	- Diving speed: vertical 0.22 m/s and horizontal 0.7 m/s
[188]	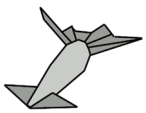	- Flying squid-inspired drone with multiple degree of freedom fins and jet propulsion - Weight of 0.6 kg - Dimensions: 78 cm × 48 cm × 60 cm	- Lift coefficient significantly higher during spread wings than folded
[189]		- Bio-inspired fixed wing based on Mantas and Eagles with landing wheels - Weight of 475 g - Wing dimensions: 38 cm × 30 cm	- Maximum lift-to-drag ratio of 4.045 in aerial asymmetric mode - Maximum lift-to-drag ratio of 3.864 in symmetric aquatic mode

Table 5. *Cont.*

Drone [Ref]	Schematic	Design Purpose and Configuration	Performance and Findings
Aerial Aquatic Drones			
Robomoth [190]		- Drone with flapping wings and can glide on water surface - Weight of 2.487 g - Wingspan: 9 cm, Length: 9 cm	- Maximum gliding speed of 17.1 cm/s at 40 Hz, with a maximum power consumption of 570.9 mW at 50 Hz
[191,192]		- Design of flapping wing aerial aquatic insect-scale drone with the ability to fly and swim - Weight of 175 mg	- Transition take-off speed of 2.5 m/s
Aerial Climbing Drones			
Drone [Ref]	**Schematic**	**Design Purpose and Configuration**	**Performance and Findings**
ICAROS [193]		- Design of a dynamic fixed-wing climbing drone with microstructures for wall perching - Weight of 350 g - Wingspan of 0.72 m and the chord length of 0.18 m	- Climbing achieved at 0.135 m/s - Gliding achieved at 5.3 m/s
S-MAD [194,195]		- Design of microspine fixed-wing drone for wall perching - Weight of 330 g	- Specific resistance of 7, at a vertical speed of 5 m/s
[196]		- Autonomous perching of flapping wing drones with claw gripper for tree perching - Weight of 700 g	- Low forward flight velocity before landing ensures gripping forces remain below 150 N
Aerial Wall-Climbing Robot			
Drone [Ref]	**Schematic**	**Design Purpose and Configuration**	**Performance and Findings**
[197]		- Pterodactyl-inspired climbing, winged, legged drone with flapping wings and claws	- Successful flying, walking, and climbing demonstration
[198]	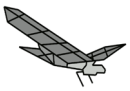	- Design of flapping wing drone that can perch with claws - Weight of 1.5 kg	- Can perch on landing platform with gliding speed up to 5 m/s
[199]		- Design of bat-inspired flapping wing perching drone with soft legs for walking and perching - Weight of 60 g	- Maximum thrust of 94 g and 24 N shear strength
RoSeGu [200]	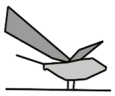	- Seagull-inspired ornithopter perching on wire with claws - Weight of 476 g - Length of 522 mm and wingspan of 786 mm	- Achieved and maintained pitch and yaw angles in testing
Triphibian Drones			
Drone [Ref]	**Schematic**	**Design Purpose and Configuration**	**Performance and Findings**
RoboFly [201]	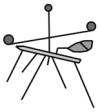	- Small insect drone with flapping wings and three legs that can be used on land and water surface - Leg diameter of 0.5 m and leg length of 50 mm	- Stable hovering at 0.08 m - Unstable water landings - Water surface take-off with lift-to-weight ratio of 3.4

Bio-inspired tri-modal designs allow for flexible and adaptable locomotion in three modes. Common triphibian drones include miniature insect drones and water striders. Due to their small sizes and simplified locomotion, these demonstrate low energy consumption and versatile kinematics. With that said the main issue with these designs is that they typically have small payloads and can only traverse the water surface due to their fragile structures. Consequently, AWCR drones include winged designs with perching capabilities and potential terrestrial adaptability. These allow for flexible movements in both close- and long-range environments with adaptive designs. On the other hand, these designs are currently not suited to wind turbine inspections due to not having the ability to efficiently hover and or hold the required high payload components.

4.4. Hybrid Designs

Hybrid drones (as illustrated in Figure 14) optimise the different actuation techniques from different types of locomotion and apply them to the environment in which they are deployed [202,203]. In particular, hybrid designs combine features from both rotor-based and bio-inspired concepts. This section will discuss current hybrid designs as a means of assessing their suitability for wind turbine inspections.

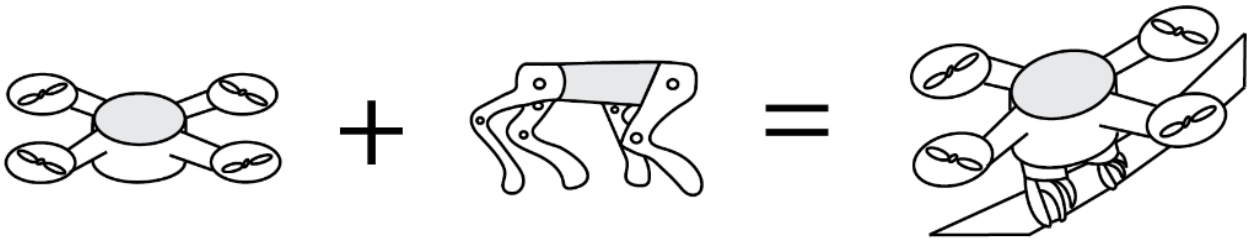

Figure 14. An example of a hybrid drone design.

Table 6 (and as previously illustrated in Figure 10) shows that hybrid terrestrial bimodal designs are increasingly popular due to their versatility and adaptability. Common TA drones include propeller-based drones with legs, resulting in effective hovering flight with flexible and manoeuvrable terrestrial locomotion. Despite that, these designs do not have compatible adhesive mechanisms for close-range operations and have limited stability on non-linear surfaces. Following this, amphibious drones usually involve legged spherical designs, allowing for efficient underwater explorations with manoeuvrable terrestrial locomotion. Regardless, these drones also suffer from having no adhesive capabilities with high energy consumption in all modes. WCR designs commonly involve wheels with microspines for adhesion, allowing for energy-efficient wall climbing and passive climbing capabilities. Nonetheless, these designs are usually slow during climbing operations and lack the payload capacity to be useful for wind turbine inspections. AA drones typically employ underwater propeller drones, with locomotion capabilities inspired by fish. This allows for stable performance in both modes as well as adaptive morphology for better transitions. However, they have no capabilities for close-range operations, and the system requires complex and adaptable control algorithms. Following this, AC drones involve UAVs with perching claws or microspines, resulting in effective perching onto walls from aerial modes. In contrast, these designs are optimised for flat and small surfaces and, as such, need to be tested in non-linear large-scale environments.

Table 6. Examples of hybrid multimodal drones.

Terrestrial Aerial Drones			
Drone [Ref]	**Schematic**	**Design Purpose and Configuration**	**Performance and Findings**
M4 [204]	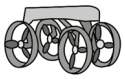	- A drone with adaptive propeller wheels with legged kinematics for flexible locomotion - Weight of 6 kg - Dimensions: 0.7 m × 0.35 m × 0.35 m	- Drone can climb 45-degree slopes with two wheels as well as fly, roll, walk, crouch, balance, tumble, scout, and loco-manipulate successfully
DALER [205]	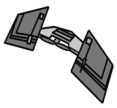	- A fixed-wing drone with adaptive wings that can act as wheels - Weight of 450 g - Wingspan of 60 cm	- Can operate on different terrains and in forward flight
[206]		- A legged Quadcopter setup with two legs	- Maximum payload of 40 N - Aerial battery life of 30 min - Ground battery life of 360 min
Leonardo [207]		- A bi-copter drone with two multiple degrees of freedom legs - Weight of 2.58 kg - Height of 75 cm	- Nominal walking speed of 20 cm/s and flying speed of 1 m/s
Amphibious Drones			
Drone [Ref]	**Schematic**	**Design Purpose and Configuration**	**Performance and Findings**
[208]		- Turtle-inspired spherical drone design with legged wheels for land movements - Diameter of 250 mm	- Maximum walking speed of 62.1 cm/s at a 10-degree incline
ASRobot [209,210]	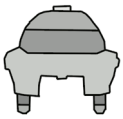	- Development of amphibious spherical drone and legged thrusters for underwater and land - Weight of 6.7 kg - Diameter of 300 mm	- Maximum speed in walking is 6.1 cm/s - Maximum speed underwater is 4.5 cm/s
Wall-Climbing Robots			
Drone [Ref]	**Schematic**	**Design Purpose and Configuration**	**Performance and Findings**
µTugs [211,212]	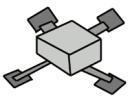	- Design of small drone with legs/wheels with gecko gripper pads attached - Weight of 13 g - Dimensions: 150 mm × 25 m × 20 mm	- Seven 17 g drones can pull 375 N loads
[213]	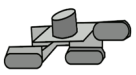	- Gecko-inspired tracked wheel drone with microstructures on the wheels - Weight of 4.92 kg	- Can move faster than legged wall-climbing drones with required shear force of 48.31 N
[214]	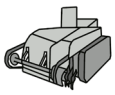	- Clingfish-inspired wall-climbing drone design with tracked wheels with microstructures - Weight of 1.3 kg - Dimensions: 35.5 cm × 24.8 cm × 9.5 cm	- Stable climbing carrying loads up to 1100 g

Table 6. *Cont.*

Aerial Aquatic Drones			
Drone [Ref]	**Schematic**	**Design Purpose and Configuration**	**Performance and Findings**
[215]		- Quadcopter drone with the ability to operate underwater and hitchhike using remora disc - Weight of 950 g - Dimensions: 40 cm × 40 cm × 14 cm	- Self-folding propellers have better transitions with less transition time for same thrust
Acutus [216]	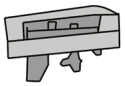	- Design of aerial underwater submarine-shaped drone actuated using rotor and fins	- Stable performance in air and water modes with maximum thrust of 50 N
SailMAV [217]	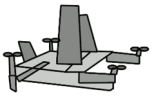	- Aerial aquatic drone design with adaptive foldable wings for sailing and quadcopter setup for flying - Weight of 520 g	- Stable flight at 10.8 m/s - Swimming in water tank at 6 m/s demonstrated
Aerial Climbing Drones			
Drone [Ref]	**Schematic**	**Design Purpose and Configuration**	**Performance and Findings**
[218]	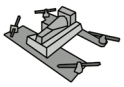	- Adaptive design for a perching UAV with foldable perching structure - Weight of 650 g - Wheelbase: 280 mm × 350 mm	- Bi-stable arm is rigid in flight but will conform to its target in 0.97 s when perching
HEDGEHOG [219]	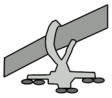	- Design of passive perching mechanism for drones using quadcopter with soft claws - Weight of 402 g - Diameter of 200 mm; height of 185 mm	- Stable perching on branches of 86 mm diameter
SCAMP [220]	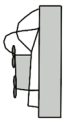	- Design of climbing-flying quadcopter drone with microspine array for climbing - Weight of 38 g	- Average angular acceleration during climbing was 4.4 times smaller than without (63 rad/s^2) - Successfully climbed various vertical surfaces
Aerial Wall-Climbing Robot			
Drone [Ref]	**Schematic**	**Design Purpose and Configuration**	**Performance and Findings**
SNAG [221]	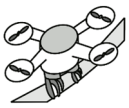	- Bird-perching quadcopter drone with claws	- Reliable perching on different branches in less than 50 ms
[222]	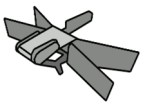	- Robotic insect that can land and climb off vertical surfaces using flapping wings and wheels	- Flying to climbing in 0.4 s and vice versa in 0.7 s
[223]	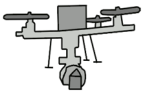	- Avian-inspired claw mechanism for UAVs of quadcopter setup with soft claws - Weight of 700 g	- Claws held the UAV at tilt angle of 19.4 degrees before slipping

Table 6. *Cont.*

Triphibian Drones			
Drone [Ref]	**Schematic**	**Design Purpose and Configuration**	**Performance and Findings**
[224]		- Swan-inspired triphibian drone design with quadcopter aerofoil chassis and paddle wheels	- Lift-to-drag ratio of 30–35 with 3–5 degrees angle of attack and operation in all three modes
AmphiSTAR [225]		- Basilisk lizard-inspired triphibian with foldable quadcopter with thrusters for all modes - Weight of 246 g - Dimensions: 245 mm × 260 mm	- Crawling speed is 3.6 m/s and aerial gliding speed is 1.5 m/s
3DTR [226]	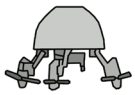	- Design of propeller clutch unit for triphibian with spherical design with legged thrusters	- Rotational speed of clutch system increases linearly with voltage increase with a rate of 831 rev/V

Hybrid tri-modal designs provide the ability to expand the operating conditions even further. Triphibian drones come in many forms, such as legged spherical designs, for effective operations in all environmental mediums. These designs provide improved flexibility and adaptability in comparison to other solutions. Be that as it may, these designs also do not have mechanisms for close-range operations. Consequently, common AWCR drones involve UAV designs with legs or wheels with adhesive mechanisms. This allows for simplified control by using UAV control for flight with more flexible perching and terrestrial locomotion using legs and claws. On the other hand, mechanical perching mechanisms can harm wind turbine structures and are not suitable for different scales of operation.

5. Locomotion Mechanisms and Selection Optimisation

5.1. Overview

One big factor that contributes to the design process is to choose the correct actuation methods for the locomotion required, hence ensuring that the drone can effectively operate in the required environments. In this section, various actuation methods are evaluated and discussed in the context of their suitability for wind turbine inspections. As these drones are expected to operate both onshore and offshore, we considered climbing locomotion for close-range inspections, aerial locomotion for long-range inspections, terrestrial locomotion for transportation and land operations and aquatic locomotion for underwater inspections.

5.2. Climbing Locomotion

Climbing locomotion is essential for wind turbine inspection drones in situations that require proximity for close-range sensors to operate effectively. However, without a method of stabilising and attaching the drone to the surface, the drone would either slip off the surface or consume a large amount of energy to sustain its position on top of the blade. There are many diverse types of actuators that can be used to allow the drone to stick onto the surface (illustrated in Figure 15), such that the drone can operate in unconventional modes, including vertical or upside-down motions (as demonstrated in Figure 7a).

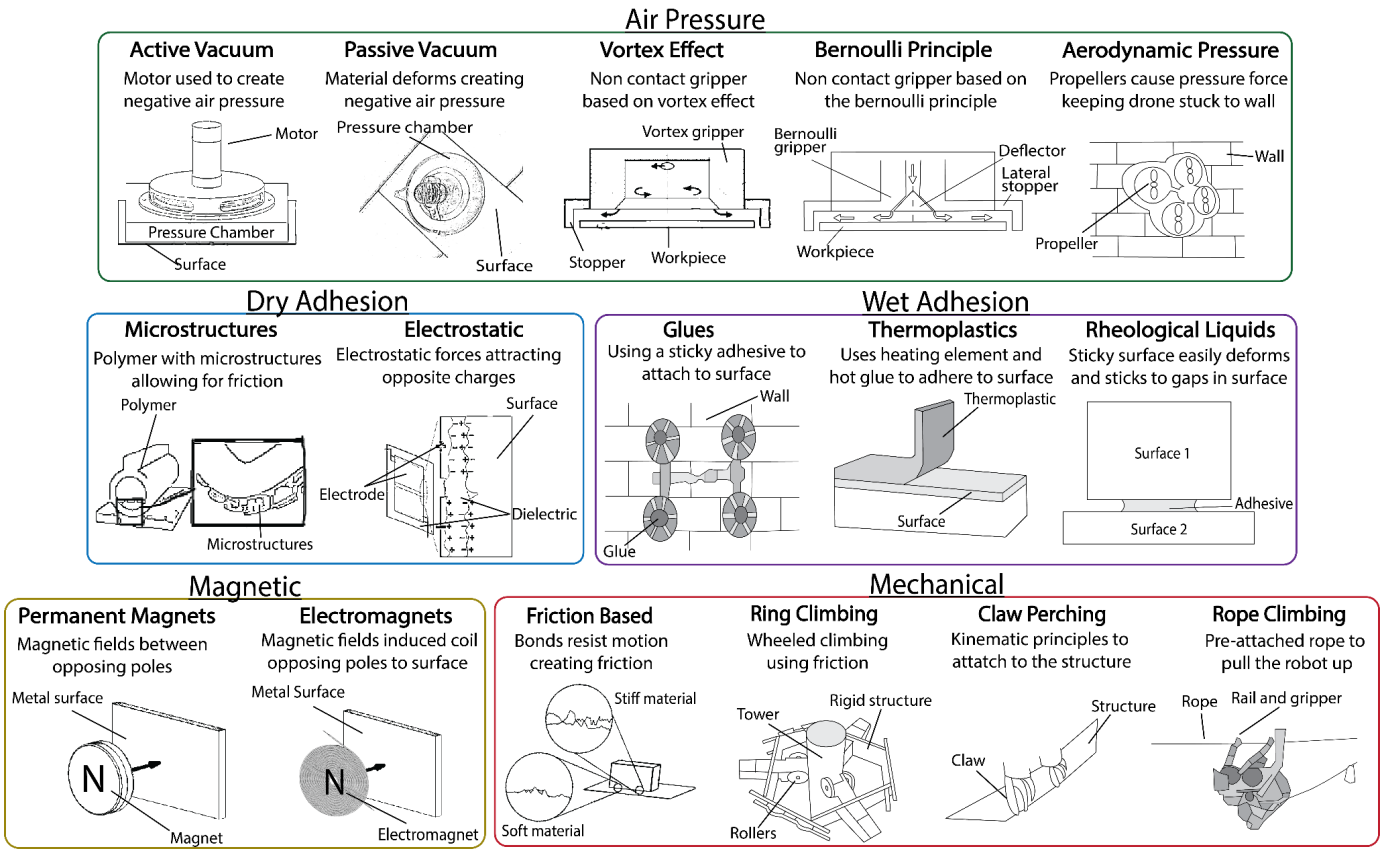

Figure 15. Different methods of attachment adopted within climbing drones.

There have been many studies outlining the effectiveness of different modes of adhesion and perching for drones. In their thorough examination of gripping devices for industrial robots (IRs), Mykhailyshyn et al. [227] emphasised the significance of gripper design optimisation for a range of tasks and environments, emphasising efficiency and adaptability. One example method for this is flexible vacuum-combined pneumatic gripping devices (CPGDs), which enable access to geometrically constrained areas with conventional wheeled or tracked systems whilst using pneumatic adhesion methods. Another adhesive method is that of the contactless Bernoulli Gripping Device (BGD) for manipulating objects with displaced centres of mass [228,229]. Tomar et al. [230] clarified the power–shear relationship essential for Bernoulli pad equilibrium. In fact, the use of Bernoulli pads presents a viable approach as an adhesive pad for wall-climbing drones since they can produce enough shear forces for efficient adhesion and cleaning while simultaneously reducing the total weight of the robotic system.

Other types of adhesive systems include the use of gas-lubricated vibration-based adhesion in order to achieve high specific normal adhesive stress, maintaining adhesion on a range of surfaces including flat, curved and inverted orientations [231]. Venturi-vortex grippers [232], on the other hand, demonstrate high grip performance, compactness and versatility, offering stable and non-contact gripping. Finally, aerodynamic pressure methods using drone propellers provide a good solution for pneumatic gripping. In spite of that, these are not generally flexible and usually not suitable due to the need to transition from aerial to vertical climbing modes, unless coupled with other modes of locomotion, such as within multimodal drones [233].

In addition to pneumatic grippers, there are a multitude of other adhesive modes [234], including magnets and electromagnets, which have very good performances on metallic surfaces. Following this, rheological liquids may provide a means to be simultaneously

used with magnets to further allow sticking onto non-magnetic surfaces, yet on smooth surfaces, the performance can deteriorate and generally works best with legged drones [235]. Scarselli et al. [236] also showed that thermoplastics have very good performance, but if the surface is dirty, the performance degrades, and if adhesion becomes too strong, then it may damage the surface.

Methods that employ friction, such as rubber wheels, claws, wires and clamps, are also promising approaches to this problem as they provide high flexibility and high adhesive capabilities [37,237–239]. However, these methods are not sustainable long-term due to the expected wearing of the material. Also, the friction contact has the potential to damage the surface due to the high contact with the surface; as such, this approach may not be very suitable for wind turbine inspections. Additionally, the demonstration of the idea of tentacle grippers opens up an interesting possibility for robotic designs in wind turbine inspections due to their adaptable and multidirectional gripping abilities [240]. Notably, there is the bio-inspired solution proposed by Wang et al. [241], building on the adhesive abilities and locomotion of Beaufortia kweichowensis, which uses paired girdle muscles and two anisotropic suckers to enable it to crawl on vertical surfaces, both forwards and backwards, while still adhering to the substrate.

Electrostatic adhesion is another method that relies on the principles of static electricity with high voltage [242–244]. This can effectively attach to a surface as long as it can gather static charge for a very high range of surfaces [245]. That said, this requires a high source of voltage. Finally, the use of microstructures provides an almost passive method for adhesion that provides a strong bond [211,246,247]. These provide particularly good insight into future adhesion technologies; nonetheless, they may not be the most suitable due to their design complexity. Overall, these designs are inspired by nature and, as such, demonstrate remarkably high flexibility.

All the previously discussed methods of realising climbing locomotion are assessed and contrasted in Table 7, highlighting the benefits and drawbacks of each approach within the context of their suitability for the wind turbine inspection missions. In this table, all concepts are ranked from very high (5) to very low (1), where average (3) is the median rank, dependent on the level of the given category. Surface is only ranked as flexible or limited due to limited ranking criteria.

Table 7. Assessment of the different climbing locomotion methods in the context of their suitability for wind turbine inspection missions.

Type	Strength	Manoeuvrability	Surface	Repeatability	Energy/Cost
Friction	High	Very High	Flexible	Average	High
Ring	High	Average	Limited	High	High
Claw	High	Low	Limited	High	Average
Rope	High	Average	Limited	High	High
Permanent Magnets	Very High	Low	Limited	Very High	Very Low
Electromagnets	Average	High	Limited	Very High	Very High
Rheological Liquids	Average	Average	Flexible	High	Very High
Glues	Average	Very Low	Flexible	Very Low	Very Low
Thermoplastics	Very High	Average	Flexible	Very Low	Low
Active Vacuum	High	Very High	Flexible	High	Very High
Passive Vacuum	Very Low	High	Flexible	High	Very Low
Vortex Effect	High	Very High	Flexible	High	Very High
Bernoulli Principle	High	Very High	Flexible	High	Very High
Aerodynamic Pressure	High	Low	Flexible	High	Very High
Microstructures	High	High	Flexible	High	Average
Electrostatic	High	High	Flexible	High	High

Following the previous assessment, methods such as friction, active/passive vacuum, vortex, Bernoulli, electrostatics and microstructures provide particularly good performance due to their high adhesive strength, surface flexibility and repeatability. However, due to the need for strong adhesion with high payloads, while minimising the damage to the wind turbine surface, Bernoulli grippers and microstructures can be considered the optimal candidates for the application in hand, depending on the scale and application of the deployed drone.

5.3. Aerial Locomotion

Aerial locomotion is essential for long-range inspections, particularly when inspecting the blades and upper sections of the tower. That said, it can be beneficial for some close-range inspection scenarios such as acoustic sensing, which can be conducted with a UAV when configured correctly [248]. Overall, there are three main types of aerial locomotion (as seen in Figure 7b), including fixed-wing, rotary wing and flapping wing configurations. Each of these configurations provides various benefits and drawbacks for wind turbine inspections, which will be further touched upon in this section.

Fixed-wing drones provide an efficient method of forward flight for long distances and high speeds due to their relatively low energy consumption They originally targeted missions that involve surveillance, e.g., [249,250]; however, these missions are actually not far, in terms of mission requirements, from long-range inspection missions. Fixed-wing drones can come in many different configurations [251], and as highlighted by Yayli et al. [252], Masood and Wei [253] and Qiao et al. [254], their operations include different factors required to optimise aircraft designs while also considering the different possible configurations of the system and the different mission profiles. While they provide an efficient method for high-speed forward flight suitable for long-range inspections, most wind turbine close-range inspections typically require low speeds with mostly hovering flight, making them unsuitable for such inspection scenarios.

On the other hand, rotary wing drones provide a viable alternative for low-speed and hovering flight. These can come in many different forms, such as helicopter and multirotor configurations (such as quadcopters). That said, helicopter configurations are considered more complex and expensive to realise at small form factors, even though they are more stable and efficient [255]. On the other hand, the stability and responsiveness of multirotor drones can be enhanced by applying various different control methods, such as Proportional–Integral–Derivative (PID) and sliding mode control (SMC) [256–259]. These drones are by far the most popular configuration, and by optimising various factors such as the materials used and the propeller configurations, their performance can be further improved. As such, these are very commonly used for the different wind turbine inspection scenarios and can be considered the current state of the art [260,261].

Finally, flapping wing drones provide an innovative method for increased agility and flexibility in difficult environments [262]. That said, their development has been limited up to now, both because the biomechanics of flapping flight itself is complex and because there has been limited industrial interest in both the simulation and construction of such drones. That said, in recent years, we have witnessed significant efforts to enhance our aerodynamic understanding of flapping flight, and the reader is referred to [263–267] for more focused discussions. Moreover, several research attempts have had notable success in demonstrating successful bird-like [262,268] and insect-like [269,270] prototypes that show good promise for future implementations. In fact, by optimising various factors, such as optimising the flapping profiles and wing geometries, flapping wing flights can be further improved for more efficient locomotion [271–276]. This improved efficiency is crucial to enable feasible and cost-effective wind turbine inspections, hence further developments

in this direction are needed to ensure flapping wing designs are real contenders for wind turbine inspection deployment.

Overall, rotary wing configurations are currently deemed the most suitable for wind turbine inspection applications. While the energy consumption is lower during forward flight in fixed-wing configurations, hovering flight is a completely different matter, and this mode is deemed necessary for successful inspection capability. On the other hand, flapping wing configurations can still be considered to be in the initial developmental stage and currently need further work to improve their effectiveness and efficiency to be able to compete with the currently more well-developed rotary platforms.

5.4. Terrestrial Locomotion

Terrestrial locomotion is useful and critical to the inspection of wind turbines when considering transportation to and from the control station and between turbines. The drone may also need to perch on the wind turbines, which is useful for close-range inspections of both the blades and the tower in a more thorough manner. In general, there are many diverse types of terrestrial drones, and these can be generally classified into the distinct categories illustrated in Figure 7c, detailing the mechanisms employed by each type of locomotion.

Wheeled locomotion is the simplest method of terrestrial locomotion from both design and control angles. Over the years, there have been many innovative drone designs involving wheels, such as the vibration-driven drone [277] and wheel-legged drones [278–280]. These designs demonstrate the low kinematic complexity of wheeled locomotion while employing innovative mechanisms for more versatile motion. Another variant of wheeled locomotion is that of tracked locomotion, which wraps a set of wheels in a tracked belt for better performance in rough environments [281–283] (with the different tracked configurations demonstrated in [284]). Other tracked solutions, including the designs by Ben-Tzvi and Saab [285] and Nagatani et al. [286], illustrate how tracked solutions can be used in innovative multimodal terrestrial solutions, such as hybrid tracked legged locomotion to traverse complex environments and hybrid wheel-tracked systems for multi-directional adaptability.

Other solutions involve using bioinspired mechanisms. One popular mechanism used is that of legged locomotion, which demonstrates higher manoeuvrability and flexibility in rough and unknown terrains [287]. Legged drone designs [288–290] illustrate the importance of the control system employed to traverse complex terrains due to the complexity of the system. Other studies demonstrate the learning ability of legged drones and how different algorithms can be used to improve the system [291,292]. Bioinspired solutions also include multi-DOF locomotion, which demonstrates even higher manoeuvrability for complex environments. Example designs include soft drones such as those developed by Park and Cha [293], Chen et al. [294], and Shah et al. [295], demonstrating adaptable motion using caterpillar motion at a small scale. Other examples include earthworm and snake-like locomotion [296–298]. These demonstrate unparalleled flexibility; however, they require more research to be used in practice.

Overall, it can be inferred that wheeled locomotion would be the most suitable for the application at hand. While the other solutions are either more robust or more flexible, which are important considerations for the current application, the complexity, energy consumption and potential effect on the blade surface make them a less desirable choice for long and cost-effective deployments.

5.5. Aquatic Locomotion

Aquatic locomotion is essential to the complete inspection of offshore wind turbines as a good portion of the tower and the system is typically buried underwater. Robotic navigation in such environments is difficult due to the need to navigate a denser fluid than air and the need to be sufficiently waterproofed and robust. Many diverse types of aquatic locomotion can be used, and these can be split into three categories, as illustrated in Figure 7d. These all have their respective advantages and disadvantages, and in this section, these will be highlighted and addressed in terms of wind turbine inspections.

Rotor-based locomotion is the simplest approach to underwater locomotion. This uses rotors to propel the drone underwater and can be classified into multiple sub-categories [299]. Example ROV designs can be found in the studies conducted by Ray et al. [300], Aguirre-Castro et al. [301], and Zulkarnain et al. [302], which were designed to be remotely controlled from a distance. This is in contrast to AUV designs [303], which are designed to operate autonomously without operator intervention. Other novel strategies include the Variable Buoyancy System (VBS) [304], which provides a lightweight and compact buoyancy control system that allows vehicles to function well in both air and water without sacrificing performance.

Bio-inspired locomotion can provide more flexible and adaptable locomotion that can be used in different applications. A popular inspiration in this direction is that of aquatic legs, such as those used by ducks, frogs and mudskippers, allowing for amphibious locomotion [305–308], as well as other designs using turtle flipper configurations for more versatile kinematics [309–311]. While these designs provide increased manoeuvrability, there are other designs that do not require legs, providing even more flexibility in different environments by imitating fish in nature [312–316].

Overall, based on the above discussions, it seems that rotor locomotion is currently the most suitable for the application at hand, as while the other solutions may be more flexible, which is important, their complexity and energy consumption make them less suitable for long and cost-effective deployments.

6. Control and Navigation Considerations

6.1. Overview

In this section, different control/navigation aspects involved in multimodal drones will be briefly highlighted. Our discussions will focus on three main aspects: control platforms, control strategies and navigation and autonomy.

6.2. Control Platforms

To control the locomotion of multimodal drones, an appropriate control platform is needed that is powerful enough while optimising costs and the simplicity of the system. There are several options for such a platform; however, the most common types include:

- Off-the-shelf solutions (e.g., Pixhawk PX4).
- Microcontroller (e.g., Arduino Nano/Uno/Mega).
- Microprocessor (e.g., Raspberry Pi 5).
- Remote computation with (e.g., Host PC with Robot Operating System).

All these options have been used previously on different drones within different applications, with each of these solutions having different trade-offs.

Off-the-shelf solutions are the simplest methods to control a drone. This is due to the little software programming required and the limited hardware ports available [317,318]. These platforms typically abstract the control of the system, which is ideal for users who want a quick solution that just works. However, the main issue with such systems is the lack of versatility, i.e., if the controller is not fit for purpose, then this system cannot be

used standalone. This type of system has been used within a multitude of drones for different modes of locomotion, including aerial, terrestrial and aquatic modes individually, e.g. [319–324].

Microcontrollers, on the other hand, are far more versatile and allow for much more low-level programming [325–328]. These platforms are usually reasonably cheap, which makes them a popular choice. However, these platforms are usually not very powerful and cannot handle very complex computations. As such, microcontrollers are usually used for small-scale systems, making them a less useful option as a standalone solution. There are more powerful microcontroller solutions; however, for these, the price increases significantly. There have been many drone designs that have been presented using microcontrollers, including many simple terrestrial, aerial and aquatic drones, e.g. [329–335].

Microprocessors provide another method for controlling drones using an operating system while still allowing for hardware interactions [336,337]. This method has more power and memory than microcontrollers while still allowing for significant low-level hardware interactions. Microprocessors also allow for on-board communication, such as WiFi and Bluetooth, which are needed for data communication. As such, they provide a reasonable compromise between a low-power microcontroller and an expensive processor. As such, for systems that are not too computationally demanding but require reasonable performance, this solution provides a good compromise. It is therefore not surprising to see a multitude of designs currently relying on this controller platform, e.g. [301,338–343].

Finally, remote computation with a Robot Operating System (ROS) provides a powerful control solution [344,345]. By running all the computationally demanding algorithms on a separate powerful machine, the actual robot can have a low power board in return, which thereby lowers energy consumption. However, this requires a very strong and robust communication link between the drone and the host computer, leading to an easy point of failure for the system. As such, in some cases, a custom processor board is made to provide the required processing power while minimising the complexity as much as possible. However, this requires much more time beforehand to set up the system. These solutions are also used extensively with a multitude of drones of different types, e.g. [346–352].

Based on the above and depending on the application, different systems can be used. As multimodal drones are reasonably complex systems that typically require a more complex level of control, microcontrollers may not be ideal in such cases. Also, as inspection tasks need to be as robust as possible, remote computation may not be ideal. However, more complex sensor computations can be analysed on a remote computer to reduce the power usage of the multimodal drone. As such, the remaining options are off-the-shelf solutions and microprocessors. Both provide sensible solutions; however, for custom drones that need proprietary controllers, microprocessors (such as the Raspberry Pi 5) provide a viable solution due to their versatility and reasonable computation power.

6.3. Controller Strategies

Another important aspect is the control strategy itself for each of the previously discussed locomotion methods to ensure stable and effective operation. There are many different algorithms to deploy such a strategy, as summarised in Table 8. These can be classified as basic-level control algorithms and more advanced methods. There are many designs in which basic control algorithms are all that are needed to control the system. However, for more complex multimodal systems that have many mechanisms and complex chassis designs, more advanced systems would seem to be more appropriate. For more information on advanced control systems, the reader is referred to [353].

Table 8. Comparison of different control strategies.

Controller	Block Diagram	Advantages	Disadvantages
	Basic		
Open Loop	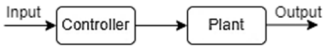	Low complexity and remarkably simple	Sensitive to disturbances
Bang-Bang	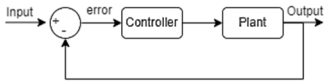	Simple to implement with fast response time	Not suitable for fine control
PID	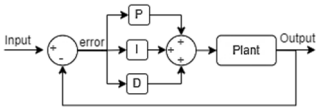	Stable and accurate with a wide range of uses	Parameter tuning is more complex
	Advanced		
Adaptive	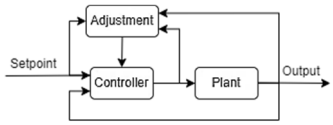	Real time parameter adjustments	More complex and requires detailed data
Multivariable	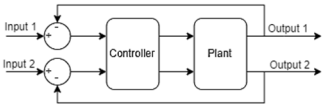	Can control systems with multiple inputs and outputs	Complex to design and computationally intensive
Fuzzy	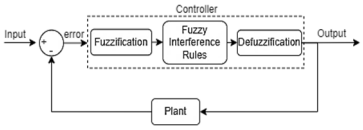	Non-linear and complex systems, and robust to noise	Tuning subjective and time consuming
Model Predictive	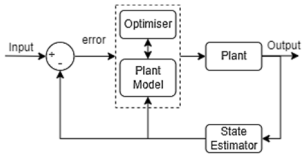	Optimises over future horizon and has excellent performance for complex systems	Requires accurate model of system and is computationally intensive
Robust	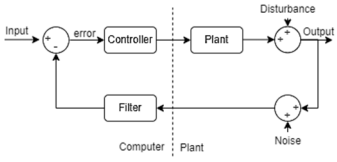	Maintains performance despite uncertainties	Requires extensive training and validation
Neural Network	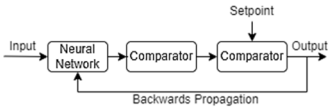	Models' complex systems while improving with training	Requires large amount of training data
Optimal	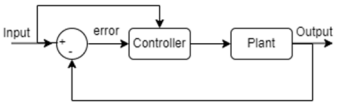	Minimises cost-function for better performance	Requires accurate system model and overly complex

Based on the comparison shown in Table 8, PID as a controller would provide better results than open loop or bang-bang due to its accuracy and stability. On the other hand, if the system to control is non-linear and/or may need to be re-tuned constantly, more advanced control is needed. In such cases, fuzzy and adaptive controllers should be considered as these better suit non-linear systems and minimise noise while adjusting control parameters in real time.

6.4. Navigation and Autonomy

Autonomy is the act of allowing the system to operate without the need for human intervention. This can come at multiple levels, ranging from no autonomy to full autonomy, as illustrated in Figure 16.

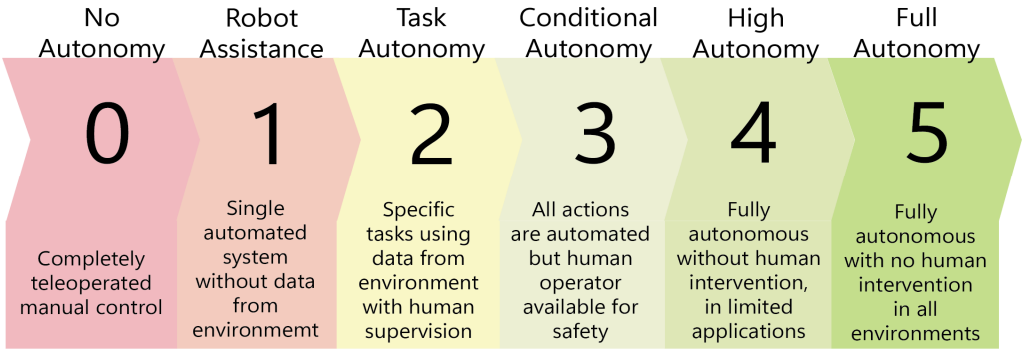

Figure 16. Illustration of the different levels of autonomy.

For typical wind turbine inspection tasks, the aim is usually to have a drone that can operate with conditional or high-level automation at levels 3 or 4. This is to ensure that personnel are minimally required for drone deployments, as well as to maintain the safety of the system. To achieve this, the drone must be aware of its own location, as well as its surroundings. There are multiple methods that can be used to achieve this, using different types of sensors. These can be classed as proprioceptive or exteroceptive sensors, respectively, and will be briefly highlighted together with the different navigation techniques.

The first type of sensor used for localisation and autonomy is the proprioceptive sensor, such as an accelerometer or encoder. These can be used to position the drone using odometry and feedback control systems to estimate the errors induced by the drone using methods, such as dead-reckoning [354]. The second type of sensor, typically used for sensor fusion and mapping, is the exteroceptive sensor, such as sonar and LiDAR. These can be used to map out the environment or use the obstacles in the environment to correct the position data of the drone, providing a more accurate estimation and, hence, a more accurate navigation result. Example navigation methods include LiDAR SLAM, Visual SLAM, GPS and bug algorithms. These all come with their advantages and disadvantages, as summarised in Table 9.

A combination of proprioceptive and exteroceptive sensors is typically needed to ensure that the drone can navigate effectively. From Table 9, it can be inferred that GPS is the preferred localisation method in wind turbine environments, with LiDAR SLAM used as a backup when the system fails or when the drone is deployed in other applications, such as in confined spaces. Moreover, sensor fusion can provide optimal results for autonomous navigation. Examples of this can be performed with Kalman filters for linear data and extended Kalman filters or particle filters for non-linear data [354]. It is useful to note that sensor fusion can be used to combine proprioceptive sensors with exteroceptive sensors for accurate validation between inertial data and environmental data. However, sensor fusion can also be used to merge different methods of navigation, such as GPS and LiDAR SLAM. By gathering data from both sensors, the drone can gain a better-informed position of where it is in space and where the structures are. By combining these algorithms together while utilising the onboard inspection sensors, the navigation accuracy is improved significantly without the need for additional electronics, leading to a more effective autonomous system.

Table 9. A comparison of different navigation methods using exteroceptive sensors.

Method	Sensors and Method	Advantages	Disadvantages
LIDAR SLAM [355]	- Fusion between LiDAR for environment data and IMU for drone data. - Map of environment used for accurate navigation of surroundings.	- High-resolution. - No prior knowledge of the surroundings needed. - Can be used in a variety of different environments.	- Expensive. - Limited range, and some weather conditions can impact performance. - Computationally demanding. - Struggles to detect transparent materials.
Visual SLAM [356]	- Fusion between camera for environment data and IMU for drone data. - Map of environment used for accurate navigation	- Accurate. - Real-time operation. - Comparatively cheap. - Can be implemented on a variety of platforms.	- Small field of view. - Accuracy affected by lighting. - Computationally expensive. - Sensor calibration can be difficult and time-consuming.
GPS [357]	- Global Satellites triangulate position. - Needs at least 4 satellites to operate in three dimensions.	- Can navigate on a global scale. - Receivers are accessible and reasonably priced. - More user-friendly.	- Structures can block radar. - Inaccuracy due to building reflections or weak satellite coverage. - Electromagnetic interference. - Limited vertical accuracy. - Can use a lot of battery power. - Location accurate to within a few meters.
Bug Algorithm [358]	- Sonar or Laser Distance Sensor - Obstacle avoidance algorithm where drone continuously adjusts direction to goal optimally	- Easy-to-implement - Drone can go across complicated surroundings with few collisions - Moves the drone efficiently	- Estimation errors can result in navigational mistakes. - Does not ensure optimal path. - Limited performance in complex situations.

It is also useful to note that the sensors used for autonomy and navigation can be re-used for inspection purposes simultaneously. Examples of this include using LiDAR scans for both SLAM navigation and 3D laser scanning (which utilises the same 3D map) and ultrasound sensors for both ultrasound inspection and bug algorithms for navigation using distance measurements. As such, these sensors can be re-used and utilised concurrently to ensure that their potential is maximised and the payload is optimised effectively. This can significantly reduce the system costs and payloads by selecting the payload sensors such that they can be reused for both inspections and navigation.

6.5. Mode Transitions

Based on our earlier analysis, the following locomotion modes seem to be good starting design selections for a multimodal design:

- Bernoulli Pad and Gecko Gripper for Climbing.
- Quadrotor for Aerial.
- Wheels for Terrestrial.
- Reconfigurable Quadrotor for Aquatic.

For any multimodal drone, mode transitions are critical to the operation of the drone. As such, effective transition mechanisms are required to optimise the new operation effectively. Table 10 briefly mentions a few strategies to transition from each environment to the next for the above-selected configurations.

Table 10. Methods of transition from different operating modes.

Involved Modes		A to B	B to A
A	**B**		
Land	**Air**	Lift off from ground using propellers	Land carefully on ground landing on wheels
Land	**Water**	Drive carefully into water and deploy Variable Buoyancy System (VBS) system to go underwater	Use propellers and VBS to reach water surface then use wheels to reach land
Land	**Climbing**	Change orientation then attach to surface	Touch Ground, detach from surface and change orientation safely
Air	**Water**	Land in water using propellers and then use VBS to go underwater	Use propellers to generate enough lift to exit the water–air barrier
Air	**Climbing**	Land on target, while using propellers for stability until adhesion mechanism deployed	Deploy propellers for safety, de-attach adhesion and then fly off
Water	**Climbing**	Swim to correct orientation and then attach accordingly to surface	De-attach from surface and then deploy underwater locomotion

7. Overall Discussions and Conclusions

7.1. Drone Features and Design Decisions

There are many designs that are currently being used for wind turbine inspections. However, these drones mostly operate in a single-mode configuration on a single wind turbine, completing a single type of inspection. For long-range deployments, aerial drones are usually used due to their unmatched coverage capabilities. These aerial drones can thus provide an overview of the issues identified on wind turbine blades, as well as other structures, allowing for reduced costs and downtime. Even so, this approach can be prone to errors from factors such as weather or low-quality imaging. Also, the depth of scanning is not always optimised and, as such, close-range inspections are usually employed in parallel.

Notably, ring-climbing drone designs, while effective in their operation for wind turbine towers and blades, must maintain contact with the tower whether by using wheels or wires, each providing its own set of advantages and disadvantages. The main advantage of these approaches is their robustness and ability to operate successfully on a single turbine with high payloads. Despite that, these designs can cause additional wear to the turbine towers due to the constant friction from the wheels or the tension in the cables. Also, these drones have no way of being transferred from one turbine to the next without significant work from the operators; as such, for effective operations, these drones would have to be designed in exceedingly high quantities, which can be costly and inefficient. Other approaches to close-range inspections include walking drones, which are more flexible and retrievable. In contrast, legged drones are complex in terms of control and design while having high power consumption and being slower than other alternatives. As such, for long deployments, legged drones may not be the best option. As such, a solution that can combine the robustness and high payloads of ring solutions while being reusable from turbine to turbine would be ideal. One method to achieve this includes drones that can attach to the required structure with a strong and efficient adhesive, such as PWCRs. These have the potential to achieve reasonably high payloads while allowing the drone to be used on multiple structures with less complexity.

For offshore environments, there is an additional need for aquatic inspections of the submerged tower components and the mooring system. This is essential for the continued upkeep of the wind turbine. However, conventional methods cannot traverse these environments; hence, aquatic drones provide an interesting challenge to the field. There have been many successful designs and simulations in this direction, yet these drones

have many challenges to improve upon including waterproofing, drag reduction and, hence, better power economy, as well as sensing/navigation technology challenges.

Finally, while terrestrial drones are not used in the field of wind turbine inspections due to being out of range for most of the important components, these drones have shown promise in many different fields such as bridge and object inspections. Also, terrestrial drones have been shown to be excellent for the transportation of many different systems and personnel and, as such, is an important direction to consider when observing this ever-changing field.

It goes without saying that adequate and efficient methods for actuation are key to the success of robotic deployments. For climbing locomotion, Bernoulli pads and gecko pads can be considered the best choices due to Bernoulli pads being highly effective and offering non-contact, therefore not affecting the inspection surface. Regardless, for the deployable sensor package, a strong passive contact adhesive is required for low energy and longevity. As such, gecko grippers fit the sensor package need, potentially via a microrobot. For terrestrial locomotion, wheeled actuation offers simplicity and energy efficiency in comparison to other methods. As for aerial locomotion, quadcopter locomotion is currently the most suitable mainly due to reasonable performance during hovering, which is key for this application. However, future advancements in flapping wing robotics hold promise to create a step change in the field, not because they are better hoverers but rather due to the additional features of agility and versatility that they can potentially offer. Finally, like aerial locomotion, rotor-based actuation is likely the best current option for aquatic locomotion due to its simplicity and low cost (as well as the potential of re-using current quadcopter hardware). That said, there is a notable rise in the design and deployment of ever-improving bio-inspired configurations, which have future potential to change the current inspection practices.

7.2. Collaborative and Multimodal Drone Designs

Single-mode drones operate independently and this is inefficient not only in terms of resources and energy but also the high number of personnel needed to deploy these systems. This is exemplified in Table 3, where climbing drones are configured as ring climbers as well as other configurations that are difficult to deploy. This increases the inspection interval required for more thorough inspections, which means that low levels of damage are likely not detected early, allowing them to evolve further. Collaborative and multimodal drones are showing ever-increasing promise in this field to improve and optimise wind turbine inspections by lowering the number of individual drones required and the communication required for the system's effective operation, thereby lowering the costs and the required personnel needed to deploy, monitor, operate and inspect these drones. Collaborative drones have been demonstrated in recent years, providing a good way to inspect different parts of wind turbines and transfer one drone from one turbine to the next. This is also exemplified in Table 3, showing how collaborative drones have been seen to deploy modular climbing solutions, such as the Goliath and Bladebug [88,89]. These solutions reduce the time and difficulty required to deploy climbing drones, which contributes to lower maintenance costs. However, this does not resolve the matter of having many different drones, each with its own costs and required personnel. That said, collaborative drones do provide insight into inspecting multiple parts of the wind turbine in different ways during the same deployment. As such, multimodal drones provide another approach to tackle this problem. Fit-to-purpose examples include PWCRs, which are drones that can climb on wall-like structures using pneumatics. On the other hand, these designs have not been tested in wind turbine locations and may consume large amounts of energy,

yet still less energy than a multitude of separate drones. Hence, this provides an interesting venture in the field of wind turbine inspections.

A hybrid approach to multimodal drones can be beneficial to achieving the required outcome with the lowest possible complexity, while also maximising the efficiency of the design. These drones combine the best features of both rotor-based and bio-inspired actuation to achieve the required task in an optimal fashion. Examples of this include multi-rotor wheels that have additional joints, allowing them to operate as legs for unconventional environments, as well as wall-climbing drones that use wheeled locomotion with bio-inspired microspine adhesive techniques. These examples indeed demonstrate the benefits of combining various methods of locomotion. Notably, we illustrate here that rotor-based designs lead to simple configurations with very few complexities, such as wheeled quadcopters and magnetic wheeled WCRs. However, these cannot be applied to varying environments and are limited in how they are used. Consequently, bio-inspired designs allow for a greater range of motion by imitating kinematic mechanisms seen in nature, such as those seen in duck and turtle mechanisms for swimming and bird-perching mechanisms using claws and winged aerial flight.

While these designs and sensing selections provide useful insights, they require further research to enhance their stability, control and energy efficiency. As such, when considering wind turbine inspections, these factors should be optimised for effective close-range, long-range and aquatic inspections.

7.3. Final Comments

Based on the environment in which wind turbines are deployed and their design, the designed drone should be able to inspect all aspects of the turbine blade, which could involve locomotion at a 90° angle or even upside down. Such a drone will typically also need to be able to carry a significant payload, containing the sensors required to conduct the inspections and the core electronics and mechanics for the system. Therefore, the optimisation of payload configuration and weight can have a drastic impact on the whole drone's design, especially when considering cases requiring vertical and upside-down inspections. In addition, this drone will be required to operate in harsh and turbulent conditions so it must be able to withstand these conditions accordingly.

Overall, drones can significantly help in optimising the workflow involved with wind turbine inspections, reducing the risk to human workers, reducing downtime and increasing the efficiency of the inspection process. Bio-inspired drones can be seen to have a greater adaptability to the environment with much smoother operations, and in certain cases, they can have a lower energy consumption rate (as the actuation used by animals saves unnecessary energy loss for different modes of operation). Finally, multimodal drones can further improve the adaptability to the environment and enable more efficient operations. Despite that, no design currently addresses this issue effectively for wind turbine farm inspection in a multitude of modes of operation, including the deployment phase, the long-range phase, the close-range phase, the retrieval phase and the underwater inspection phase. As such, more research is needed to address this challenge, allowing for an actuation system that can morph between these different modes of operation as smoothly as possible.

As pointed out in this paper, we believe that an ideal multimodal drone should effectively combine relevant rotor-based and bio-inspired methods to achieve streamlined performance. An example of how this can be achieved is to use a multi-rotor setup for aerial and aquatic locomotion, wheeled locomotion for terrestrial locomotion and Bernoulli or gecko grippers for climbing modes. However, as climbing is a complex task, other bio-inspired techniques such as those inspired by caterpillar and snail locomotion should

also be considered. This would allow effective locomotion that features adhesive strength while conserving energy, which is a drawback of pneumatic adhesives. It should be noted that the previous examples are just a few possible options and should not limit future endeavours to come up with different proposals. That said, what we proposed is mainly a result of the current advances in this vibrant field.

Supplementary Materials: The following supporting information can be downloaded at: https://www.mdpi.com/article/10.3390/drones9010004/s1, Lists of studies used to create the histograms in Figures 3, 8 and 10.

Author Contributions: Conceptualization, A.O., A.N. and M.R.A.N.; methodology, A.O. and M.R.A.N.; investigation, A.O. and M.R.A.N.; data curation, A.O.; writing—original draft preparation, A.O.; writing—review and editing, A.A. and M.R.A.N.; visualization, A.O. and M.R.A.N.; supervision, A.N., A.A. and M.R.A.N. All authors have read and agreed to the published version of the manuscript.

Funding: This research received no external funding.

Data Availability Statement: The data presented in this study are contained within the paper and its Supplementary Materials.

Conflicts of Interest: The authors declare no conflicts of interest.

References

1. Nordin, M.H.; Sharma, S.; Khan, A.; Gianni, M.; Rajendran, S.; Sutton, R. Collaborative Unmanned Vehicles for Inspection, Maintenance, and Repairs of Offshore Wind Turbines. *Drones* **2022**, *6*, 137. [CrossRef]
2. Liu, Y.; Hajj, M.; Bao, Y. Review of robot-based damage assessment for offshore wind turbines. *Renew. Sustain. Energy Rev.* **2022**, *158*, 112187. [CrossRef]
3. Mitchell, D.; Blanche, J.; Zaki, O.; Roe, J.; Kong, L.; Harper, S.; Robu, V.; Lim, T.; Flynn, D. Symbiotic System of Systems Design for Safe and Resilient Autonomous Robotics in Offshore Wind Farms. *IEEE Access* **2021**, *9*, 141421–141452. [CrossRef]
4. United Nations THE 17 GOALS | Sustainable Development. Available online: https://sdgs.un.org/goals (accessed on 22 September 2024).
5. Iqbal, J.; Al-Zahrani, A.; Alharbi, S.A.; Hashmi, A. Robotics Inspired Renewable Energy Developments: Prospective Opportunities and Challenges. *IEEE Access* **2019**, *7*, 174898–174923. [CrossRef]
6. Mitchell, D.; Blanche, J.; Harper, S.; Lim, T.; Gupta, R.; Zaki, O.; Tang, W.; Robu, V.; Watson, S.; Flynn, D. A review: Challenges and opportunities for artificial intelligence and robotics in the offshore wind sector. *Energy AI* **2022**, *8*, 100146. [CrossRef]
7. Yang, C.; Zhou, H.; Liu, X.; Ke, Y.; Gao, B.; Grzegorzek, M.; Boukhers, Z.; Chen, T.; See, J. BladeView: Toward Automatic Wind Turbine Inspection With Unmanned Aerial Vehicle. *IEEE Trans. Autom. Sci. Eng.* **2024**, 1–16. [CrossRef]
8. Masita, K.; Hasan, A.; Shongwe, T. Defects Detection on 110 MW AC Wind Farm's Turbine Generator Blades Using Drone-Based Laser and RGB Images with Res-CNN3 Detector. *Appl. Sci.* **2023**, *13*, 13046. [CrossRef]
9. Taefi, T.T.; Roswag, M.; Peklar, G. Wingbeat Over Wind Turbines: Autonomous Drones for Acoustic Bat Detection in Operational Wind Farms. In Proceedings of the 2024 International Conference on Artificial Intelligence, Computer, Data Sciences and Applications (ACDSA), Victoria, Seychelles, 1–2 February 2024; pp. 1–5.
10. Yung, K.H.Y. A New Digital Twin Model of Floating Offshore Wind Turbine for Cost-Effective Structural Health Monitoring. In Proceedings of the All-Energy Exhibition and Conference 2024, Glasgow, UK, 14–15 June 2024; Xiao, Q., Incecik, A., Thompson, P., Eds.; University of Strathclyde: Glasgow, UK, 2024. [CrossRef]
11. Okenyi, V.; Bodaghi, M.; Mansfield, N.; Afazov, S.; Siegkas, P. A review of challenges and framework development for corrosion fatigue life assessment of monopile-supported horizontal-axis offshore wind turbines. *Ships Offshore Struct.* **2024**, *19*, 1–15. [CrossRef]
12. Rojas, S.; Michalaros, D.; Rincon, J.; Arrieta, A.F. Bioinspired Self-Stiffening Wing for Multimodal Locomotion. In Proceedings of the 2024 IEEE 7th International Conference on Soft Robotics (RoboSoft), San Diego, CA, USA, 14–17 April 2024; pp. 1004–1009.
13. Chellapurath, M.; Stenius, I. Underwater Robot with Bioinspired Multimodal Locomotion Expands the Scope of Ocean Exploration. In Proceedings of the OCEANS 2024, Singapore, 15–18 April 2024; pp. 1–6.
14. Wu, S.; Shao, M.; Wu, S.; He, Z.; Wang, H.; Zhang, J.; You, Y. Design and Demonstration of a Tandem Dual-Rotor Aerial–Aquatic Vehicle. *Drones* **2024**, *8*, 100. [CrossRef]

15. Qin, G.; Xu, Y.; He, W.; Qi, Q.; Zheng, L.; Hu, H.; Cheng, Y.; Zuo, C.; Zhang, D.; Ji, A. Design and Development of an Air–Land Amphibious Inspection Drone for Fusion Reactor. *Drones* **2024**, *8*, 190. [CrossRef]
16. Chen, G.; Yan, L.; Cao, A.; Zhu, X.; Ding, H.; Lin, Y. Novel Design and Computational Fluid Dynamic Analysis of a Foldable Hybrid Aerial Underwater Vehicle. *Drones* **2024**, *8*, 669. [CrossRef]
17. Herraiz, Á.H.; Marugán, A.P.; Ramirez, I.S.; Papaelias, M.; Márquez, F.P.G. A novel walking robot based system for non-destructive testing in wind turbines. *E-J. Nondestruct. Test.* **2019**, *24*.
18. Rinaldi, G.; Thies, P.; Johanning, L. Current Status and Future Trends in the Operation and Maintenance of Offshore Wind Turbines: A Review. *Energies* **2021**, *14*, 2484. [CrossRef]
19. Alex. *Global Wind Report 2024*; Global Wind Energy Council: Lisbon, Portugal, 2024. Available online: https://gwec.net/global-wind-report-2024/ (accessed on 27 May 2024).
20. Bath, A. *Global Wind Report 2023*; Global Wind Energy Council: Lisbon, Portugal, 2023. Available online: https://gwec.net/globalwindreport2023/ (accessed on 9 November 2023).
21. FrazerNash. *Review of Technical Assumptions and Generation Costs Floating Offshore Wind: Levelised Cost of Energy Review*; FrazerNash Consultancy: Bristol, UK, 2023.
22. Röckmann, C.; Lagerveld, S.; Stavenuiter, J. Operation and Maintenance Costs of Offshore Wind Farms and Potential Multi-use Platforms in the Dutch North Sea. In *Aquaculture Perspective of Multi-Use Sites in the Open Ocean: The Untapped Potential for Marine Resources in the Anthropocene*; Buck, B.H., Langan, R., Eds.; Springer International Publishing: Cham, Switzerland, 2017; pp. 97–113. [CrossRef]
23. Ritchie, H.; Rosado, P.; Roser, M. Energy Production and Consumption. *Oxford Our World Data*. 2024. Available online: https://ourworldindata.org/energy-production-consumption (accessed on 21 March 2024).
24. IEA Renewables 2023—Analysis. 2024. Available online: https://www.iea.org/reports/renewables-2023 (accessed on 21 March 2024).
25. Liu, Y.; Tao, T.; Zhao, X.; Zhang, C.; Ma, Y. Support vector regression-based fatigue damage assessment method for wind turbine nacelle chassis. *Structures* **2021**, *33*, 759–768. [CrossRef]
26. Zhao, Y.; Zhang, Y.; Zhou, Q.; Bian, X.; Lyu, W. Lightning damage on GFRP materials of wind turbines under positive first return stroke. *Electr. Power Syst. Res.* **2023**, *215*, 108978. [CrossRef]
27. Mishnaevsky, L.; Hasager, C.B.; Bak, C.; Tilg, A.-M.; Bech, J.I.; Doagou Rad, S.; Fæster, S. Leading edge erosion of wind turbine blades: Understanding, prevention and protection. *Renew. Energy* **2021**, *169*, 953–969. [CrossRef]
28. Sareen, A.; Sapre, C.A.; Selig, M.S. Effects of leading edge erosion on wind turbine blade performance. *Wind Energy* **2014**, *17*, 1531–1542. [CrossRef]
29. Keegan, M.H. *Wind Turbine Blade Leading Edge Erosion: An Investigation of Rain Droplet and Hailstone Impact Induced Damage Mechanisms*; University of Strathclyde: Glasgow, UK, 2014.
30. Chuang, Z.; Li, C.; Liu, S.; Li, X.; Li, Z.; Zhou, L. Numerical analysis of blade icing influence on the dynamic response of an integrated offshore wind turbine. *Ocean. Eng.* **2022**, *257*, 111593. [CrossRef]
31. Yirtici, O.; Tuncer, I.H.; Ozgen, S. Ice Accretion Prediction on Wind Turbines and Consequent Power Losses. *J. Phys. Conf. Ser.* **2016**, *753*, 022022. [CrossRef]
32. Juhl, M.; Hauschild, M.Z.; Dam-Johansen, K. Sustainability of corrosion protection for offshore wind turbine towers. *Prog. Org. Coat.* **2024**, *186*, 107998. [CrossRef]
33. Sun, K.; Xu, Z.; Li, S.; Jin, J.; Wang, P.; Yue, M.; Li, C. Dynamic response analysis of floating wind turbine platform in local fatigue of mooring. *Renew. Energy* **2023**, *204*, 733–749. [CrossRef]
34. Pacheco, J.; Pimenta, F.; Pereira, S.; Cunha, Á.; Magalhães, F. Fatigue Assessment of Wind Turbine Towers: Review of Processing Strategies with Illustrative Case Study. *Energies* **2022**, *15*, 4782. [CrossRef]
35. Yang, Y.; Bashir, M.; Li, C.; Wang, J. Investigation on mooring breakage effects of a 5 MW barge-type floating offshore wind turbine using F2A. *Ocean. Eng.* **2021**, *233*, 108887. [CrossRef]
36. Dimitrova, M.; Aminzadeh, A.; Meiabadi, M.S.; Sattarpanah Karganroudi, S.; Taheri, H.; Ibrahim, H. A Survey on Non-Destructive Smart Inspection of Wind Turbine Blades Based on Industry 4.0 Strategy. *Appl. Mech.* **2022**, *3*, 1299–1326. [CrossRef]
37. Leon Rodriguez, H.; Sattar, T.P.; Bridge, B. Climbing ring robot for inspection of offshore wind turbines. *Ind. Robot. Int. J.* **2009**, *36*, 326–330. [CrossRef]
38. Katsaprakakis, D.A.; Papadakis, N.; Ntintakis, I. A Comprehensive Analysis of Wind Turbine Blade Damage. *Energies* **2021**, *14*, 5974. [CrossRef]
39. Chen, X.; Eder, M.A. A Critical Review of Damage and Failure of Composite Wind Turbine Blade Structures. *IOP Conf. Ser. Mater. Sci. Eng.* **2020**, *942*, 012001. [CrossRef]
40. Civera, M.; Surace, C. Non-Destructive Techniques for the Condition and Structural Health Monitoring of Wind Turbines: A Literature Review of the Last 20 Years. *Sensors* **2022**, *22*, 1627. [CrossRef]

41. García Márquez, F.P.; Peco Chacón, A.M. A review of non-destructive testing on wind turbines blades. *Renew. Energy* **2020**, *161*, 998–1010. [CrossRef]
42. SGS. In-Service Inspection Solution for Renewable Energy for Wind Power Turbines. Available online: https://www.sgs.com/en-lb/news/2023/08/in-service-inspection-solution-for-renewable-energy-for-wind-power-turbines (accessed on 8 December 2024).
43. Prokopets, E. Guide to Wind Turbine Drone Inspection and Maintenance. Voliro. 2024. Available online: https://voliro.com/blog/wind-turbine-drone-inspection/ (accessed on 8 December 2024).
44. Wieme, J.; Mollazade, K.; Malounas, I.; Zude-Sasse, M.; Zhao, M.; Gowen, A.; Argyropoulos, D.; Fountas, S.; Van Beek, J. Application of hyperspectral imaging systems and artificial intelligence for quality assessment of fruit, vegetables and mushrooms: A review. *Biosyst. Eng.* **2022**, *222*, 156–176. [CrossRef]
45. Analytik. Nano HP VNIR Hyperspectral Imaging Sensor | Nano-Hyperspec. Analytik Ltd. 2024. Available online: https://analytik.co.uk/product/hyperspectral-imaging-nano-hyperspec-vnir-camera/ (accessed on 8 December 2024).
46. Innoter. Hyperspectral Imaging. GEO Innoter. Available online: https://innoter.com/en/articles/hyperspectral-imaging/ (accessed on 8 December 2024).
47. Nakatsuji, R. Headwall Hyperspectral Sensor System Launched Into Space. Headwall Photonics. Available online: https://headwallphotonics.com/headwall-hyperspectral-sensor-system-launched-into-space/ (accessed on 8 December 2024).
48. DPREVIEW. Side-by-Side Camera Comparison: Digital Photography Review: Digital Photography Review. Available online: https://www.dpreview.com/products/compare/cameras (accessed on 9 December 2024).
49. PASS. FLIR Thermal Cameras For Sale | Huge Range of Thermal Imagers. Available online: https://www.pass-thermal.co.uk/brands/flir-thermal-cameras?p=4 (accessed on 10 December 2024).
50. Blackview. How Far That a FLIR Camera Can See?—Blackview Blog. Available online: https://www.blackview.hk/blog/guides/how-far-can-flir-camera-see (accessed on 8 December 2024).
51. Anritsu. XR75 Dual X-Ray. Available online: https://www.anritsu.com/en-gb/product-inspection/products/x-ray/dual-x (accessed on 8 December 2024).
52. Amadeo. Portable X-Ray Machines | Low-Weight, Flexible & High Performance. Available online: https://www.or-technology.com/en/products/human/amadeo-p-systems.html (accessed on 10 December 2024).
53. RobotShop. LIDAR, Laser Scanners & Rangefinders. RobotShop UK. Available online: https://uk.robotshop.com/collections/lidar (accessed on 10 December 2024).
54. RobotShop. Search: 11 Results Found for "mm-Wave Radar". RobotShop UK. Available online: https://uk.robotshop.com/search?q=mm-wave+radar&type=product (accessed on 10 December 2024).
55. Global Sources. Stonkam 1080p 24ghz Radar Detector System, Detection Range: 0.1~20m (0.33ft-65.6ft), Parking Radar, Radar Detection System, Parking Sensor—Buy China Wholesale Radar Detection $300 | Globalsources.com. Global Sources. Available online: https://www.globalsources.com/Car-radar/Radar-Detection-1178649419p.htm (accessed on 8 December 2024).
56. Sørensen, F.F.; Mai, C.; Olsen, O.M.; Liniger, J.; Pedersen, S. Commercial Optical and Acoustic Sensor Performances under Varying Turbidity, Illumination, and Target Distances. *Sensors* **2023**, *23*, 6575. [CrossRef] [PubMed]
57. Instrotech. Acoustic/Sonic Inspection—Imaging & Inspection. Available online: https://instrotech.com/industrial-imaging/acoustic-sonic-imaging.html?product_list_order=price (accessed on 8 December 2024).
58. Vallen Systeme. Acoustic Emission Sensors. 2017. Available online: https://www.vallen.de/wp-content/uploads/2019/03/sov.pdf (accessed on 8 December 2024).
59. RS. Vibration Sensors | Piezoelectric Sensors | RS. Available online: https://uk.rs-online.com/web/c/automation-control-gear/sensors/vibration-sensors/?sortBy=price&sortType=DESC (accessed on 10 December 2024).
60. Sonatest. Digital Ultrasonic Flaw Detector | Wave | Sonatest. Available online: https://sonatest.com/products/flaw-detectors/wave (accessed on 8 December 2024).
61. PASS. Ultrasonic Detection. Available online: https://www.tester.co.uk/process-and-industrial/condition-monitoring/ultrasonic-detection (accessed on 8 December 2024).
62. Baumer. Functionality of Ultrasonic Sensors. Available online: https://www.baumer.com/us/en/a/Know-how_Function_Ultrasonic-sensors (accessed on 8 December 2024).
63. RS. 528 for "Strain Gauge" | RS. Available online: https://uk.rs-online.com/web/c/?searchTerm=strain+gauge&sortType=DESC&sortBy=price (accessed on 10 December 2024).
64. BVT Technologies. AC2 Electrochemical Sensor. Available online: https://bvt.cz/produkt/ac2/ (accessed on 8 December 2024).
65. Frontline Safety. Drager EC Electrochemical Sensor for Hydrogen (H2). Frontline Safety. Available online: https://www.frontline-safety.co.uk/drager-ec-electrochemical-sensor-for-hydrogen-h2 (accessed on 10 December 2024).
66. Yang, B.; Sun, D. Testing, inspecting and monitoring technologies for wind turbine blades: A survey. *Renew. Sustain. Energy Rev.* **2013**, *22*, 515–526. [CrossRef]

67. Du, Y.; Zhou, S.; Jing, X.; Peng, Y.; Wu, H.; Kwok, N. Damage detection techniques for wind turbine blades: A review. *Mech. Syst. Signal Process.* **2020**, *141*, 106445. [CrossRef]
68. Kaewniam, P.; Cao, M.; Alkayem, N.F.; Li, D.; Manoach, E. Recent advances in damage detection of wind turbine blades: A state-of-the-art review. *Renew. Sustain. Energy Rev.* **2022**, *167*, 112723. [CrossRef]
69. Xia, J.; Zou, G. Operation and maintenance optimization of offshore wind farms based on digital twin: A review. *Ocean. Eng.* **2023**, *268*, 113322. [CrossRef]
70. Yue, Y.; Tian, J.; Bai, Y.; Jia, K.; He, J.; Luo, D.; Chen, T. Applicability Analysis of Inspection and Monitoring Technologies in Wind Turbine Towers. *Shock. Vib.* **2021**, *2021*, 5548727. [CrossRef]
71. Kabbabe Poleo, K.; Crowther, W.J.; Barnes, M. Estimating the impact of drone-based inspection on the Levelised Cost of electricity for offshore wind farms. *Results Eng.* **2021**, *9*, 100201. [CrossRef]
72. Netland, Ø.; Jenssen, G.D.; Skavhaug, A. The Capabilities and Effectiveness of Remote Inspection of Wind Turbines. *Energy Procedia* **2015**, *80*, 177–184. [CrossRef]
73. Langåker, H.-A.; Kjerkreit, H.; Syversen, C.L.; Moore, R.J.; Holhjem, Ø.H.; Jensen, I.; Morrison, A.; Transeth, A.A.; Kvien, O.; Berg, G.; et al. An autonomous drone-based system for inspection of electrical substations. *Int. J. Adv. Robot. Syst.* **2021**, *18*, 17298814211002973. [CrossRef]
74. Alsayed, A.; Nabawy, M.R.; Arvin, F. Autonomous Aerial Mapping Using a Swarm of Unmanned Aerial Vehicles. In *AIAA AVIATION 2022 Forum*; American Institute of Aeronautics and Astronautics: Reston, VA, USA, 2022.
75. Besada, J.A.; Bergesio, L.; Campaña, I.; Vaquero-Melchor, D.; López-Araquistain, J.; Bernardos, A.M.; Casar, J.R. Drone Mission Definition and Implementation for Automated Infrastructure Inspection Using Airborne Sensors. *Sensors* **2018**, *18*, 1170. [CrossRef]
76. Nooralishahi, P.; Ibarra-Castanedo, C.; Deane, S.; López, F.; Pant, S.; Genest, M.; Avdelidis, N.P.; Maldague, X.P.V. Drone-Based Non-Destructive Inspection of Industrial Sites: A Review and Case Studies. *Drones* **2021**, *5*, 106. [CrossRef]
77. Ameli, Z.; Aremanda, Y.; Friess, W.A.; Landis, E.N. Impact of UAV Hardware Options on Bridge Inspection Mission Capabilities. *Drones* **2022**, *6*, 64. [CrossRef]
78. Alsayed, A.; Nabawy, M.R.A. Indoor Stockpile Reconstruction Using Drone-Borne Actuated Single-Point LiDARs. *Drones* **2022**, *6*, 386. [CrossRef]
79. Pinto, L.R.; Vale, A.; Brouwer, Y.; Borbinha, J.; Corisco, J.; Ventura, R.; Silva, A.M.; Mourato, A.; Marques, G.; Romanets, Y.; et al. Radiological Scouting, Monitoring and Inspection Using Drones. *Sensors* **2021**, *21*, 3143. [CrossRef]
80. Ashour, R.; Taha, T.; Mohamed, F.; Hableel, E.; Kheil, Y.A.; Elsalamouny, M.; Kadadha, M.; Rangan, K.; Dias, J.; Seneviratne, L.; et al. Site Inspection Drone: A Solution for Inspecting and Regulating Construction Sites. In Proceedings of the 2016 IEEE 59th International Midwest Symposium on Circuits and Systems (MWSCAS), Abu Dhabi, United Arab Emirates, 16–19 October 2016; pp. 1–4.
81. Alsayed, A.; Nabawy, M.R.A. Stockpile Volume Estimation in Open and Confined Environments: A Review. *Drones* **2023**, *7*, 537. [CrossRef]
82. Kamran, M. Chapter 7—Microgrid and Hybrid Energy Systems. In *Fundamentals of Smart Grid Systems*; Kamran, M., Ed.; Academic Press: Cambridge, MA, USA, 2023; pp. 299–363. [CrossRef]
83. Khalid, O.; Hao, G.; Desmond, C.; Macdonald, H.; Devoy McAuliffe, F.; Dooly, G.; Hu, W. Applications of robotics in floating offshore wind farm operations and maintenance: Literature review and trends. *Wind Energy* **2022**, *25*, 1880–1899. [CrossRef]
84. Shafiee, M.; Zhou, Z.; Mei, L.; Dinmohammadi, F.; Karama, J.; Flynn, D. Unmanned Aerial Drones for Inspection of Offshore Wind Turbines: A Mission-Critical Failure Analysis. *Robotics* **2021**, *10*, 26. [CrossRef]
85. Lee, I. Service Robots: A Systematic Literature Review. *Electronics* **2021**, *10*, 2658. [CrossRef]
86. Charron, N.; McLaughlin, E.; Phillips, S.; Goorts, K.; Narasimhan, S.; Waslander, S.L. Automated Bridge Inspection Using Mobile Ground Robotics. *J. Struct. Eng.* **2019**, *145*, 04019137. [CrossRef]
87. Phillips, S.; Narasimhan, S. Automating Data Collection for Robotic Bridge Inspections. *J. Bridge Eng.* **2019**, *24*, 04019075. [CrossRef]
88. Jiang, Z.; Jovan, F.; Moradi, P.; Richardson, T.; Bernardini, S.; Watson, S.; Weightman, A.; Hine, D. A multirobot system for autonomous deployment and recovery of a blade crawler for operations and maintenance of offshore wind turbine blades. *J. Field Robot.* **2022**, *40*, 73–93. [CrossRef]
89. Bernardini, S.; Jovan, F.; Jiang, Z.; Watson, S.; Weightman, A.; Moradi, P.; Richardson, T.; Sadeghian, R.; Sareh, S. A Multi-Robot Platform for the Autonomous Operation and Maintenance of Offshore Wind Farms. *Blue Sky Idea Pap.* **2020**, 1696–1700. Available online: https://dl.acm.org/doi/abs/10.5555/3398761.3398956 (accessed on 10 December 2024).
90. Liu, J.-H.; Padrigalan, K. Design and Development of a Climbing Robot for Wind Turbine Maintenance. *Appl. Sci.* **2021**, *11*, 2328. [CrossRef]
91. Lee, D.G.; Oh, S.; Son, H.I. Maintenance Robot for 5-MW Offshore Wind Turbines and its Control. *IEEE/ASME Trans. Mechatron.* **2016**, *21*, 2272–2283. [CrossRef]

92. Jeon, M.; Kim, B.G.; Hong, D. Maintenance robot for wind power blade cleaning. In Proceedings of the International Symposium on Automation and Robotics in Construction, Eindhoven, The Netherlands, 26–29 June 2012; Volume 11, p. 377. [CrossRef]
93. Elkmann, N.; Felsch, T.; Förster, T. Robot for Rotor Blade Inspection. In Proceedings of the 2010 1st International Conference on Applied Robotics for the Power Industry, Montreal, ON, Canada, 5–7 October 2010; pp. 1–5. [CrossRef]
94. Lim, S.; Park, C.-W.; Hwang, J.-H.; Kim, D.-Y.; Kim, T.-K. The Inchworm Type Blade Inspection Robot System. In Proceedings of the 2012 9th International Conference on Ubiquitous Robots and Ambient Intelligence (URAI), Daejeon, Republic of Korea, 26–28 November 2012; pp. 604–607. [CrossRef]
95. Stokkeland, M.; Klausen, K.; Johansen, T.A. Autonomous Visual Navigation of Unmanned Aerial Vehicle for Wind Turbine Inspection. In Proceedings of the 2015 International Conference on Unmanned Aircraft Systems (ICUAS), Denver, CO, USA, 9–12 June 2015; pp. 998–1007. [CrossRef]
96. Schäfer, B.E.; Picchi, D.; Engelhardt, T.; Abel, D. Multicopter Unmanned Aerial Vehicle for Automated Inspection of Wind Turbines. In Proceedings of the 2016 24th Mediterranean Conference on Control and Automation (MED), Athens, Greece, 21–24 June 2016; pp. 244–249. [CrossRef]
97. Car, M.; Markovic, L.; Ivanovic, A.; Orsag, M.; Bogdan, S. Autonomous Wind-Turbine Blade Inspection Using LiDAR-Equipped Unmanned Aerial Vehicle. *IEEE Access* **2020**, *8*, 131380–131387. [CrossRef]
98. Zhao, C.; Thies, P.R.; Johanning, L. Offshore inspection mission modelling for an ASV/ROV system. *Ocean. Eng.* **2022**, *259*, 111899. [CrossRef]
99. Sivčev, S.; Omerdić, E.; Dooly, G.; Coleman, J.; Toal, D. Towards Inspection of Marine Energy Devices Using ROVs: Floating Wind Turbine Motion Replication. In Proceedings of the ROBOT 2017: Third Iberian Robotics Conference, Sevilla, Spain, 22–24 November 2017; Ollero, A., Sanfeliu, A., Montano, L., Lau, N., Cardeira, C., Eds.; Springer International Publishing: Cham, Switzerland, 2018; pp. 196–211. [CrossRef]
100. Jacobi, M. Autonomous inspection of underwater structures. *Robot. Auton. Syst.* **2015**, *67*, 80–86. [CrossRef]
101. Gorma, W.; Post, M.A.; White, J.; Gardner, J.; Luo, Y.; Kim, J.; Mitchell, P.D.; Morozs, N.; Wright, M.; Xiao, Q. Development of Modular Bio-Inspired Autonomous Underwater Vehicle for Close Subsea Asset Inspection. *Appl. Sci.* **2021**, *11*, 5401. [CrossRef]
102. Franko, J.; Du, S.; Kallweit, S.; Duelberg, E.; Engemann, H. Design of a Multi-Robot System for Wind Turbine Maintenance. *Energies* **2020**, *13*, 2552. [CrossRef]
103. Song, Y.; Kim, T.; Lee, M.; Rho, S.; Kim, J.; Kang, J.; Yu, S.-C. Development of Safety-Inspection-Purpose Wall-Climbing Robot Utilizing Aerial Drone with Lifting Function. In Proceedings of the 2021 18th International Conference on Ubiquitous Robots (UR), Gangneung, Republic of Korea, 12–14 July 2021; pp. 411–416. [CrossRef]
104. Myeong, W.C.; Jung, K.Y.; Jung, S.W.; Jung, Y.H.; Myung, H. Development of a Drone-Type Wall-Sticking and Climbing Robot. In Proceedings of the 2015 12th International Conference on Ubiquitous Robots and Ambient Intelligence (URAI), Goyang, Republic of Korea, 28–30 October 2015; pp. 386–389. [CrossRef]
105. Myeong, W.; Jung, K.; Jung, S.; Jeong, Y.; Myung, H. Drone-Type Wall-Climbing Robot Platform For Structural Health Monitoring. 2015. Available online: https://www.semanticscholar.org/paper/Drone-Type-Wall-Climbing-Robot-Platform-For-Health-Myeong-Jung/e868f1a86c2ff1e6a83bb862e2c2b53c000de613 (accessed on 9 December 2024).
106. Jung, S.; Shin, J.-U.; Myeong, W.; Myung, H. Mechanism and System Design of MAV(Micro Aerial Vehicle)-Type Wall-Climbing Robot for Inspection of Wind Blades and Non-Flat Surfaces. In Proceedings of the 2015 15th International Conference on Control, Automation and Systems (ICCAS), Busan, Republic of Korea, 13–16 October 2015; pp. 1757–1761. [CrossRef]
107. Myeong, W.; Myung, H. Development of a Wall-Climbing Drone Capable of Vertical Soft Landing Using a Tilt-Rotor Mechanism. *IEEE Access* **2019**, *7*, 4868–4879. [CrossRef]
108. Ottaviano, E.; Rea, P.; Cavacece, M.; Figliolini, G. Mechatronic Design of a Wall-Climbing Drone for the Inspection of Structures and Infrastructure. In *Innovations in Mechatronics Engineering*; Machado, J., Soares, F., Trojanowska, J., Yildirim, S., Eds.; Springer International Publishing: Cham, Switzerland, 2022; pp. 460–467. [CrossRef]
109. Mintchev, S.; Floreano, D. Adaptive Morphology: A Design Principle for Multimodal and Multifunctional Robots. *IEEE Robot. Autom. Mag.* **2016**, *23*, 42–54. [CrossRef]
110. Ramirez, J.P.; Hamaza, S. Multimodal Locomotion: Next Generation Aerial–Terrestrial Mobile Robotics. *Adv. Intell. Syst.* **2023**, 2300327. [CrossRef]
111. Kalantari, A.; Spenko, M. Modeling and Performance Assessment of the HyTAQ, a Hybrid Terrestrial/Aerial Quadrotor. *IEEE Trans. Robot.* **2014**, *30*, 1278–1285. [CrossRef]
112. Mintchev, S.; Floreano, D. A Multi-Modal Hovering and Terrestrial Robot with Adaptive Morphology. In Proceedings of the 2nd International Symposium on Aerial Robotics, Philadelphia, PA, USA, 11–12 June 2018. Available online: https://infoscience.epfl.ch/handle/20.500.14299/146873 (accessed on 10 December 2024).
113. Fabris, A.; Kirchgeorg, S.; Mintchev, S. A Soft Drone with Multi-modal Mobility for the Exploration of Confined Spaces. In Proceedings of the 2021 IEEE International Symposium on Safety, Security, and Rescue Robotics (SSRR), Sevilla, Spain, 8–10 November 2022; pp. 48–54. [CrossRef]

114. Kossett, A.; D'Sa, R.; Purvey, J.; Papanikolopoulos, N. Design of an Improved Land/Air Miniature Robot. In Proceedings of the 2010 IEEE International Conference on Robotics and Automation, Anchorage, AK, USA, 3–7 May 2010; pp. 632–637. [CrossRef]
115. Tanaka, K.; Zhang, D.; Inoue, S.; Kasai, R.; Yokoyama, H.; Shindo, K.; Matsuhiro, K.; Marumoto, S.; Ishii, H.; Takanishi, A. A Design of a Small Mobile Robot with a Hybrid Locomotion Mechanism of Wheels and Multi-Rotors. In Proceedings of the 2017 IEEE International Conference on Mechatronics and Automation (ICMA), Takamatsu, Japan, 6–9 August 2017; pp. 1503–1508. [CrossRef]
116. Fan, D.D.; Thakker, R.; Bartlett, T.; Miled, M.B.; Kim, L.; Theodorou, E.; Agha-mohammadi, A. Autonomous Hybrid Ground/Aerial Mobility in Unknown Environments. In Proceedings of the 2019 IEEE/RSJ International Conference on Intelligent Robots and Systems (IROS), Venetian Macao, Macau, 3–8 November 2019; pp. 3070–3077. [CrossRef]
117. Hoji, R.; Maeyama, S.; Kono, T.; Takei, T.; Yuta, S. Position Control for Half-Drone Wheeled Inverted Pendulum Robot. In Proceedings of the 2021 IEEE International Conference on Mechatronics and Automation (ICMA), Takamatsu, Japan, 8–11 August 2021; pp. 651–656. [CrossRef]
118. Dias, T.; Basiri, M. BogieCopter: A Multi-Modal Aerial-Ground Vehicle for Long-Endurance Inspection Applications. *arXiv* **2023**, arXiv:2303.01933. [CrossRef]
119. Swamy, S.R.; Sasnur, S.S.; Sai, P.G.; Naga, S.B.; Kharvi, V.S. Design and Development of Unmanned Ground and Aerial Vehicle with The Concept of Integration of Drone and Rover. Available online: http://13.232.72.61:8080/jspui/handle/123456789/5248 (accessed on 29 January 2024).
120. Li, Y.; Lu, H.; Nakayama, Y.; Kim, H.; Serikawa, S. Automatic road detection system for an air–land amphibious car drone. *Future Gener. Comput. Syst.* **2018**, *85*, 51–59. [CrossRef]
121. Zhao, S.; Ruggiero, F.; Fontanelli, G.A.; Lippiello, V.; Zhu, Z.; Siciliano, B. Nonlinear Model Predictive Control for the Stabilization of a Wheeled Unmanned Aerial Vehicle on a Pipe. *IEEE Robot. Autom. Lett.* **2019**, *4*, 4314–4321. [CrossRef]
122. Greco, M.; Leccese, F.; Giarnetti, S.; De Francesco, E. A Multiporpouse Amphibious Rover (MAR) as Platform in Archaeological Field. In Proceedings of the 2022 IMEKO TC4 International Conference on Metrology for Archaeology and Cultural Heritage, Calabria, Italy, 19–21 October 2022; IMEKO: Consenza, Italy, 2023; pp. 252–256. [CrossRef]
123. Ge, Y.; Gao, F.; Chen, W. A transformable wheel-spoke-paddle hybrid amphibious robot. *Robotica* **2024**, *42*, 701–727. [CrossRef]
124. Klein, M.A.; Boxerbaum, A.S.; Quinn, R.D.; Harkins, R.; Vaidyanathan, R. SeaDog: A Rugged Mobile Robot for Surf-Zone Applications. In Proceedings of the 2012 4th IEEE RAS & EMBS International Conference on Biomedical Robotics and Biomechatronics (BioRob), Rome, Italy, 24–27 June 2012; pp. 1335–1340. [CrossRef]
125. Muthusamy, S.; Duraisamy, S.; Ramachandran, M.; Karthikeyan, J.; David, J.I.; Kumar Settu, H.; Rathinasamy, A. A Novel Method for Design and Development of Hybrid Land and Water Buoyancy Trash Collecting Robot. In Proceedings of the 2024 International Conference on Intelligent and Innovative Technologies in Computing, Electrical and Electronics (IITCEE), Bangalore, India, 24–25 January 2024; pp. 1–5. [CrossRef]
126. Nilas, P.; Ngo, T. A Multi-Terrain Spherical Amphibious Robot for On-Land, In-Water, and Underwater Operation. 2019. Available online: https://www.semanticscholar.org/paper/A-Multi-Terrain-Spherical-Amphibious-Robot-for-,-,-Nilas-Ngo/9338074270f7611466c872420342e780ac7b0520 (accessed on 11 June 2024).
127. Li, L.; Guo, J.; Guo, S. Characteristic Evaluation on Land for a Novel Amphibious Spherical Robot. In Proceedings of the 2015 IEEE International Conference on Mechatronics and Automation (ICMA), Beijing, China, 2–5 August 2015; pp. 1100–1105. [CrossRef]
128. Wagner, M.; Chen, X.; Nayyerloo, M.; Wang, W.; Chase, J.G. A Novel Wall Climbing Robot Based on Bernoulli Effect. In Proceedings of the 2008 IEEE/ASME International Conference on Mechtronic and Embedded Systems and Applications, Beijing, China, 12–15 October 2008; pp. 210–215. [CrossRef]
129. Navaprakash, N.; Ramachandraiah, U.; Muthukumaran, G.; Rakesh, V.; Singh, A.P. Modeling and Experimental Analysis of Suction Pressure Generated by Active Suction Chamber Based Wall Climbing Robot with a Novel Bottom Restrictor. *Procedia Comput. Sci.* **2018**, *133*, 847–854. [CrossRef]
130. Muthugala, M.A.V.J.; Vega-Heredia, M.; Mohan, R.E.; Vishaal, S.R. Design and Control of a Wall Cleaning Robot with Adhesion-Awareness. *Symmetry* **2020**, *12*, 122. [CrossRef]
131. Mahmood, S.K.; Bakhy, S.H.; Tawfik, M.A. Magnetic–type Climbing Wheeled Mobile Robot for Engineering Education. *IOP Conf. Ser. Mater. Sci. Eng.* **2020**, *928*, 022145. [CrossRef]
132. Eto, H.; Asada, H.H. Development of a Wheeled Wall-Climbing Robot with a Shape-Adaptive Magnetic Adhesion Mechanism. In Proceedings of the 2020 IEEE International Conference on Robotics and Automation (ICRA), Paris, France, 31 May–31 August 2020. [CrossRef]
133. Horn, A.C.; Pinheiro, P.M.; Grando, R.B.; da Silva, C.B.; Neto, A.A.; Drews, P.L.J. A Novel Concept for Hybrid Unmanned Aerial Underwater Vehicles Focused on Aquatic Performance. In Proceedings of the 2020 Latin American Robotics Symposium (LARS), 2020 Brazilian Symposium on Robotics (SBR) and 2020 Workshop on Robotics in Education (WRE), Natal, Brazil, 9–12 November 2020; pp. 1–6. [CrossRef]

134. Aoki, V.M.; Pinheiro, P.M.; Drews-Jr, P.L.J.; Cunha, M.A.B.; Tuchtenhagen, L.G. Analysis of a Hybrid Unmanned Aerial Underwater Vehicle Considering the Environment Transition. In Proceedings of the 2021 Latin American Robotics Symposium (LARS), 2021 Brazilian Symposium on Robotics (SBR), and 2021 Workshop on Robotics in Education (WRE), Natal, Brazil, 11–15 October 2021; pp. 90–95. [CrossRef]
135. Debruyn, D.; Zufferey, R.; Armanini, S.F.; Winston, C.; Farinha, A.; Jin, Y.; Kovac, M. MEDUSA: A Multi-Environment Dual-Robot for Underwater Sample Acquisition. *IEEE Robot. Autom. Lett.* **2020**, *5*, 4564–4571. [CrossRef]
136. Liu, X.; Dou, M.; Huang, D.; Gao, S.; Yan, R.; Wang, B.; Cui, J.; Ren, Q.; Dou, L.; Gao, Z.; et al. TJ-FlyingFish: Design and Implementation of an Aerial-Aquatic Quadrotor with Tiltable Propulsion Units. In Proceedings of the 2023 IEEE International Conference on Robotics and Automation (ICRA), London, UK, 29 May–2 June 2023; pp. 7324–7330. [CrossRef]
137. Maia, M.M.; Soni, P.; Diez, F.J. Demonstration of an Aerial and Submersible Vehicle Capable of Flight and Underwater Navigation with Seamless Air-Water Transition. *arXiv* **2015**, arXiv:1507.01932. [CrossRef]
138. Le, P.H.; Wang, Z.; Hirai, S. Origami Structure Toward Floating Aerial Robot. In Proceedings of the 2015 IEEE International Conference on Advanced Intelligent Mechatronics (AIM), Busan, Republic of Korea, 7–11 July 2015; pp. 1565–1569. [CrossRef]
139. Albers, A.; Trautmann, S.; Howard, T.; Nguyen, T.A.; Frietsch, M.; Sauter, C. Semi-Autonomous Flying Robot for Physical Interaction with Environment. In Proceedings of the 2010 IEEE Conference on Robotics, Automation and Mechatronics, Singapore, 28–30 June 2010; pp. 441–446. [CrossRef]
140. Ding, X.; Yu, Y. Motion Planning and Stabilization Control of a Multipropeller Multifunction Aerial Robot. *IEEE/ASME Trans. Mechatron.* **2013**, *18*, 645–656. [CrossRef]
141. Myeong, W.; Song, S.; Myung, H. Development of a Wall-Climbing Drone with a Rotary Arm for Climbing Various-Shaped Surfaces. In Proceedings of the 2018 15th International Conference on Ubiquitous Robots (UR), Honolulu, HI, USA, 26–30 June 2018; pp. 687–692. [CrossRef]
142. Myeong, W.; Jung, S.; Yu, B.-U.; Chris, T.; Song, S.; Myung, H. Development of Wall-climbing Unmanned Aerial Vehicle System for Micro-Inspection of Bridges. Presented at the IEEE International Conference on Robotics and Automation, Montreal, QC, Canada, 20–24 May 2019. Available online: https://www.semanticscholar.org/paper/Development-of-Wall-climbing-Unmanned-Aerial-System-Myeong-Jung/b12cce6d9509b6cc93ab5df1e0fa0f435b9b011d (accessed on 11 June 2024).
143. Lee, H.; Yu, B.; Tirtawardhana, C.; Kim, C.; Jeong, M.; Hu, S.; Myung, H. CAROS-Q: Climbing Aerial RObot System Adopting Rotor Offset With a Quasi-Decoupling Controller. *IEEE Robot. Autom. Lett.* **2021**, *6*, 8490–8497. [CrossRef]
144. Hsiao, Y.-H.; Bai, S.; Zhou, Y.; Jia, H.; Ding, R.; Chen, Y.; Wang, Z.; Chirarattananon, P. Energy efficient perching and takeoff of a miniature rotorcraft. *Commun. Eng.* **2023**, *2*, 1–14. [CrossRef]
145. Liu, Y.; Sun, G.; Chen, H. Impedance Control of a Bio-Inspired Flying and Adhesion Robot. In Proceedings of the 2014 IEEE International Conference on Robotics and Automation (ICRA), Hong Kong, China, 31 May–7 June 2014; pp. 3564–3569. [CrossRef]
146. Liang, P.; Gao, X.; Gao, R.; Zhang, Q.; Li, M. Analysis of the aerodynamic performance of a twin-propelled wall-climbing robot based on computational fluid dynamics method. *AIP Adv.* **2022**, *12*, 015022. [CrossRef]
147. Liang, P.; Gao, X.; Zhang, Q.; Gao, R.; Li, M.; Xu, Y.; Zhu, W. Design and Stability Analysis of a Wall-Climbing Robot Using Propulsive Force of Propeller. *Symmetry* **2021**, *13*, 37. [CrossRef]
148. Liang, P.; Gao, X.; Zhang, Q.; Li, M.; Gao, R.; Xu, Y. Analysis and experimental research on motion stability of wall-climbing robot with double propellers. *Adv. Mech. Eng.* **2021**, *13*, 168781402110477. [CrossRef]
149. David, N.B.; Zarrouk, D. Design and Analysis of FCSTAR, a Hybrid Flying and Climbing Sprawl Tuned Robot. *IEEE Robot. Autom. Lett.* **2021**, *6*, 6188–6195. [CrossRef]
150. Huang, C.; Liu, Y.; Wang, K.; Bai, B. Land–Air–Wall Cross-Domain Robot Based on Gecko Landing Bionic Behavior: System Design, Modeling, and Experiment. *Appl. Sci.* **2022**, *12*, 3988. [CrossRef]
151. Hossain, R.; Chisty, N. Design and Implementation of a Wall Climbing Robot. *Int. J. Comput. Appl.* **2018**, *179*, 1–5. [CrossRef]
152. Kadar, F.; Tătar, M.O. A Review on Mobile Robots with Multimodal Locomotion. In Proceedings of the SYROM 2022 & ROBOTICS 2022, Iasi, Romania, 17–18 November 2022; Doroftei, I., Nitulescu, M., Pisla, D., Lovasz, E.-C., Eds.; Mechanisms and Machine Science; Springer International Publishing: Cham, Switzerland, 2023; pp. 337–349. [CrossRef]
153. Canelon, D.; Westlake, S.; Wang, Y.; Papanikolopoulos, N. Design and Characterization of a Multi-Domain Unmanned Vehicle Operating in Aerial, Terrestrial, and Underwater Environments. In Proceedings of the 2021 International Conference on Unmanned Aircraft Systems (ICUAS), Athens, Greece, 15–18 June 2021; pp. 1466–1471. [CrossRef]
154. Guo, J.; Zhang, K.; Guo, S.; Li, C.; Yang, X. Design of a New Type of Tri-habitat Robot. In Proceedings of the 2019 IEEE International Conference on Mechatronics and Automation (ICMA), Tianjin, China, 4–7 August 2019; pp. 1508–1513. [CrossRef]
155. Evangeliou, N.; Chaikalis, D.; Giakoumidis, N.; Tzes, A. Mechatronic Design of an Amphibious Drone. In Proceedings of the 2023 9th International Conference on Automation, Robotics and Applications (ICARA), Abu Dhabi, United Arab Emirates, 10–12 February 2023; pp. 230–233. [CrossRef]
156. Sharma, P.; Ab, A.S. Conceptual Design and Non-Linear Analysis of Triphibian Drone. *Procedia Comput. Sci.* **2018**, *133*, 448–455. [CrossRef]

157. Zhong, G.; Cao, J.; Chai, X.; Bai, Y. Design and Performance Analysis of a Triphibious Robot With Tilting-Rotor Structure. *IEEE Access* **2021**, *9*, 10871–10879. [CrossRef]
158. Kawasaki, K.; Zhao, M.; Okada, K.; Inaba, M. MUWA: Multi-field universal wheel for air-land vehicle with quad variable-pitch propellers. In Proceedings of the 2013 IEEE/RSJ International Conference on Intelligent Robots and Systems, Tokyo, Japan, 3–7 November 2013; pp. 1880–1885. [CrossRef]
159. Eswaran, P.; Tamilmani, B.; Karna, D.R.; Arif, A.M.; Susheel, R.N.; Kumar, B.S.; Raju, K.R. Triphibian—An urban future transportation system. *IOP Conf. Ser. Mater. Sci. Eng.* **2020**, *764*, 012035. [CrossRef]
160. Shrestha, E.; Davis, B.; Hrishikeshavan, V.; Chopra, I. All-Terrain Cyclocopter Capable of Aerial, Terrestrial, and Aquatic Modes. *J. Am. Helicopter Soc.* **2021**, *66*, 1–10. [CrossRef]
161. Lock, R.J.; Burgess, S.C.; Vaidyanathan, R. Multi-modal locomotion: From animal to application. *Bioinspir. Biomim.* **2013**, *9*, 011001. [CrossRef] [PubMed]
162. Ortega-Jimenez, V.M.; Jusufi, A.; Brown, C.E.; Zeng, Y.; Kumar, S.; Siddall, R.; Kim, B.; Challita, E.J.; Pavlik, Z.; Priess, M.; et al. Air-to-land transitions: From wingless animals and plant seeds to shuttlecocks and bio-inspired robots. *Bioinspir. Biomim.* **2023**, *18*, 051001. [CrossRef] [PubMed]
163. Shin, W.D.; Park, J.; Park, H.-W. Bio-Inspired Design of a Gliding-Walking Multi-Modal Robot. In Proceedings of the 2018 IEEE/RSJ International Conference on Intelligent Robots and Systems (IROS), Madrid, Spain, 1–5 October 2018; pp. 8158–8164. [CrossRef]
164. Shin, W.D.; Park, J.; Park, H.-W. Development and experiments of a bio-inspired robot with multi-mode in aerial and terrestrial locomotion. *Bioinspir. Biomim.* **2019**, *14*, 056009. [CrossRef] [PubMed]
165. Bachmann, R.J.; Boria, F.J.; Vaidyanathan, R.; Ifju, P.G.; Quinn, R.D. A biologically inspired micro-vehicle capable of aerial and terrestrial locomotion. *Mech. Mach. Theory* **2009**, *44*, 513–526. [CrossRef]
166. Paulson, L.D. Biomimetic robots. *Computer* **2004**, *37*, 48–53. [CrossRef]
167. Peterson, K.; Fearing, R.S. Experimental Dynamics of Wing Assisted Running for a Bipedal Ornithopter. In Proceedings of the 2011 IEEE/RSJ International Conference on Intelligent Robots and Systems, San Francisco, CA, USA, 25–30 September 2011; pp. 5080–5086. [CrossRef]
168. Peterson, K.; Birkmeyer, P.; Dudley, R.; Fearing, R.S. A wing-assisted running robot and implications for avian flight evolution. *Bioinspir. Biomim.* **2011**, *6*, 046008. [CrossRef]
169. Kashem, S.; Sufyan, H. A novel design of an aquatic walking robot having webbed feet. *Int. J. Autom. Comput.* **2017**, *14*, 576–588. [CrossRef]
170. Kashem, S.B.A.; Tabassum, M.; Chai, M. A Novel Design of an Amphibious Robot Having Webbed Feet as Duck. In Proceedings of the 2017 International Conference on Computer and Drone Applications (IConDA), Kuching, Malaysia, 9–11 November 2017; pp. 17–21. [CrossRef]
171. Kashem, S.B.A.; Jawed, S.; Ahmed, J.; Qidwai, U. Design and Implementation of a Quadruped Amphibious Robot Using Duck Feet. *Robotics* **2019**, *8*, 77. [CrossRef]
172. Baines, R.; Patiballa, S.K.; Booth, J.; Ramirez, L.; Sipple, T.; Garcia, A.; Fish, F.; Kramer-Bottiglio, R. Multi-environment robotic transitions through adaptive morphogenesis. *Nature* **2022**, *610*, 283–289. [CrossRef]
173. Dudek, G.; Giguere, P.; Prahacs, C.; Saunderson, S.; Sattar, J.; Torres-Mendez, L.; Jenkin, M.; German, A.; Hogue, A.; Ripsman, A.; et al. AQUA: An Amphibious Autonomous Robot. *Computer* **2007**, *40*, 46–53. [CrossRef]
174. Georgiades, C.; German, A.; Hogue, A.; Liu, H.; Prahacs, C.; Ripsman, A.; Sim, R.; Torres, L.-A.; Zhang, P.; Buehler, M.; et al. AQUA: An Aquatic Walking Robot. In Proceedings of the 2004 IEEE/RSJ International Conference on Intelligent Robots and Systems (IROS) (IEEE Cat. No.04CH37566), Sendai, Japan, 28 September–2 October 2004; Volume 4, pp. 3525–3531. [CrossRef]
175. Chen, Y.; Doshi, N.; Goldberg, B.; Wang, H.; Wood, R.J. Controllable water surface to underwater transition through electrowetting in a hybrid terrestrial-aquatic microrobot. *Nat. Commun.* **2018**, *9*, 2495. [CrossRef]
176. Chen, Z.; Hu, Q.; Chen, Y.; Wei, C.; Yin, S. Water Surface Stability Prediction of Amphibious Bio-Inspired Undulatory Fin Robot. In Proceedings of the 2021 IEEE/RSJ International Conference on Intelligent Robots and Systems (IROS), Prague, Czech Republic, 27 September–1 October 2021; pp. 7365–7371. [CrossRef]
177. Crespi, A.; Badertscher, A.; Guignard, A.; Ijspeert, A.J. AmphiBot I: An amphibious snake-like robot. *Robot. Auton. Syst.* **2005**, *50*, 163–175. [CrossRef]
178. Yang, Q.; Yu, J.; Tan, M.; Wang, W. Preliminary Development of a Biomimetic Amphibious Robot Capable of Multi-Mode Motion. In Proceedings of the 2007 IEEE International Conference on Robotics and Biomimetics (ROBIO), Sanya, China, 15–18 December 2007; pp. 769–774. [CrossRef]
179. Yu, J.; Yang, Q.; Ding, R.; Tan, M.; Yu, J.; Yang, Q.; Ding, R.; Tan, M. Terrestrial and Underwater Locomotion Control for a Biomimetic Amphibious Robot Capable of Multimode Motion. In *Motion Control*; IntechOpen: London, UK, 2010. [CrossRef]

180. Yue, T.; Bloomfield-Gadêlha, H.; Rossiter, J. Friction-driven Three-Foot Robot Inspired by Snail Movement. In Proceedings of the 2021 IEEE International Conference on Robotics and Automation (ICRA), Xi'an, China, 30 May–5 June 2021; pp. 9820–9825. [CrossRef]
181. Goldman, D.I.; Chen, T.S.; Dudek, D.M.; Full, R.J. Dynamics of rapid vertical climbing in cockroaches reveals a template. *J. Exp. Biol.* **2006**, *209*, 2990–3000. [CrossRef] [PubMed]
182. Liu, G.; Liu, Y.; Wang, X.; Wu, X.; Mei, T. Design and Experiment of a Bioinspired Wall-Climbing Robot Using Spiny Grippers. In Proceedings of the 2016 IEEE International Conference on Mechatronics and Automation, Harbin, China, 7–10 August 2016; pp. 665–670. [CrossRef]
183. Zhang, H.; Wang, W.; Gonzalez-Gomez, J.; Zhang, J.; Zhang, H.; Wang, W.; Gonzalez-Gomez, J.; Zhang, J. A Bio-Inspired Small-Sized Wall-Climbing Caterpillar Robot. In *Mechatronic Systems Applications*; IntechOpen: London, UK, 2010. [CrossRef]
184. Lin, T.-H.; Chiang, P.-C.; Putranto, A. Multispecies hybrid bioinspired climbing robot for wall tile inspection. *Autom. Constr.* **2024**, *164*, 105446. [CrossRef]
185. Siddall, R.; Kovač, M. Launching the AquaMAV: Bioinspired design for aerial-aquatic robotic platforms. *Bioinspir. Biomim.* **2014**, *9*, 031001. [CrossRef]
186. Armanini, S.F.; Siddall, R.; Kovac, M. Modelling and Simulation of a Bioinspired Aquatic Micro Aerial Vehicle. In *AIAA Aviation 2019 Forum*; American Institute of Aeronautics and Astronautics: Reston, VA, USA, 2019. [CrossRef]
187. Qin, K.; Tang, W.; Zhong, Y.; Liu, Y.; Xu, H.; Zhu, P.; Yan, D.; Yang, H.; Zou, J. An Aerial–Aquatic Robot with Tunable Tilting Motors Capable of Multimode Motion. *Adv. Intell. Syst.* **2023**, *5*, 2300193. [CrossRef]
188. Hou, T.; Yang, X.; Su, H.; Jiang, B.; Chen, L.; Wang, T.; Liang, J. Design and Experiments of a Squid-Like Aquatic-Aerial Vehicle with Soft Morphing Fins and Arms. In Proceedings of the 2019 International Conference on Robotics and Automation (ICRA), Montreal, QC, Canada, 20–24 May 2019; pp. 4681–4687. [CrossRef]
189. Gu, L.; Xiang, Y.; Gong, Z.; Tao, B. Bio-Inspired Wing with Bistable Morphing Airfoils for Aquatic-Aerial Robots. *IEEE Robot. Autom. Lett.* **2024**, *9*, 6704–6711. [CrossRef]
190. Chen, Y.; Liu, Y.; Liu, T.; Li, H.; Qu, S.; Yang, W. Design and analysis of an untethered micro flapping robot which can glide on the water. *Sci. China Technol. Sci.* **2022**, *65*, 1749–1759. [CrossRef]
191. Chen, Y.; Wang, H.; Helbling, E.F.; Jafferis, N.T.; Zufferey, R.; Ong, A.; Ma, K.; Gravish, N.; Chirarattananon, P.; Kovac, M.; et al. A biologically inspired, flapping-wing, hybrid aerial-aquatic microrobot. *Sci. Robot.* **2017**, *2*, eaao5619. [CrossRef] [PubMed]
192. Chen, Y.; Helbling, E.F.; Gravish, N.; Ma, K.; Wood, R.J. Hybrid Aerial and Aquatic Locomotion in an at-Scale Robotic Insect. In Proceedings of the 2015 IEEE/RSJ International Conference on Intelligent Robots and Systems (IROS), Hamburg, Germany, 28 September–3 October 2015; pp. 331–338. [CrossRef]
193. Dickson, J.D.; Clark, J.E. Design of a Multimodal Climbing and Gliding Robotic Platform. *IEEE/ASME Trans. Mechatron.* **2013**, *18*, 494–505. [CrossRef]
194. Lussier Desbiens, A.; Cutkosky, M.R. Landing and Perching on Vertical Surfaces with Microspines for Small Unmanned Air Vehicles. *J. Intell. Robot Syst.* **2010**, *57*, 313–327. [CrossRef]
195. Mehanovic, D.; Rancourt, D.; Desbiens, A.L. Fast and Efficient Aerial Climbing of Vertical Surfaces Using Fixed-Wing UAVs. *IEEE Robot. Autom. Lett.* **2019**, *4*, 97–104. [CrossRef]
196. Zufferey, R.; Tormo-Barbero, J.; Feliu-Talegón, D.; Nekoo, S.R.; Acosta, J.Á.; Ollero, A. How ornithopters can perch autonomously on a branch. *Nat. Commun.* **2022**, *13*, 7713. [CrossRef]
197. Chatterjee, S.; Roberts, B.; Lind, R. Pterodrone: A Pterodactyl-Inspired Unmanned Air Vehicle That Flies, Walks, Climbs, and Sails. In *WIT Transactions on Ecology and the Environment 2010*; University of Pisa: Pisa, Italy, 2010; pp. 301–316. [CrossRef]
198. Pérez-Sánchez, V.; Gómez-Tamm, A.E.; García-Rubiales, F.J.; Arrue, B.; Ollero, A. Analysis of Forces Involved in the Perching Maneuver of Flapping-Wing Aerial Systems and Development of an Ultra-Lightweight Perching System. In Proceedings of the 2021 International Conference on Unmanned Aircraft Systems (ICUAS), Athens, Greece, 15–18 June 2021; pp. 1284–1290. [CrossRef]
199. Lau, G.-K.; Wu, C.-C.; Ren, Z.-X.; Wakler, S.; Lin, S.-C.; Tseng, K.-Y.; Lu, C.-C. Lightweight Perching Mechanisms for Flapping-wing Drones. In Proceedings of the 2023 International Conference on Advanced Robotics and Intelligent Systems (ARIS), Taipei, Taiwan, 30 August–1 September 2023; pp. 1–6. [CrossRef]
200. Pan, Y.; Göktogan, A. Quasi-Static Balance of a Bioinspired Robotic-Seagull Ornithopter Perching on a Wire. Environmental Science. 2017. Available online: https://www.semanticscholar.org/paper/Quasi-Static-Balance-of-a-Bioinspired-Ornithopter-a-Pan-G%C3%B6ktogan/aa29d322840f3bbdc563180d0af6f443805006ba (accessed on 11 June 2024).
201. Chukewad, Y.M.; James, J.; Singh, A.; Fuller, S. RoboFly: An Insect-Sized Robot With Simplified Fabrication That Is Capable of Flight, Ground, and Water Surface Locomotion. *IEEE Trans. Robot.* **2021**, *37*, 2025–2040. [CrossRef]
202. Russo, M.; Ceccarelli, M. A Survey on Mechanical Solutions for Hybrid Mobile Robots. *Robotics* **2020**, *9*, 32. [CrossRef]

203. Dinelli, C.; Racette, J.; Escarcega, M.; Lotero, S.; Gordon, J.; Montoya, J.; Dunaway, C.; Androulakis, V.; Khaniani, H.; Shao, S.; et al. Configurations and Applications of Multi-Agent Hybrid Drone/Unmanned Ground Vehicle for Underground Environments: A Review. *Drones* **2023**, *7*, 136. [CrossRef]
204. Sihite, E.; Kalantari, A.; Nemovi, R.; Ramezani, A.; Gharib, M. Multi-Modal Mobility Morphobot (M4) with appendage repurposing for locomotion plasticity enhancement. *Nat. Commun.* **2023**, *14*, 3323. [CrossRef] [PubMed]
205. Daler, L.; Lecoeur, J.; Hählen, P.B.; Floreano, D. A Flying Robot with Adaptive Morphology for Multi-Modal Locomotion. In Proceedings of the 2013 IEEE/RSJ International Conference on Intelligent Robots and Systems, Detroit, MI, USA, 1–5 October 2013; pp. 1361–1366. [CrossRef]
206. Ceccarelli, M.; Cafolla, D.; Russo, M.; Carbone, G. Design Issues for a Walking-Flying Robot. In *Mechanism and Machine Science*; Sen, D., Mohan, S., Ananthasuresh, G.K., Eds.; Springer: Singapore, 2021; pp. 267–277. [CrossRef]
207. Kim, K.; Spieler, P.; Lupu, E.-S.; Ramezani, A.; Chung, S.-J. A bipedal walking robot that can fly, slackline, and skateboard. *Sci. Robot.* **2021**, *6*, eabf8136. [CrossRef]
208. Li, M.; Guo, S.; Hirata, H.; Ishihara, H. A roller-skating/walking mode-based amphibious robot. *Robot. Comput. Integr. Manuf.* **2017**, *44*, 17–29. [CrossRef]
209. Xing, H.; Shi, L.; Hou, X.; Liu, Y.; Hu, Y.; Xia, D.; Li, Z.; Guo, S. Design, modeling and control of a miniature bio-inspired amphibious spherical robot. *Mechatronics* **2021**, *77*, 102574. [CrossRef]
210. Xing, H.; Guo, S.; Shi, L.; Hou, X.; Liu, Y.; Liu, H. Design, modeling and experimental evaluation of a legged, multi-vectored water-jet composite driving mechanism for an amphibious spherical robot. *Microsyst. Technol.* **2020**, *26*, 475–487. [CrossRef]
211. Christensen, D.L.; Hawkes, E.W.; Suresh, S.A.; Ladenheim, K.; Cutkosky, M.R. μTugs: Enabling microrobots to deliver macro forces with controllable adhesives. In Proceedings of the 2015 IEEE International Conference on Robotics and Automation (ICRA), Seattle, WA, USA, 26–30 May 2015; pp. 4048–4055. [CrossRef]
212. Christensen, D.L.; Suresh, S.A.; Hahm, K.; Cutkosky, M.R. Let's All Pull Together: Principles for Sharing Large Loads in Microrobot Teams. *IEEE Robot. Autom. Lett.* **2016**, *1*, 1089–1096. [CrossRef]
213. Li, H.; Sun, X.; Chen, Z.; Zhang, L.; Wang, H.; Wu, X. Design of a wheeled wall climbing robot based on the performance of bio-inspired dry adhesive material. *Robotica* **2022**, *40*, 611–624. [CrossRef]
214. Liu, J.; Xu, L.; Chen, S.; Xu, H.; Cheng, G.; Li, T.; Yang, Q. Design and Realization of a Bio-inspired Wall Climbing Robot for Rough Wall Surfaces. In *Intelligent Robotics and Applications*; Yu, H., Liu, J., Liu, L., Ju, Z., Liu, Y., Zhou, D., Eds.; Springer International Publishing: Cham, Switzerland, 2019; pp. 47–59. [CrossRef]
215. Li, L.; Wang, S.; Zhang, Y.; Song, S.; Wang, C.; Tan, S.; Zhao, W.; Wang, G.; Sun, W.; Yang, F.; et al. Aerial-aquatic robots capable of crossing the air-water boundary and hitchhiking on surfaces. *Sci. Robot.* **2022**, *7*, eabm6695. [CrossRef] [PubMed]
216. Vyas, A.; Puppala, R.; Sivadasan, N.; Molawade, A.; Ranganathan, T.; Thondiyath, A. Modelling and Dynamic Analysis of a Novel Hybrid Aerial—Underwater Robot—Acutus. In Proceedings of the OCEANS 2019, Marseille, France, 17–20 June 2019; pp. 1–6. [CrossRef]
217. Zufferey, R.; Ancel, A.O.; Raposo, C.; Armanini, S.F.; Farinha, A.; Siddall, R.; Berasaluce, I.; Zhu, H.; Kovac, M. SailMAV: Design and Implementation of a Novel Multi-Modal Flying Sailing Robot. *IEEE Robot. Autom. Lett.* **2019**, *4*, 2894–2901. [CrossRef]
218. Zheng, P.; Xiao, F.; Nguyen, P.H.; Farinha, A.; Kovac, M. Metamorphic aerial robot capable of mid-air shape morphing for rapid perching. *Sci. Rep.* **2023**, *13*, 1297. [CrossRef] [PubMed]
219. Kirchgeorg, S.; Mintchev, S. HEDGEHOG: Drone Perching on Tree Branches with High-Friction Origami Spines. *IEEE Robot. Autom. Lett.* **2022**, *7*, 602–609. [CrossRef]
220. Pope, M.T.; Kimes, C.W.; Jiang, H.; Hawkes, E.W.; Estrada, M.A.; Kerst, C.F.; Roderick, W.R.T.; Han, A.K.; Christensen, D.L.; Cutkosky, M.R. A Multimodal Robot for Perching and Climbing on Vertical Outdoor Surfaces. *IEEE Trans. Robot.* **2017**, *33*, 38–48. [CrossRef]
221. Roderick, W.R.T.; Cutkosky, M.R.; Lentink, D. Bird-inspired dynamic grasping and perching in arboreal environments. *Sci. Robot.* **2021**, *6*, eabj7562. [CrossRef] [PubMed]
222. Li, Q.; Li, H.; Shen, H.; Yu, Y.; He, H.; Feng, X.; Sun, Y.; Mao, Z.; Chen, G.; Tian, Z.; et al. An Aerial–Wall Robotic Insect That Can Land, Climb, and Take Off from Vertical Surfaces. *Research* **2022**, *6*, 0144. [CrossRef]
223. Askari, M.; Shin, W.D.; Lenherr, D.; Stewart, W.; Floreano, D. Avian-Inspired Claws Enable Robot Perching or Walking. *IEEE/ASME Trans. Mechatron.* **2023**, *29*, 1856–1866. [CrossRef]
224. Kong, J.; Niu, S.; Lu, P.; Li, A.; Xiang, X.; Zhao, W.; Zhou, Z. Design of a Bio-inspired Water-Ground-Air Amphibious and Cross Domain Robot Platform. In Proceedings of the 2022 IEEE International Conference on Robotics and Biomimetics (ROBIO), Jinghong, China, 5–9 December 2022; pp. 2177–2182. [CrossRef]
225. Cohen, A.; Zarrouk, D. Design, Analysis and Experiments of a High-Speed Water Hovering Amphibious Robot: AmphiSTAR. *IEEE Access* **2023**, *11*, 80874–80885. [CrossRef]

226. Chen, Y.; Guo, S.; Yin, H.; Li, A.; Liu, M. Design of Clutch Units of the Propulsion System for the Three-Dimension Triphibian Robot. In Proceedings of the 2023 IEEE International Conference on Mechatronics and Automation (ICMA), Harbin, China, 6–9 August 2023; pp. 1947–1952. [CrossRef]
227. Mykhailyshyn, R.; Savkiv, V.; Maruschak, P.; Xiao, J. A systematic review on pneumatic gripping devices for industrial robots. *Transport* **2022**, *37*, 201–231. [CrossRef]
228. Savkiv, V.; Mykhailyshyn, R.; Duchon, F. Gasdynamic analysis of the Bernoulli grippers interaction with the surface of flat objects with displacement of the center of mass. *Vacuum* **2019**, *159*, 524–533. [CrossRef]
229. Savkiv, V.; Mykhailyshyn, R.; Duchon, F.; Fendo, O. Justification of design and parameters of Bernoulli–vacuum gripping device. *Int. J. Adv. Robot. Syst.* **2017**, *14*, 1729881417741740. [CrossRef]
230. Tomar, A.S.; Kamensky, K.M.; Mejia-Alvarez, R.; Hellum, A.M.; Mukherjee, R. A scaling relationship between power and shear for Bernoulli pads at equilibrium. *Flow* **2022**, *2*, E29. [CrossRef]
231. Weston-Dawkes, W.P.; Adibnazari, I.; Hu, Y.-W.; Everman, M.; Gravish, N.; Tolley, M.T. Gas-Lubricated Vibration-Based Adhesion for Robotics. *Adv. Intell. Syst.* **2021**, *3*, 2100001. [CrossRef]
232. Lee, Y.H.; Kim, J.H.; Sung, J. Enhanced Non-Contact Grip Force and Swirl Stability by a Combined Venturi–Vortex Air Head. *Materials* **2021**, *14*, 7123. [CrossRef]
233. Wei, Y.; Zhang, Q.; Gao, X.; Liang, P.; Li, M.; Li, K. Aerodynamic Analysis of a Wall-Climbing Robot with Dual-propeller. In Proceedings of the 2022 IEEE International Conference on Mechatronics and Automation (ICMA), Guilin, China, 7–10 August 2022; pp. 1537–1542. [CrossRef]
234. Vlasova, N.S.; Bykov, N.V. The Problem of Adhesion Methods and Locomotion Mechanism Development for Wall-Climbing Robots. *AIP Conf. Proc.* **2023**, *2549*, 210015. [CrossRef]
235. Watanabe, M.; Wiltsie, N.; Hosoi, A.E.; Iagnemma, K. Characteristics of controllable adhesion using magneto-rheological fluid and its application to climbing robotics. In Proceedings of the 2013 IEEE/RSJ International Conference on Intelligent Robots and Systems, Tokyo, Japan, 3–7 November 2013; pp. 2315–2320. [CrossRef]
236. Scarselli, G.; Quan, D.; Murphy, N.; Deegan, B.; Dowling, D.; Ivankovic, A. Adhesion Improvement of Thermoplastics-Based Composites by Atmospheric Plasma and UV Treatments. *Appl. Compos. Mater.* **2021**, *28*, 71–89. [CrossRef]
237. Relation between friction and adhesion. *Proc. R. Soc. Lond. A* **1950**, *202*, 244–253. [CrossRef]
238. Zhu, Y.; He, X.; Zhang, P.; Guo, G.; Zhang, X. Perching and Grasping Mechanism Inspired by a Bird's Claw. *Machines* **2022**, *10*, 656. [CrossRef]
239. Fang, G.; Cheng, J. Design and Implementation of a Wire Rope Climbing Robot for Sluices. *Machines* **2022**, *10*, 1000. [CrossRef]
240. Festo. TentacleGripper | Festo GB. Available online: https://www.festo.com/gb/en/e/about-festo/research-and-development/bionic-learning-network/highlights-from-2015-to-2017/tentaclegripper-id_33321/ (accessed on 26 February 2024).
241. Wang, J.; Ji, C.; Wang, W.; Zou, J.; Yang, H.; Pan, M. An adhesive locomotion model for the rock-climbing fish, Beaufortia kweichowensis. *Sci. Rep.* **2019**, *9*, 16571. [CrossRef]
242. Okamoto, S.; Akitsu, Y.; Shigemune, H. Electrostatic Adhesion Technology Based on a Folded Paper. In Proceedings of the 2023 IEEE 12th Global Conference on Consumer Electronics (GCCE), Nara, Japan, 10–13 October 2023; pp. 1038–1039. [CrossRef]
243. Louati, H.; Zouzou, N.; Tilmatine, A.; Zouaghi, A.; Ouiddir, R. Experimental investigation of an electrostatic adhesion device used for metal/polymer granular mixture sorting. *Powder Technol.* **2021**, *391*, 301–310. [CrossRef]
244. Liu, R.; Chen, R.; Shen, H.; Zhang, R. Wall Climbing Robot Using Electrostatic Adhesion Force Generated by Flexible Interdigital Electrodes. *Int. J. Adv. Robot. Syst.* **2013**, *10*, 36. [CrossRef]
245. Ruffatto, D.; Parness, A.; Spenko, M. Improving controllable adhesion on both rough and smooth surfaces with a hybrid electrostatic/gecko-like adhesive. *J. R. Soc. Interface* **2014**, *11*, 20131089. [CrossRef] [PubMed]
246. Heepe, L.; Kovalev, A.E.; Varenberg, M.; Tuma, J.; Gorb, S.N. First mushroom-shaped adhesive microstructure: A review. *Theor. Appl. Mech. Lett.* **2012**, *2*, 014008. [CrossRef]
247. Lakkannavar, V.; Yogesha, K.B.; Prasad, C.D.; Srinivasa, G.; Mathapati, M. Assessment of the Microstructure, Adhesion and Elevated Temperature Erosion Resistance of Plasma-Sprayed NiCrAlY/cr3C2/h-Bn Composite Coating. Results Surf. *Interfaces* **2024**, *17*, 100289. [CrossRef]
248. García Márquez, F.P.; Bernalte Sánchez, P.J.; Segovia Ramírez, I. Acoustic inspection system with unmanned aerial vehicles for wind turbines structure health monitoring. *Struct. Health Monit.* **2022**, *21*, 485–500. [CrossRef]
249. Abdelrahman, M.; ElNomrossy, M.; Nabawy, M. Development of Mini Unmanned Air Vehicles. In Proceedings of the 13th International Conference on Aerospace Sciences and Aviation Technology, Cairo, Egypt, 26–28 May 2009.
250. McNeal, G.S. *Drones and the Future of Aerial Surveillance*; Social Science Research Network: Rochester, NY, USA, 2015; p. 2498116. Available online: https://papers.ssrn.com/abstract=2498116 (accessed on 31 October 2024).
251. Gundlach, J. *Designing Unmanned Aircraft Systems*; American Institute of Aeronautics and Astronautics, Inc.: Reston, VA, USA, 2014. [CrossRef]

252. Yayli, U.; Kimet, C.; Duru, A.; Cetir, O.; Torun, U.; Aydogan, A.; Padmanaban, S.; Ertas, A. Design optimization of a fixed wing aircraft. *Adv. Aircr. Spacecr. Sci.* **2017**, *4*, 65–80. [CrossRef]
253. Masood, K.; Wei, Z. Detailed Flight Performance Analysis of a Fixed Wing UAV. In Proceedings of the Infotech, Garden Grove, CA, USA, 19–21 June 2012. [CrossRef]
254. Qiao, N.; Ma, T.; Wang, X.; Wang, J.; Fu, J.; Xue, P. An approach for formation design and flight performance prediction based on aerodynamic formation unit: Energy-saving considerations. *Chin. J. Aeronaut.* **2024**, *37*, 77–91. [CrossRef]
255. Liang, O. Quadcopter VS Helicopter—Why Not Scale Up, Full Size Drone. Available online: https://oscarliang.com/quadcopter-helicopter-compare-cons-pro/ (accessed on 11 July 2024).
256. Katiar, A.; Rashdi, R.; Ali, Z.; Baig, U. Control and Stability Analysis of Quadcopter. In Proceedings of the 2018 International Conference on Computing, Mathematics and Engineering Technologies (iCoMET), Sukkur, Pakistan, 3–4 March 2018; pp. 1–6. [CrossRef]
257. Ali, M.Z.; Ahmed, A.; Afridi, H.K. Control System Analysis and Design of Quadcopter in the Presence of Unmodelled Dynamics and Disturbances. *IFAC-Pap.* **2020**, *53*, 8840–8846. [CrossRef]
258. Chamberlain, B.; Sheikh, W. Design and Implementation of a Quadcopter Drone Control System for Photography Applications. In Proceedings of the 2022 Intermountain Engineering, Technology and Computing (IETC), Orem, UT, USA, 14–15 May 2022; pp. 1–7. [CrossRef]
259. Thu, K.M.; Gavrilov, A.I. Designing and Modeling of Quadcopter Control System Using L1 Adaptive Control. *Procedia Comput. Sci.* **2017**, *103*, 528–535. [CrossRef]
260. Tatale, O.; Anekar, N.; Phatak, S.; Sarkale, S. Quadcopter: Design, Construction and Testing. *Int. J. Res. Eng. Appl. Manag.* **2019**, *4*, 1–7. [CrossRef]
261. Balayan, A.; Mallick, R.; Dwivedi, S.; Saxena, S.; Haorongbam, B.; Sharma, A. Optimal Design of Quadcopter Chassis Using Generative Design and Lightweight Materials to Advance Precision Agriculture. *Machines* **2024**, *12*, 187. [CrossRef]
262. Tanaka, S.; Asignacion, A.; Nakata, T.; Suzuki, S.; Liu, H. Review of Biomimetic Approaches for Drones. *Drones* **2022**, *6*, 320. [CrossRef]
263. Shyy, W.; Aono, H.; Chimakurthi, S.K.; Trizila, P.; Kang, C.-K.; Cesnik, C.E.S.; Liu, H. Recent progress in flapping wing aerodynamics and aeroelasticity. *Prog. Aerosp. Sci.* **2010**, *46*, 284–327. [CrossRef]
264. Xuan, H.; Hu, J.; Yu, Y.; Zhang, J. Recent progress in aerodynamic modeling methods for flapping flight. *AIP Adv.* **2020**, *10*, 020701. [CrossRef]
265. Sane, S.P. The aerodynamics of insect flight. *J. Exp. Biol.* **2003**, *206*, 4191–4208. [CrossRef] [PubMed]
266. Chin, D.D.; Lentink, D. Flapping wing aerodynamics: From insects to vertebrates. *J. Exp. Biol.* **2016**, *219*, 920–932. [CrossRef] [PubMed]
267. Broadley, P.; Nabawy, M.R.A.; Quinn, M.K.; Crowther, W.J. Dynamic experimental rigs for investigation of insect wing aerodynamics. *J. R. Soc. Interface* **2022**, *19*, 20210909. [CrossRef] [PubMed]
268. Harvey, C.; Gamble, L.L.; Bolander, C.R.; Hunsaker, D.F.; Joo, J.J.; Inman, D.J. A review of avian-inspired morphing for UAV flight control. *Prog. Aerosp. Sci.* **2022**, *132*, 100825. [CrossRef]
269. Phan, H.V.; Park, H.C. Insect-inspired, tailless, hover-capable flapping-wing robots: Recent progress, challenges, and future directions. *Prog. Aerosp. Sci.* **2019**, *111*, 100573. [CrossRef]
270. Nabawy, M.R.A.; Marcinkeviciute, R. Scalability of resonant motor-driven flapping wing propulsion systems. *R. Soc. Open Sci.* **2021**, *8*, 210452. [CrossRef]
271. Nabawy, M.R.A.; Crowther, W.J. Aero-optimum hovering kinematics. *Bioinspir. Biomim.* **2015**, *10*, 044002. [CrossRef]
272. Nabawy, M.R.A.; Crowther, W.J. Optimum hovering wing planform. *J. Theor. Biol.* **2016**, *406*, 187–191. [CrossRef]
273. Nabawy, M.; Crowther, W. Is Flapping Flight Aerodynamically Efficient? In Proceedings of the 32nd AIAA Applied Aerodynamics Conference, Atlanta, GA, USA, 16–20 June 2014. [CrossRef]
274. Li, H.; Nabawy, M.R.A. Wing Planform Effect on the Aerodynamics of Insect Wings. *Insects* **2022**, *13*, 459. [CrossRef] [PubMed]
275. Nabawy, M.R.A. A simple model of wake capture aerodynamics. *J. R. Soc. Interface* **2023**, *20*, 20230282. [CrossRef]
276. Li, H.; Nabawy, M.R.A. Detachment of leading-edge vortex enhances wake capture force production. *J. Fluid Mech.* **2024**, *995*, A6. [CrossRef]
277. Korendiy, V.; Kachur, O. Locomotion characteristics of a wheeled vibration-driven robot with an enhanced pantograph-type suspension. *Front. Robot. AI* **2023**, *10*, 1239137. [CrossRef]
278. Zhang, C.; Liu, T.; Song, S.; Wang, J.; Meng, M.Q.-H. Dynamic wheeled motion control of wheel-biped transformable robots. *Biomim. Intell. Robot.* **2022**, *2*, 100027. [CrossRef]
279. Thueer, T.; Siegwart, R. Kinematic Analysis and Comparison of Wheeled Locomotion Performance. In *Proceedings of the 10th ESA Workshop on Advanced Space Technologies for Robotics and Automation (ASTRA)*; ETH Zurich: Zürich, Switzerland, 2008; 8p.

280. Amar, F.; Grand, C.; Besseron, G.; Plumet, F. Performance Evaluation of Locomotion Modes of an Hybrid Wheel-Legged Robot for Self-Adaptation to Ground Conditions. In Proceedings of the ASTRA'04, 8th ESA Workshop on Advanced Space Technologies for Robotics and Automation, Noordwijk, The Netherlands, 2–4 November 2004.
281. Shafaei, S.M.; Mousazadeh, H. Experimental comparison of locomotion system performance of ground mobile robots in agricultural drawbar works. *Smart Agric. Technol.* **2023**, *3*, 100131. [CrossRef]
282. Bruzzone, L.; Nodehi, S.E.; Fanghella, P. Tracked Locomotion Systems for Ground Mobile Robots: A Review. *Machines* **2022**, *10*, 648. [CrossRef]
283. Morales, J.; Martinez, J.L.; Mandow, A.; Garcia-cerezo, A.J.; Gomez-gabriel, J.M.; Pedraza, S. Power Analysis for a Skid-Steered Tracked Mobile Robot. In Proceedings of the 2006 IEEE International Conference on Mechatronics, Budapest, Hungary, 3–5 July 2006; pp. 420–425. [CrossRef]
284. Zamanov, V.; Dimitrov, A. Tracked Locomotion and Manipulation Robots. *Probl. Eng. Cybern. Robot.* **2012**, *65*, 75–84.
285. Ben-Tzvi, P.; Saab, W. A Hybrid Tracked-Wheeled Multi-Directional Mobile Robot. *J. Mech. Robot.* **2019**, *11*, 041008. [CrossRef]
286. Nagatani, K.; Kinoshita, H.; Yoshida, K.; Tadakuma, K.; Koyanagi, E. Development of leg-track hybrid locomotion to traverse loose slopes and irregular terrain. *J. Field Robot.* **2011**, *28*, 950–960. [CrossRef]
287. Torres-Pardo, A.; Pinto-Fernández, D.; Garabini, M.; Angelini, F.; Rodriguez-Cianca, D.; Massardi, S.; Tornero, J.; Moreno, J.C.; Torricelli, D. Legged locomotion over irregular terrains: State of the art of human and robot performance. *Bioinspir. Biomim.* **2022**, *17*, 061002. [CrossRef]
288. Souza, L.; Mohr, F.; Alencar, B. Analysis, Prototyping and Locomotion Control of a Quadruped Robot. In Proceedings of the 2023 Latin American Robotics Symposium (LARS), 2023 Brazilian Symposium on Robotics (SBR), and 2023 Workshop on Robotics in Education (WRE), Salvador, Brazil, 9–11 October 2023; pp. 129–134. [CrossRef]
289. Garcia Bermudez, F.L.; Julian, R.C.; Haldane, D.W.; Abbeel, P.; Fearing, R.S. Performance Analysis and Terrain Classification for a Legged Robot over Rough Terrain. In Proceedings of the 2012 IEEE/RSJ International Conference on Intelligent Robots and Systems, Vilamoura-Algarve, Portugal, 7–12 October 2012; pp. 513–519. [CrossRef]
290. Čížek, P.; Zoula, M.; Faigl, J. Design, Construction, and Rough-Terrain Locomotion Control of Novel Hexapod Walking Robot With Four Degrees of Freedom Per Leg. *IEEE Access* **2021**, *9*, 17866–17881. [CrossRef]
291. Ha, S.; Lee, J.; van de Panne, M.; Xie, Z.; Yu, W.; Khadiv, M. Learning-based legged locomotion; state of the art and future perspectives. *arXiv* **2024**, arXiv:2406.01152. [CrossRef]
292. Smith, L.; Kew, J.C.; Peng, X.B.; Ha, S.; Tan, J.; Levine, S. Legged Robots that Keep on Learning: Fine-Tuning Locomotion Policies in the Real World. *arXiv* **2021**, arXiv:2110.05457. [CrossRef]
293. Park, T.; Cha, Y. Soft mobile robot inspired by animal-like running motion. *Sci. Rep.* **2019**, *9*, 14700. [CrossRef] [PubMed]
294. Chen, R.; Yuan, Z.; Guo, J.; Bai, L.; Zhu, X.; Liu, F.; Pu, H.; Xin, L.; Peng, Y.; Luo, J.; et al. Legless soft robots capable of rapid, continuous, and steered jumping. *Nat. Commun.* **2021**, *12*, 7028. [CrossRef]
295. Shah, D.S.; Powers, J.P.; Tilton, L.G.; Kriegman, S.; Bongard, J.; Kramer-Bottiglio, R. A soft robot that adapts to environments through shape change. *Nat. Mach. Intell.* **2020**, *3*, 51–59. [CrossRef]
296. Das, R.; Babu, S.P.M.; Visentin, F.; Palagi, S.; Mazzolai, B. An earthworm-like modular soft robot for locomotion in multi-terrain environments. *Sci. Rep.* **2023**, *13*, 1571. [CrossRef]
297. Zhang, X.; Naughton, N.; Parthasarathy, T.; Gazzola, M. Friction modulation in limbless, three-dimensional gaits and heterogeneous terrains. *Nat. Commun.* **2021**, *12*, 6076. [CrossRef] [PubMed]
298. Zhou, X.; Zhang, Y.; Qiu, Z.; Shan, Z.; Cai, S.; Bao, G. Locomotion control of a rigid-soft coupled snake robot in multiple environments. *Biomim. Intell. Robot.* **2024**, *4*, 100148. [CrossRef]
299. He, Y.; Wang, D.B.; Ali, Z.A. A review of different designs and control models of remotely operated underwater vehicle. *Meas. Control.* **2020**, *53*, 1561–1570. [CrossRef]
300. Ray, S.; Bhowal, R.; Patel, P.; Panaiyappan K, A. An Overview of the Design and Development of a 6 DOF Remotely Operated Vehicle for Underwater Structural Inspection. In Proceedings of the 2021 International Conference on Communication, Control and Information Sciences (ICCISc), Idukki, India, 16–18 June 2021; Volume 1, pp. 1–6. [CrossRef]
301. Aguirre-Castro, O.A.; Inzunza-González, E.; García-Guerrero, E.E.; Tlelo-Cuautle, E.; López-Bonilla, O.R.; Olguín-Tiznado, J.E.; Cárdenas-Valdez, J.R. Design and Construction of an ROV for Underwater Exploration. *Sensors* **2019**, *19*, 5387. [CrossRef] [PubMed]
302. Zulkarnain, O.W.; Redhwan, A.A.M.; Baba, N.B.; Fadhil, M.N.; Rosni, S. Design and Development of SelamDrone Underwater ROV Manoeuvring Control. *J. Phys. Conf. Ser.* **2021**, *1874*, 012081. [CrossRef]
303. Cadena, A. Design and construction of an Autonomous Underwater Vehicle for the launch of a small UAV. In Proceedings of the 2009 IEEE International Conference on Technologies for Practical Robot Applications, Woburn, MA, USA, 9–10 November 2009; pp. 78–83. [CrossRef]
304. MacLeod, M.; Bryant, M. Variable Buoyancy System for Unmanned Multi-Domain Vehicles. In *Active and Passive Smart Structures and Integrated Systems*; SPIE: Bellingham, WA, USA, 2016; Volume 9799, pp. 607–615. [CrossRef]

305. Zhang, S.; Zhou, Y.; Xu, M.; Liang, X.; Liu, J.; Yang, J. AmphiHex-I: Locomotory Performance in Amphibious Environments with Specially Designed Transformable Flipper Legs. *IEEE/ASME Trans. Mechatron.* **2016**, *21*, 1720–1731. [CrossRef]
306. Zhu, J.; Fang, T.; Xu, M.; Zhou, Y.; Huang, W.; Zhang, S. Initial Development of an Amphibious Robot with Flexible Straight Flipper-Legs. In Proceedings of the 2018 IEEE International Conference on Real-time Computing and Robotics (RCAR), Kandima, Maldives, 1–5 August 2018; pp. 417–420. [CrossRef]
307. Guo, N.; Bai, Z.; Gao, W.; Chen, H.; Zhang, S. Passively Deformable Flipper Legs for An Amphibious Quadruped. In Proceedings of the 2021 IEEE International Conference on Real-time Computing and Robotics (RCAR), Xining, China, 15–19 July 2021; pp. 738–743. [CrossRef]
308. Wang, S.; Fan, J.; Pan, Y.; Liu, G.; Liu, Y. Design and Analysis of Adaptive Flipper With Origami Structure for Frog-Inspired Swimming Robot. *IEEE Robot. Autom. Lett.* **2024**, *9*, 1262–1269. [CrossRef]
309. Chikere, N.; McElroy, J.; Ozkan-Aydin, Y. Embodied Design for Enhanced Flipper-Based Locomotion in Complex Terrains. *arXiv* **2024**, arXiv:2405.13948. [CrossRef]
310. Low, K.H.; Zhou, C.; Ong, T.W.; Yu, J. Modular Design and Initial Gait Study of an Amphibian Robotic Turtle. In Proceedings of the 2007 IEEE International Conference on Robotics and Biomimetics (ROBIO), Sanya, China, 15–18 December 2007; pp. 535–540. [CrossRef]
311. Yao, G.; Liang, J.; Wang, T.; Yang, X.; Shen, Q.; Zhang, Y.; Wu, H.; Tian, W. Development of A Turtle-Like Underwater Vehicle Using Central Pattern Generator. In Proceedings of the 2013 IEEE International Conference on Robotics and Biomimetics (ROBIO), Shenzhen, China, 12–14 December 2013; pp. 44–49. [CrossRef]
312. Li, Y.; Xu, Y.; Wu, Z.; Ma, L.; Guo, M.; Li, Z.; Li, Y. A comprehensive review on fish-inspired robots. *Int. J. Adv. Robot. Syst.* **2022**, *19*, 17298806221103707. [CrossRef]
313. Raj, A.; Thakur, A. Fish-inspired robots: Design, sensing, actuation, and autonomy—A review of research. *Bioinspir. Biomim.* **2016**, *11*, 031001. [CrossRef] [PubMed]
314. Singh, S.; Ahmad, S.; Amrr, S.M.; Khan, S.A.; Islam, N.; Gari, A.A.; Algethami, A.A. Modeling and Control Design for an Autonomous Underwater Vehicle Based on Atlantic Salmon Fish. *IEEE Access* **2022**, *10*, 97586–97599. [CrossRef]
315. Papadopoulos, E.; Apostolopoulos, E.; Tsigkourakos, P. Design, Control, and Experimental Performance of a Teleoperated Robotic Fish. In Proceedings of the 2009 17th Mediterranean Conference on Control and Automation, Thessaloniki, Greece, 24–26 June 2009; pp. 766–771. [CrossRef]
316. Peter, B.; Ratnaweera, R.; Fischer, W.; Pradalier, C.; Siegwart, R.Y. Design and Evaluation of a Fin-Based Underwater Propulsion System. In Proceedings of the 2010 IEEE International Conference on Robotics and Automation, Anchorage, AK, USA, 3–7 May 2010; pp. 3751–3756. [CrossRef]
317. Ardupilot. Pixhawk Wiring Quick Start | PX4 Guide (Main). Available online: https://docs.px4.io/main/en/assembly/quick_start_pixhawk.html (accessed on 4 November 2024).
318. Ardupilot. Standard Configuration | PX4 Guide (Main). Available online: https://docs.px4.io/main/en/config/ (accessed on 4 November 2024).
319. Wang, S.; Dai, X.; Ke, C.; Quan, Q. RflySim: A Rapid Multicopter Development Platform for Education and Research Based on Pixhawk and MATLAB. In Proceedings of the 2021 International Conference on Unmanned Aircraft Systems (ICUAS), Athens, Greece, 15–18 June 2021; pp. 1587–1594.
320. Jothikrishna, K.; Rithika, S.M.; Swetha, S.V.; Kavitha, K. Remotely Operated Underwater Vehicle (ROV). In Proceedings of the 2023 2nd International Conference on Advancements in Electrical, Electronics, Communication, Computing and Automation (ICAECA), Coimbatore, India, 16–17 June 2023; pp. 1–4. [CrossRef]
321. Nowakowski, M.; Berger, G.S.; Braun, J.; Mendes, J.A.; Bonzatto Junior, L.; Lima, J. Advance Reconnaissance of UGV Path Planning Using Unmanned Aerial Vehicle to Carry Our Mission in Unknown Environment. In Proceedings of the Robot 2023: Sixth Iberian Robotics Conference, University of Coimbra, Coimbra, Portugal, 22–24 November 2023; Marques, L., Santos, C., Lima, J.L., Tardioli, D., Ferre, M., Eds.; Springer Nature Switzerland: Cham, Switzerland, 2024; pp. 50–61. [CrossRef]
322. Толок, І.; Myasischev, O.O.; Lienkov, S.V.; Overchuk, V.V.; Lytvynenko, N.I.; Zinchuk, A.G. Large-Capacity Quadcopter's Designing on the Controllers of the Pixhawk Cube Family. 2022. Available online: http://repositsc.nuczu.edu.ua/handle/123456789/20829 (accessed on 4 November 2024).
323. Gunturu, R.; Durgaa, K.N.; Harshaa, T.S.; Ahamed, S.F. Development of Drone Based Delivery System Using Pixhawk Flight Controller. In Proceedings of the 2nd International Conference on IoT, Social, Mobile, Analytics & Cloud in Computational Vision & Bio-Engineering (ISMAC-CVB 2020), Tiruchengodu, India, 29–30 October 2020; p. 3734801. [CrossRef]
324. Kusmirek, S.; Socha, V.; Malich, T.; Socha, L.; Hylmar, K.; Hanakova, L. Dynamic Flight Tracking: Designing System for Multirotor UAVs With Pixhawk Autopilot Data Verification. *IEEE Access* **2024**, *12*, 109806–109821. [CrossRef]
325. Arduino. Arduino Uno Rev3. Available online: https://store.arduino.cc/products/arduino-uno-rev3 (accessed on 4 November 2024).
326. Farnell. DFR0478 DFROBOT, IoT Microcontroller Board, FireBeetle, ESP32, Arduino Development Boards | Farnell UK. Available online: https://uk.farnell.com/dfrobot/dfr0478/firebeetle-esp32-iot-mcu-arduino/dp/3517881 (accessed on 4 November 2024).

327. Farnell. STM32 Embedded Development Kits—ARM | Farnell UK. Available online: https://uk.farnell.com/c/embedded-computers-education-maker-boards/arm/embedded-development-kits-arm?silicon-family-name=stm32 (accessed on 4 November 2024).
328. RS. Microchip PIC18F4520-I/P, 8bit PIC Microcontroller, PIC18F, 40MHz, 32 kB, 256 B Flash, 40-Pin PDIP | RS. Available online: https://uk.rs-online.com/web/p/microcontrollers/6230819 (accessed on 4 November 2024).
329. Murtaza, Z.; Mehmood, N.; Jamil, M.; Ayaz, Y. Design and implementation of low cost remote-operated unmanned ground vehicle (UGV). In Proceedings of the 2014 International Conference on Robotics and Emerging Allied Technologies in Engineering (iCREATE), Islamabad, Pakistan, 22–24 April 2014; pp. 37–41. [CrossRef]
330. Krucsó, L.; Erdei, T.I.; Kapusi, T.P.; Husi, G. Designing an ATmega328 Microcontroller Based Gesture-controlled IoT UGV Unit and Creating a Camera System Using Linux Distribution. *Recent Innov. Mechatron.* **2019**, *6*, 1–7.
331. Marzbanrad, A.; Sharafi, J.; Eghtesad, M.; Kamali, R. Design, Construction and Control of a Remotely Operated Vehicle (ROV). In Proceedings of the ASME 2011 International Mechanical Engineering Congress and Exposition, Denver, CO, USA, 11–17 November 2011; American Society of Mechanical Engineers Digital Collection. ASME: New York, NY, USA, 2012; pp. 1295–1304. [CrossRef]
332. Syukron, M.; Mardiyah, N.; Wahono; Rosikhin, A.; Sari, Z. The application of ROV (remotely operated vehicle) of the micro-controller submarine as a tool to take sample of water and soil contaminated by waste. *AIP Conf. Proc.* **2019**, *2088*, 020016. [CrossRef]
333. Lee, D.; Moon, S. Implementation of a drone using the PID control of an 8-bit microcontroller. *Asia-Pac. J. Multimed. Serv. Converg. Art Humanit. Sociol.* **2016**, *6*, 81–90. [CrossRef]
334. Spoorthi, S.; Shadaksharappa, B.; Suraj, S.; Manasa, V.K. Freyr drone: Pesticide/fertilizers spraying drone—An agricultural approach. In Proceedings of the 2017 2nd International Conference on Computing and Communications Technologies (ICCCT), Allahabad, India, 23–24 February 2017; pp. 252–255. [CrossRef]
335. Ghosh, A.; Roy, H.; Dhar, S. Arduino Quadcopter. In Proceedings of the 2018 Fourth International Conference on Research in Computational Intelligence and Communication Networks (ICRCICN), Kolkata, India, 22–23 November 2018; pp. 280–283. [CrossRef]
336. Raspberry Pi. Buy a Raspberry Pi 5. Available online: https://www.raspberrypi.com/products/raspberry-pi-5/ (accessed on 4 November 2024).
337. Raspberry Pi. Getting started—Raspberry Pi Documentation. Available online: https://www.raspberrypi.com/documentation/computers/getting-started.html (accessed on 4 November 2024).
338. Brand, I.; Roy, J.; Ray, A.; Oberlin, J.; Oberlix, S. PiDrone: An Autonomous Educational Drone Using Raspberry Pi and Python. In Proceedings of the 2018 IEEE/RSJ International Conference on Intelligent Robots and Systems (IROS), Madrid, Spain, 1–5 October 2018; pp. 1–7. [CrossRef]
339. Benhadhria, S.; Mansouri, M.; Benkhlifa, A.; Gharbi, I.; Jlili, N. VAGADRONE: Intelligent and Fully Automatic Drone Based on Raspberry Pi and Android. *Appl. Sci.* **2021**, *11*, 3153. [CrossRef]
340. Westerlund, O.; Asif, R. Drone Hacking with Raspberry-Pi 3 and WiFi Pineapple: Security and Privacy Threats for the Internet-of-Things. In Proceedings of the 2019 1st International Conference on Unmanned Vehicle Systems-Oman (UVS), Muscat, Oman, 5–7 February 2019; pp. 1–10. [CrossRef]
341. Osen, O.L.; Sandvik, R.-I.; Berge Trygstad, J.; Rogne, V.; Zhang, H. A novel low cost ROV for aquaculture application. In Proceedings of the OCEANS 2017—Anchorage, Anchorage, AK, USA, 18–21 September 2017; pp. 1–7. Available online: https://ieeexplore.ieee.org/abstract/document/8232180 (accessed on 4 November 2024).
342. Tutunji, T.A.; Salah-Eddin, M.; Abdalqader, H. Unmanned Ground Vehicle Control using IoT. In Proceedings of the 2020 21st International Conference on Research and Education in Mechatronics (REM), Cracow, Poland, 9–11 December 2020; pp. 1–5. [CrossRef]
343. Chaurasia, V.; Mishra, V.; Jain, L. Brain-Bot: An Unmanned Ground Vehicle (UGV) Using Raspberry Pi and Brain Computer Interface (BCI) Technology. In *Advances in Computing and Data Sciences*; Singh, M., Gupta, P.K., Tyagi, V., Sharma, A., Ören, T., Grosky, W., Eds.; Springer: Singapore, 2017; pp. 252–261. [CrossRef]
344. Open Robotics. ROS: Home. Available online: https://www.ros.org/ (accessed on 4 November 2024).
345. Open Robotics. ROS/Tutorials/InstallingandConfiguringROSEnvironment—ROS Wiki. Available online: https://wiki.ros.org/ROS/Tutorials/InstallingandConfiguringROSEnvironment (accessed on 4 November 2024).
346. Mo, S.M. Development of a Simulation Platform for ROV Systems. Master's Thesis, NTNU, Trondheim, Norway, 2015. Available online: https://ntnuopen.ntnu.no/ntnu-xmlui/handle/11250/2350740 (accessed on 4 November 2024).
347. Hatta, M.I.F.; Widodo, N.S. Robot Operating System (ROS) in Quadcopter Flying Robot Using Telemetry System. *Int. J. Robot. Control. Syst.* **2021**, *1*, 54–65. [CrossRef]
348. Pandey, A.; Prasad, K.; Zade, S.; Babbar, A.; Singh, G.K.; Sharma, N. Implementation of simultaneous localization and mapping for TurtleBot under the ROS design framework. *Int. J. Interact. Des. Manuf.* **2024**, *18*, 3799–3812. [CrossRef]

349. Raveendran, R.; Ariram, S.; Tikanmäki, A.; Röning, J. Development of task-oriented ROS-based Autonomous UGV with 3D Object Detection. In Proceedings of the 2020 IEEE International Conference on Real-time Computing and Robotics (RCAR), Asahikawa, Japan, 28–29 September 2020; pp. 427–432. [CrossRef]
350. Conte, G.; Scaradozzi, D.; Sorbi, L.; Panebianco, L.; Mannocchi, D. ROS multi-agent structure for autonomous surface vehicles. In Proceedings of the OCEANS 2015—Genova, Genova, Italy, 18–21 May 2015; pp. 1–6. [CrossRef]
351. Ghasemi, H.; Mirfakhar, A.; Masouleh, M.T.; Kalhor, A. Control a Drone Using Hand Movement in ROS Based on Single Shot Detector Approach. In Proceedings of the 2020 28th Iranian Conference on Electrical Engineering (ICEE), Tabriz, Iran, 4–6 August 2020; pp. 1–5. [CrossRef]
352. Jain, N.; Gupta, A.K.; Mathur, P. Autonomous Drone Using ROS for Surveillance and 3D Mapping Using Satellite Map. In Proceedings of the Second International Conference on Information Management and Machine Intelligence; Goyal, D., Gupta, A.K., Piuri, V., Ganzha, M., Paprzycki, M., Eds.; Springer: Singapore, 2021; pp. 255–266. [CrossRef]
353. Airikka, P. Advanced control methods for industrial process control. *Comput. Control. Eng.* **2004**, *15*, 18–23. [CrossRef]
354. Stancu, A.; Mostafa, M.; Codres, E.; Martinez, M.; Madin, Z.; Deng, S.; Aldesouky, A. *Autonomous Mobile Robots*; The University of Manchester: Manchester, UK, 2021.
355. MATLAB. What Is SLAM (Simultaneous Localization and Mapping)—MATLAB & Simulink. Available online: https://uk.mathworks.com/discovery/slam.html (accessed on 13 March 2023).
356. Kudan. Understanding how Direct Visual SLAM works. Kudan Global. 2020. Available online: https://www.kudan.io/blog/direct-visual-slam/ (accessed on 13 March 2023).
357. Sickle, J.V. The Navigation Solution | GEOG 862: GPS and GNSS for Geospatial Professionals. Available online: https://www.e-education.psu.edu/geog862/node/1724 (accessed on 13 March 2023).
358. Choset, H. Robotic Motion Planning: Bug Algorithms. 2023. Available online: http://www.cs.columbia.edu/~allen/F15/NOTES/Chap2-Bug.pdf (accessed on 13 March 2023).